

**SOLAR CONCENTRATOR  
TECHNOLOGY DEVELOPMENT  
FOR  
SPACE BASED APPLICATIONS  
ENGINEERING REPORT ER-1001  
VOLUME I OF II**

FINAL REPORT

SOLAR CONCENTRATOR  
TECHNOLOGY DEVELOPMENT  
FOR  
SPACE BASED APPLICATIONS  
ENGINEERING REPORT, ER-1001

Dr. A. Pintz  
Principal Investigator  
Cleveland State University  
Advanced Manufacturing Center  
Cleveland, Ohio 44114

Prepared by:  
C.H. Castle, and R.R. Reimer

December 31, 1992

Project work performed under grant NCC 3-77  
NASA Lewis Resesrch Center  
Solar Dynamics and Thermal Systems Branch  
J.E. Calogeras: Chief  
Project Managers: Dr. J.M. Savino and T.S. Mroz

## List of Contributing Organizations and Personnel

### 1. NASA Lewis Research Center

Electro-Physics Branch, 5480, Bruce Banks  
Kim De Groh, Profilometer Measurement  
Don Jaworske, Profilometer Measurement

### 2. Cleveland Advanced Manufacturing Program Advanced Manufacturing Center, Cleveland State University

Frank Albert, Design and Drafting  
Arlene Ellington (student), Solar Tracker  
Ernie Hall, Manufacturing Processes and Tooling  
Paul Lin, Optical Inspection  
Ken Svitak, Lead Project Tasks  
Jeff Tishue (student), Various Tasks

### 3. Suppliers and Vendors

Tempcraft (Cleveland), Stretch Forming Tool  
A.J. Oster (Canton, OH), Aluminum Foils  
Hexcell Corporation (Dublin, OH), Honeycomb  
Advanced Polymer Sciences (Avon, OH), Epoxy  
Denton Vacuum Inc. (Cherry Hill, NJ) Vacuum Aluminizing  
Majestic Tool & Machine (Cleveland), Machining  
Modern Industries (Cleveland), Machining

## Table of Contents

### Volume I

	Page
1. Introduction -----	2
2. Summary -----	3
3. Discussion -----	4
3.1 Two Meter Concentrator Design -----	4
3.1.1 Design Specification-----	4
3.1.2 Concentrator Configuration -----	5
3.1.3 Launch Stowage -----	6
3.1.4 Concentrator Assembly Drawing -----	7
3.1.5 Panel Detail Drawing -----	7
3.1.6 Deployment Actuation -----	8
3.1.7 Shape Control -----	8
3.1.8 Reflective Surface -----	10
3.1.9 Thermoelastic Properties -----	10
3.1.10 Concentrator Efficiency -----	11
3.1.11 Budget of Surface Deviations -----	12



	Page
3.2 Panel Cross Section Analysis -----	17
3.2.1 Print Through Evaluation -----	17
3.2.2 Edge Design -----	25
3.3 Panel Fabrication -----	26
3.3.1 Concentrator Fabrication and Assembly --	26
3.3.2 Forming Aluminum Faces -----	29
3.3.3 Core Preparation -----	30
3.3.4 Component Fabrication -----	32
3.3.5 Cleaning Procedure -----	32
3.3.6 Adhesive Bonding Procedure -----	34
3.3.7 Leveling Layer Application -----	37
3.3.8 Reflective and Protective Coating -----	48
3.3.9 Edge Trimming -----	49
3.4 Inspection -----	50
3.4.1 Tool Accuracy -----	50
3.4.2 Panel Optical Inspection -----	50
3.4.3 Panel Weight -----	52
3.5 Two Panel Test Rig -----	53
4. Recommendations -----	54
Appendixes _____	55
References -----	56

List of Figures  
(Volume II)

Pg

1.	Two Meter Concentrator Geometry -----	
2.	Requirements for a Demonstrator Solar Concentrator-----	
3.	Panel Deployment Graphics -----	
4.	Rim Angle versus f/d Ratio -----	
5.	Ray Deviation versus Rim Angle -----	
6.	Deployed Concentrator -----	
7.	Stowed Concentrator -----	
8.	Panel Hinge Geometry -----	
9.	Panel Deployment Actuator -----	
10.	Assembly Jig -----	
11.	Panel Positioner Arm & Lock Spring -----	
12.	Positioner Jig -----	
13.	Temperature Gradients in LEO -----	
14.	Sources of Surface Deviations for 2 Meter Solar Concen. -	
15.	Specified Surface Deviations for 2 Meter Solar Concen. --	
16.	Types of Surface Deviations -----	
17.	Calorimetric Efficiency of 5 Ft. Dia, Fixed Dish Solar Concentrator -----	
18.	Ray Trace Results for 2 Meter Solar Concentrator -----	
19.	Probable Geometric Efficiency of Two Meter Concen. -----	
20.	Budget of Surface Deviations for 2 Meter Solar Concen. --	
21.	Honeycomb Sandwich Cross Section -----	
22.	Honeycomb Sandwich Evaluation for Print Thru & Strength--	
23,	Adhesive Curing Enclosure -----	
24.	Profilometer Chart -----	
25.	Profilometer Chart -----	
26.	Profilometer Chart -----	
27.	$\pi$ and $2\pi$ Models of Print Thru Profiles -----	
28.	Location of Max Surf Deviations for $\pi$ and $2\pi$ Models -----	
30.	Surface Slope Error versus Core Hex Size -----	
31.	Surface Slope Error versus Face Thickness -----	
32.	Double Dip Adhesive Fillet Process -----	
34.	Paste Clean and Etch Process -----	
35.	Process Evaluation No. 1 - Anodize -----	
36.	Process Evaluation No. 2 - Abrasion -----	
37.	Preferred Clean and Etch Process -----	
38.	Specimen's Prepared for Strength Evaluation -----	
39.	Lap Shear Test Specimen -----	
40.	Lap Shear Test Results -----	
41.	Honeycomb Sandwich Tensile Test Specimen -----	
42.	Honeycomb Sandwich Tensile Strength Test Results -----	
43.	Effect of Leveling Layer on Surface Specularity -----	
44.	Radial Edge Close-Out Detail -----	
45.	Potential Edge Close-Out Design -----	

List of Figures  
(Volume II)

Pg

46.	Two Meter Fabrication & Assembly Flow Chart -----
47.	Panel Fabrication Area -----
48.	Panel Fabrication Area -----
49.	Panel Fabrication Area -----
50.	Panel Fabrication Area -----
51.	Stretch Forming Tool in Trimming Fixture -----
52.	Heaters on Underside of Tool -----
53.	Stretch Former without Shroud in Place -----
54.	Stretch Former with Shroud in Place -----
55.	Stretch Former Viewed from Stretch Jaw -----
56.	HOBE Expansion -----
57.	HOBE Expansion -----
58.	HOBE Expansion -----
59.	HOBE Construction Details -----
60.	Flycutting HOBE in Milling Machine -----
61.	Panel Components, Close Up -----
62.	Panel Components, Templates & Fixtures -----
63.	Process Equipment, Tools & Aids -----
64.	Vented Hood and Chemical Dump Tanks -----
65.	Clean and Etch Drain Method -----
66.	Clean and Etch of Front Face -----
67.	Clean and Etch of Back Face -----
68.	Clean and Etch of Back Face -----
69.	Hot Air Drying of Cleaned Faces -----
70.	Hot Air Drying of Cleaned Face -----
71.	Tool in Place for Panel Lay-up Process -----
72.	Placement of Edge Stiffener Pieces -----
73.	Placement of Foam Edges and Dummy Corners -----
74.	Taping Edges in Place -----
75.	Dipping Honeycomb Core into Adhesive -----
76.	Screeding Adhesive Layer onto Dip Plate -----
77.	Screeding Adhesive Layer onto Dip Plate -----
78.	Placement of Honeycomb Core -----
79.	Honeycomb Core in Place -----
80.	Trimming Back Face with Template -----
81.	Placement of Back Face -----
82.	Back Face in Place -----
83.	Placement of Vacuum Bag -----
84.	Placement of Vacuum Bag Sealing Tape -----
85.	Stretching Vacuum Bag over Sealing Tape -----
86.	Panel Under Vacuum Bag before Cure -----
87.	Panel Under Vacuum Bag before Cure -----
88.	Placement of Oven Enclosure over Bagged Panel -----
89.	Placement of Insulation Pillows around Bagged Panel -----
90.	Programming Four Zone Temperature Controllers -----
91.	Panel Enclosed and Under Cure Heat-up -----
92.	Removal of Vacuum Bag after Panel Cure -----
93.	Removal of Tapes after Panel Cure -----

List of Figures  
(Volume II)

Pg

94.	Removal of Cured Panel -----	
95.	Panel after Rough Trim -----	
96.	Leveling Layer Spray Equipment -----	
97.	Heating Lamps and Panel Rotator -----	
98.	Traversing Mechanism -----	
99.	Traversing Mechansim -----	
100.	Views of Spray Equipment Thru Access Door -----	
101.	Vie of Traversing Unit and Filter -----	
102.	Leveling Layer Defects -----	
103.	Leveling Layer Defects -----	
104.	Vacuum Evaporation Specimens -----	
105.	Panel Mounted in Trim Tool Fixture -----	
106.	Trimming Radial Edge -----	
107.	Close-up of Radial Edge Trimming -----	
108.	Close-up of OD Edge Trimming -----	
109.	Optical Inspection Rig Schematic -----	
110.	Optical Inspection Rig, Overall View -----	
111.	Optical Inspection Rig, Plastic Target -----	
112.	Optical Inspection Rig, Light Source and Panel -----	
113.	Optical Inspection Rig, Light Source Adjustment -----	
114.	Panel No. 6 Optical Inspection Photograph -----	
115.	Close-up of Panel No. 6 Optical Inspection -----	
116.	Histogram of Panel No. 6 Circumferential Errors -----	
117.	Histogram of Panel No. 6 Radial Errors -----	
118.	Optical Inspection Rig Geometry -----	

## 1. Introduction

The National Aeronautics and Space Administration has a continuing program to develop electrical power generation systems for space applications. Photovoltaic conversion is by far the most used technology and is mature. Thermoelectric conversion using a radio-isotope heat source has been used where outer planetary space craft are too far away for absorbing significant solar energy. Other competing conversion systems are at various levels of development depending on technical and cost considerations.

Solar dynamic power (SDP) conversion is one technology that offers advantages for applications within the inner planet region. The most pronounced advantage is one of weight. Since SDP conversion efficiency can be 2 to 3 times higher than photovoltaic, the collecting surfaces are much reduced in area and therefore lighter. This becomes an advantage in allotting more weight to launched payloads. A second advantage results for low earth orbit (LEO) applications such as Space Station Freedom. The reduced area results in lower drag forces on the space craft and requires less reboost propellant to maintain orbit. A third advantage occurs because of the sun-to-shade cycling while in earth orbit. Photovoltaic systems require batteries to store energy for use when in the shade, and battery life for periods of 10 to 15 years is not presently achievable. For these reasons the Solar Dynamics and Thermal Systems Branch at NASA Lewis Research Center has funded work in developing SDP systems.

The generic SDP system uses a large parabolic solar concentrator to focus solar energy onto a power conversion device. The concentrators are large areas and must therefore be efficient and have low specific weights. Yet these surfaces must be precise and capable of being stowed in a launch vehicle and then deployed and sometimes unfurled in space. There are significant technical challenges in engineering such structures, and considerable investigation has been made to date. A grant was arranged with the Advanced Manufacturing Center at Cleveland State University to assist the NASA Lewis Research Center in evaluating this technology. Project personnel had direct experience in solar concentrator development during the 1960-70 time period. The objective of the grant was therefore to restore that technology capability while improving it with advances that have occurred since then. This report is a summary of the three year period from January 1989 through December 1991.

## 2. Summary

This grant work proceeded as a result of a preliminary six month design study at CSU/AMC, where a two meter diameter concentrator concept was proposed for further consideration. The selection process was made by working closely with NASA LeRC personnel and with their engineering specification. Based on technology that has been developed beginning in 1960, the Sunflower concept of stowage in a launch vehicle and made of adhesive bonded aluminum honeycomb sandwich panels was proposed. This technology was judged most advanced for several reasons:

1. Large light weight aluminum concentrator structures were successfully tested for launch vibration and acceleration and deployment in space.
2. Optical inspection and solar tracking tests of concentrators determined that the necessary surface accuracies can be obtained with these light weight surfaces.
3. And antenna designs based on these same aluminum concepts have successfully performed. Pioneer 10 is still transmitting after 20 years, and several Navy FltSatCom satellites continue to operate in geosynchronous orbit.

The grant tasks were devoted to developing a fabrication technique for advanced aluminum honeycomb solar concentrators, establishing a fabrication capability at CSU/AMC to build and test panels for the two meter concentrator and application of improved technology where possible. This resulted in a dedicated work area 2000 square feet in area including an optical inspection dark room and office space. All design work and fabrication was done in-house because of the unique procedures and handling required for this hardware. The following results were achieved:

1. Nine panels were fabricated using the fabrication area.
2. A precision tool for use in several process steps was designed and fabricated.
3. Clean areas were established for forming the aluminum stock and application of a leveling layer to the panel.
4. A panel oven enclosure was designed and built to control adhesive curing.
5. A panel trim fixture was designed and built.
6. An optical inspection rig was designed and built to evaluate panel surface accuracy.

Panels were successfully fabricated and inspected. The results show that a panel weight of 0.40 lb/ft<sup>2</sup> is within the 0.20 - 0.40 lb/ft<sup>2</sup> specified range, and that the surface accuracy, for the panel alone, had maximum errors of 1.1 milliradian.

Advances in technology were achieved in 1.) selection of a new epoxy adhesive which minimizes honeycomb core print thru on to the reflective face, and 2.) selection of a new leveling layer epoxy which provides the specular finish required on the reflective face. Some process refinements are required, such as improved cleanliness of the surrounding work area, but are viewed as maturation efforts toward final product quality.

### 3. DISCUSSION

#### 3.1 Two Meter Concentrator Design

A design study was completed in January 1989 (Ref. 1) and resulted in layout drawings of a two meter auto-deployable petaline solar concentrator. The geometry is shown in Figure 1 and the design specification in Figure 2. A paper describing this work was presented at the August 1989 IECEC Symposium (Ref. 2). Drawings of the concentrator assembly and panel detail are presented in Sections 3.1.4 through 3.1.7 along with deployment operation. A graphic presentation of panel deployment is shown in Figure 3 and illustrates the petaline movement of an individual panel to deployed position. This design study was based on significant advances in technology resulting from previous projects (Refs. 3 through 10). Appendixes A, B and C show selected information from References 3, 4 and 7 and will be referred to through out this report. The design also incorporates technology improvements made since those projects were completed. A 9.5 foot diameter petaline antenna (Ref. 7) was fully qualified for flight. This two meter concentrator design duplicates most of the features as a 0.7 scaled down version of the antenna.

##### 3.1.1 Design Specification

The two meter size was selected because it is large enough to produce meaningful information but is small enough to be built and tested at a lower funding level. Major considerations in the design were:

1. Auto-deployment
2. Use of proven concepts
3. And inclusion of latest technology developments

In order to ensure that the concentrator would meet the efficiency requirements for a Brayton engine conversion cycle, NASA requested that the:

1. Area concentration ratio be 2000:1 or greater
2. Surface slope deviations be typical of a normal Gaussian distribution curve where the one sigma value is one milliradian or less
3. And surface reflectance of solar energy be 0.88 or greater

The maximum solar tracking misorientation was specified at one milliradian.

The receiver aperture diameter is 1.68 inches (4.26 cm) at the area concentration ratio of 2000:1 where the concentrator outside diameter is 78.75 inches (2 meters) and the inside diameter 26.62 inches (0.6 Meter). Since the unit would be used as a demonstrator, the specification required that it be easily restowed manually and have surface protective coatings to allow terrestrial handling.

The specific weight was specified at 1-2 kg/m<sup>2</sup> (0.2-0.4 lb./ft<sup>2</sup>). This value is defined as the total weight of reflective structure, actuators, locks, positioners and support structure divided by the intercepted area of solar flux. It should be noted that accessory hardware has practical lower limits. Therefore the two meter unit will have a higher specific weight than units with diameters near the upper range of this petaline concept.

### 3.1.2 Concentrator Configuration

The geometry in Figure 1 shows an f/d ratio of 0.5 which results in a 39.375 inch focal length (1 meter) and a rim angle of 53.1 degrees. Figure 4 shows how rim angle and focal length vary with f/d ratio (for a fixed 2 meter diameter). This figure is a reduction of a CAD layout and shows rim ray misses from the focal point for a maximum surface slope deviation of 3 milliradians. These focal point misses are plotted versus rim angle on Figure 5 and the curve is fairly flat between rim angles of 30 to 60 degrees and especially between 35 and 55 degrees. The designer has considerable latitude in selecting a rim angle without seriously affecting concentration efficiency. Figure 4 shows that the larger rim angles have the advantage of shorter focal lengths while smaller rim angles have the advantage of lighter weight (less surface area of the paraboloid).



The 0.3 ratio of inside diameter to outside diameter was somewhat arbitrarily selected because no launch envelope was specified. However this ratio is considered appropriate based on previous designs (Refs. 3, 5 and 7). The two meter design utilizes reflecting surface only between the inside and outside diameters, but additional area could be added within the inside diameter as shown in Appendix C.

The stowage concept is based on the petaline configuration, and deployed and stowed views are shown in Figures 6 and 7. The unit is divided into 16 panels that are hinged at the ID so that they can be rotated to the stowed position for launch. The geometric arrangement of each panel axis is shown in Figure 8. The hinge axis is located in the plane of the paper and perpendicular to radial edge A. This simple configuration allows the efficient petaline stowage that leaves ample volume inside the stacked panels to stow other components.

Each panel has a segment of a ring attached to the outer edge, Figure 6. When the panels are rotated to the stowed position all of the segments abut end-to-end and a stacking ring is formed, Figure 7. A band placed around the outside of the ring provides a continuous hoop restraint of the ring segments. Lateral launch loads in those panels which can not efficiently resist such loads can then be transferred 90 degrees, via the stacking ring, to panels that can. The restraining band is severed in orbit to initiate deployment.

Two clevis type hinge assemblies form the hinge axis and have their fixed half attached to the mounting ring. The mounting ring transfers panel launch loads to the payload or launch vehicle and also provides a reference surface for shape control when the panels are deployed. Structural struts between the mounting ring and the launch vehicle would be properly sized, but 4 columnar struts were used for the demonstrator. Actuators, positioners and locks are discussed later.

### 3.1.3 Launch Stowage Envelope

The stowage configuration shown is not sized for a particular launch envelope and there is some freedom to modify it depending on a specific launch envelope. The design fits essentially within a 1 meter cube. The cavity receiver and other system components could very likely be stowed within the central empty space and be supported off of the mounting ring.

Stowage in a smaller cylindrical diameter can be achieved in two ways. The stacking ring can be made smaller in diameter and the panel tips would be within a diameter of about 34 inches instead of 37.8 inches as shown. The stowed volume length would not change significantly. An envelope cylinder of 24 inches diameter is a lower practical limit. In this case the number of panels would increase from 16 to 24 where the outer edge length would be reduced enough to fit. Also the inside diameter of the panels would be reduced to about 20 inches. The panel length would then be increased as would the envelope length by about 4 inches.

#### 3.1.4 Concentrator Assembly Drawing

The design study layout drawing was used as a basis for preparing the concentrator assembly drawing number 9001250 which is included in reduced size format as Appendix E. Detail parts are identified by dash number to this drawing number and are compiled in a parts list on the drawing.

#### 3.1.5 Panel Detail Drawing

The panel is the most significant component of the concentrator and was therefore detailed as drawing number 9001250-1 and is included in Appendix (F).

The panel is an adhesive bonded aluminum honeycomb sandwich construction that is heat cured while vacuum bagged against a precision tool. Other components are part of the bonded assembly as shown and include hinges, positioner, foam edges, locks and stiffeners. The panel radial edges have a 30 degree bevel profile which is necessary to allow the panels to be stowed without interference. The honeycomb cross section includes:

1. Front face at .012 inch thick.
2. Back face at .003 inch thick.
3. Honeycomb core at .250 inch thickness with hexagonal cells .250 across and made of .001 inch foil.  
(The core cells are adhesive bonded together)

The front face is spray coated with a .001 to .002 inch thick leveling layer in order to achieve a mirror-like finish. The leveling layer is then overcoated with 1000 - 1500 angstroms of aluminum to increase reflectance to solar energy and then with 1400 - 1800 angstroms of silicon oxide to protect it against terrestrial handling and orbital environmental effects.

### 3.1.6 Deployment Actuation

Figure 9 shows the spring actuator that accelerates the panel to the deployed position (photographic clarification is shown in Appendix C, pages 19 and 20). The right view shows the panel in the stowed position. The spring is extended and applies a torque around the hinge pin. The spring is fixed to the mounting bracket at the lower end and is attached to the panel hinge at the upper end via a thin flexible metal strip. When the panel is released for deployment, the spring accelerates the panel by continuously applying a torque on the 0.400 inch radius cylindrical surface. As the panel rotates about the hinge pin, the flexible strip rolls off of the cylindrical surface.

The left view shows the deployed panel where spring tension is zero. Therefore the applied deployment torque decreases linearly from maximum to zero as the panel moves from stowed to deployed positions.

### 3.1.7 Shape Control

The highest concentrator efficiency for adhesive bonded aluminum concentrators was achieved on a fixed dish assembly made as a continuous shell paraboloid reinforced at the outer diameter (Ref.4). High concentrating efficiency at concentration ratios up to 10,000:1 are achievable as discussed in Section 3.1.11.

The need to partition the concentrator for stowing in a launch vehicle reduces the achievable concentration ratio because of surface deviations not encountered with the fixed dish design. These additional errors are a result of 1). assembling the panels to the mounting ring 2). deployment on orbit and 3). thermoelastic distortion due to the orbital environment. The two meter design incorporates three features to minimize these errors as follows.

First the panels would be assembled to the mounting ring by use of the jig shown in Figure 10. The fabrication tool is placed on the bench-in fixture as shown. The mounting ring is attached to the rotating index plate and can be indexed for each of the 16 panels via an index pin. A panel is placed on the surface of the fabrication tool and the radial edge is located a distance "E" of 0.625 inch away from the tool groove at the inside and outside corners as shown. Then the hinges are shimmed and fastened to the mounting ring. This first panel is left in place during assembly of the next panel so that the .040 inch gap along the radial edge can be adjusted as shown. The panels are adjusted in pairs until all 16 have been completed. The panels can be removed, after the

hinges are fastened, by removing the hinge pins only.

The hinge pieces themselves remain assembled to the mounting ring once they are shimmed and fastened, and panel alignment is not lost.

The second feature to minimize surface deviations is associated with the positioner arm shown in Figure 11. The arm is used to control panel tip location and also locks the panel to prevent rebound away from the deployed position. The left view shows the panel stowed. As the panel deploys and nears the deployed position, center view, the tip of the arm contacts the leaf spring and deflects it downward. The spring has a rectangular hole in the end, and when the arm contacts the button stop, the hole is in position so that the spring snaps back and locks the arm in place. The design has been proven (Ref.7) and allowed repeated deployments where the panel tip was within plus or minus .002 inch of the initially adjusted position. The leaf spring wedges firmly against the positioner arm ramp surface and results in a zero backlash locked condition.

After the panels are all assembled as in Figure 10, they are then individually reassembled on the positioner jig shown in Figure 12. The fabrication tool has been removed from the bench-in fixture and replaced by the two proximity transducer assemblies shown. The one at the inside edge provides a reference measurement of the panel inside surface only (remember that this surface position was controlled on the assembly jig). However the transducer at the outer edge is used to adjust the deployed tip position. Notice that the positioner jig is placed edgewise on a table so that the Earth's 1g field acts on the stiffest section of the panel. This minimizes the effect of 1g panel deflection while positioning the tip. The gaps at the inside and outer edges ( ID and OD) can then be made equal by adjusting the tip position. This adjustment is achieved by moving the wedge piece shown in Figure 11. The wedge piece has a very slight .0002 inch-per-inch taper and therefore allows precise positioning at the panel tip. The ratio of panel length to positioner arm length is 13:1. In order to move the tip .001 the wedge must be adjusted by  $1/13 \times .001$  or .00008 inch. While this precision might seem difficult it was easily achieved (Ref.7).

### 3.1.8 Reflective Surface

The reflective front face of the panel is an aluminum foil that is as-received with a "nameplate" finish which has a high degree of specular finish. But it is not in the category of a mirror-like finish. In addition, the reflective surface takes on a fine graininess as a result of the stretch forming process. This face therefore has a significant diffuse scattering component after the panel is stretched. A leveling layer must then be applied to achieve the required specular finish. Three formulations were evaluated and will be discussed in Section 3.3.7. These formulations must withstand the low earth orbital environment, in particular atomic oxygen impact.

The leveling layer must then be coated with aluminum to raise the solar spectrum reflectance to 0.92 as a freshly deposited layer. This coating is susceptible to oxidation and handling and must be immediately overcoated with a silicon oxide protective layer. Both layers are applied by a vacuum evaporation process during the same pump down cycle. The silicon oxide reduces the solar reflectance, and a minimum of 0.88 is considered achievable.

### 3.1.9 Thermoelastic Properties

The concentrator shape on-orbit can be affected significantly by its thermoelastic properties. The primary means of heat transfer into and out of the concentrator structure is by thermal radiation. The design minimizes conductive transfer from the concentrator mounting ring to the vehicle mount points. The ideal of an isothermal condition in all orbital locations is prevented by the cyclic sun-to-shade movement into and out of the Earth's shadow and also from the variation of Earth albedo and thermal radiation incident on the concentrator as its attitude varies with respect to the Earth. A typical temperature profile is shown in Figure 13 where the reflective structure has the radiation properties noted.

The full-on to full-off solar input results in an overall variation between zero and 150 degrees F. There will also be smaller gradients under 5 degrees F from front face to back face because of structural thermal properties. These gradients cause surface deviations that affect concentration efficiency, and their magnitudes are discussed in Section 3.1.11. The front-to-back gradient is what forces the requirement of inter panel locks along the radial edges in order to stiffen the structure. Design considerations also dictate that the highest operational temperature of the structure should be below the glass transition temperature of the adhesive material.

### 3.1.10 Concentrator Efficiency

The concentrator efficiency factor is simply the ratio of solar energy reflected and concentrated through the receiver aperture to the solar energy that the concentrator structure intercepts. This factor is less than 1.0 and can be between 0.8 and 0.9 depending on the following:

1. Geometry of the paraboloid (Rim angle).
2. Area concentration ratio (Area of intercepted solar flux divided by the receiver aperture area).
3. Reflectance of solar energy by the concentrator surface.
4. Specular nature of the reflecting surface.
5. Deviation of the structure from a theoretical paraboloidal surface due to fabrication errors and thermoelastic deformation.
6. Shadow factors due to structures in front of the concentrator or between the concentrator and receiver.
7. Misorientation of the focal axis while pointing at the sun.
8. Surface degradation during mission lifetime.

All of these effects are expressed in the following equation:

$$\eta_c = \eta_1 \eta_2 \eta_3 \eta_4 \eta_5 \eta_6 \eta_7 \eta_8 = \text{EFFICIENCY FACTOR}$$

While the equation is simple, the determination of the surface deviation factor (number 5 above), is particularly difficult. As will be discussed next, there are nine sources of surface deviations associated with the petaline concept. Combining all of these surface effects into a ray trace analysis to determine is an enormous computational task. In addition the statistical distribution of these various deviations do not always follow a normal Gaussian curve. The characteristics of these deviations are only estimates until prototype hardware is built and evaluated. However, the results of previous hardware projects (Refs. 3, 4, 5, 6 and 7) and those obtained by fabricating panels for the two meter concentrator provide considerable data toward defining achievable concentrator efficiencies. Since this data is so important to the prediction of efficiency, selected portions of some previous reports are reproduced in Appendixes A, B and C.

### 3.1.11 Budget of Surface Deviations

The various deviations from a true paraboloid are usually considered individually. When this is done the deviation may not seem large relative to the design requirement of a 2000:1 concentration ratio. But when considered together these small deviations add up to produce a significant effect on concentrator efficiency. It is therefore necessary to establish a realistic budget of deviations to determine whether or not a given method of concentrator construction will meet the design requirement. This section attends to these allotments and particularly to the data that is known. The sources of surface deviations are shown in Figures 14.1 through 14.9 and are listed as follows:

1. Surface specularity.
2. Honeycomb print through.
3. Edge construction.
4. Cure tool deviations.
5. Panel replication of the tool during cure.
6. Panel assembly to mounting ring.
7. Panel deployment and position control.
8. Thermoelastic distortion on-orbit.
9. Surface degradation on-orbit.

Figure 15 defines the specified error budget for the two meter concentrator. It is a frequency distribution curve with a normal Gaussian shape and a one sigma value of one milliradian. If the combined deviations displayed this pattern while in orbit, then about 68% of all errors would occur between plus or minus one sigma and about 99% would occur between plus or minus three sigma. However, the various deviations do not always exhibit a normal curve shape, and the net effect is a curve different from normal [Appendix B, page 11]. The sources of deviations in Figure 14 for the two meter unit will now be described.

Surface specularity (Figure 14.1) is difficult to quantify because it involves tiny defects not easily measured. It is qualitatively the deviation from a "mirror-like surface". Telescope mirrors represent the ultimate "figure of merit", but fortunately concentrators for solar dynamic power systems do not require diffraction limited optics. Specularity is usually treated as an angular reflectance factor but this makes it difficult to correlate specularity with concentration ratio. Specularity is related to finish, scratches, orange peel and particles on or in the leveling

layer. These defects are hard to quantify and visual standards become important. Experience on the 5 foot fixed dish concentrator (Ref.4) indicates that the specular loss is small as will be discussed later.

Honeycomb print through (Figure 14.2) is a surface deviation that is characteristic of the sandwich structure design. In order to keep weight low, the reflective skin must be thin. Because of the shrinkage and thermal properties of the adhesive, the front face tends to dimple inward at each cell causing an imprint pattern of the honeycomb core. These surface profiles do not result in normal distribution curves. Dimpling is changed by varying face thickness, adhesive properties and fillet size. The degree of adherence to the front face is also important. A considerable amount of effort on the two meter project was put into controlling print through and will be discussed in Section 3.2.1.

Edge distortion (Figure 14.3) occurs in these light weight structures where cross sections change; along lap strip joints on shell designs (Ref.4) and along edges in petaline designs. The petaline edge construction changes shape (tapered) and material (foam) for two reasons. The taper avoids inter panel interference during stowage. It also provides close-out of the edge to avoid handling damage and peel-back of the faces away from the core. Open edged honeycomb sandwich panels would not survive without extreme care. The edge distortion related to the two meter panel is associated with adhesive properties similar to honeycomb print through cases.

The panels are fabricated by using a precision machined tool (Figure 14.4). The faces are first stretch formed over the tool, and then the same tool is used to vacuum bag and heat cure the adhesive bonded panel assembly. Machining the tool on a 3 axis CNC milling machine resulted in a paraboloidal shape satisfactory for the two meter requirements. Surface slope errors were the most critical to control.

The fabricated panel will replicate the tool surface to a degree depending on the construction materials of the tool and panel and on the fabrication process, especially cure temperature conditions. The main problem to avoid is spring back, the tendency for a panel to have less curvature than the tool (Figure 14.5). A panel placed on the tool at mid point would have gaps along the four corners. Important considerations that help avoid replication errors are 1). that the tool has the same coefficient of expansion as the panel, 2). the panel materials do not resist conformance to the tool and 3). the heat cure cycle does not place significant temperature gradients over the panel surface, especially from front to back face. The mounting ring provides structural support for



the panels but is also the attachment point where assembly deviations can occur. These deviations (Figure 14.6) are controlled by use of the assembly jig in Figure 10. The panel fabrication tool is a major component of the jig. Final assembly precision at the inside diameter and of the radial gaps between panels is achieved during this procedure.

The panel tip position (Figure 14.7) can not be precisely adjusted on the assembly jig. It is necessary to place the assembled panel edge-on-its-side as in Figure 12 so that one g deflection of the tip is minimized during tip position adjustment. The assembly jig is changed into the positioning jig by replacing the tool with two proximity transducers as shown. The wedge on the positioner arm can then be adjusted until the tip is within limits as measured by the outer transducer.

When the concentrator is deployed on-orbit, two other surface deviations are encountered; thermoelastic distortion [Figure 14.8] due to the space thermal environment and surface degradation [Figure 14.9] due to micrometeoroid or high energy particle impact during operational life. Thermal distortion depends on the incident radiation and the internally conductive properties of the panels. Atomic oxygen attack can be extensive if the protective layer is porous wherein the leveling layer can be heavily undercut.

The questions now are 1). what budget should be allocated for the various sources of deviations and 2). how well are they known at this time? To get answers it is necessary to review previous programs and also the results of the two meter project.

Before listing these results, it will be helpful to review the five generic types of deviations [Figure 16] that cause the concentrator reflected rays to miss the focal point:

1. Non parallelism of the incoming rays because of the finite size (32 arc minutes) of the solar disc, Figure 16.1.
2. Rotational (slope) errors that deviate from a true paraboloid, Figure 16.2.
3. Translational (displacement) errors that deviate from true paraboloid, Figure 16.3.
4. Misorientation of the concentrator optic axis while tracking on the center of the solar disc, Figure 16.4.
5. Scale change (shape) of the true paraboloid due to sun-to-shade temperature level cycling, Figure 16.5.

These deviations add up in countless ways to produce a characteristic flux profile in the focal plane. The profile shape depends on the frequency distribution curves for the deviation sources described in Figure 14. The difficulty in assessing the

concentration efficiency of a given fabrication method is in knowing the actual distribution curves for the various deviations. The following discussion quantifies these deviations based on previous work (Refs. 3, 4, and 7) and the present two meter concentrator project.

Generally speaking the maximum values of the deviation types are easier to determine than their distribution curves. However, as will be shown, the latter have a very significant effect on concentration efficiency. It is natural to speculate that the distribution curves will follow the normal curve shape that is often encountered in the physical world. Work to date shows this does not occur in all cases. It is important to note that there are fewer deviation sources related to fixed dish concentrators than with the petaline. Therefore the concentration efficiency for a petaline design is lower than for fixed dishes, for a given concentration ratio. The efficiency versus concentration ratio curve for fixed dishes made of adhesive bonded aluminum thus becomes the limit for the petaline designs. The deviation sources shown in Figures 14.6 through 14.8 are those found on petaline but not fixed dish concentrators. All of the concentrator hardware inspected and tested to date and discussed in this section were made of adhesive bonded aluminum. The 5 foot diameter fixed dish (Ref. 4) will be discussed first because it achieved remarkable efficiency values even to a 10,000:1 concentration ratio.

Appendix A is a selection of 5 foot concentrator information taken from several sources (Refs. 4, 8 and 9). This unit was composed of a .016 inch thick membrane paraboloidal shell with a toroidal stiffener ring attached at the outside diameter via a cylindrical skirt; Appendix A, pages 13 and 25. The concentrator was inspected by the projected grid method and surface deviation distribution curves are shown in Appendix A, pages 7 and 8. They are very close to normal Gaussian shape as shown. These curves represent about 94% of the concentrator area. The distribution curves have one sigma standard deviations of 0.46 and 0.60 milliradian. Larger surface deviations existed on the remaining 6% of area located at the eight radial seams and where the skirt attached to the shell outer diameter. Based on the calorimetric tests during solar tracking, these deviations were probably less than 3 milliradians.

The five foot dish was evaluated at NASA Langley Research Center (Refs. 8 and 9) by a ray trace procedure and also by solar calorimeter tests; Appendix A, page 14. This data is reproduced in Figure 17 to show concentrator efficiency versus concentration ratio for the three models I, II and III, that were delivered sequentially. The efficiency for model III measured 0.84 at a 10,000:1 ratio and 0.90 at a 2000:1 ratio. The calorimetric efficiency includes the reflectance factor while the geometric

efficiency does not; Appendix A, pages 14 and 15. These efficiencies were measured at zero misorientation and without thermoelastic distortions that could occur on-orbit. However the data show that fabrication deviations were held to low values. Petaline concentrators, like the two meter unit, can therefore use the fixed dish results as a performance benchmark. The objective in a petaline design is therefore to minimize deviations defined in Figures 14.6 and 14.7 that are not associated with the fixed dish and in Figure 14.8 which can be more pronounced in the multipiece petaline structure.

Information regarding petaline surface deviations is available (Refs. 3 and 7). The Sunflower report (Ref. 3) includes an extensive analysis of surface deviations; how they affect the focal plane flux profile and ultimately how efficiency versus concentration ratio is affected. Appendix B is a selection of information from that project report. Pages 6, 8 and 9 illustrate the analytical results. Page 6 shows five cases of widely different distribution curves and also case 6, which represents the combined distribution curve determined for the various sources of Sunflower surface deviations. It is significant that, except for case 3, the other four distribution curves were encountered. Case 4 is the normal Gaussian curve. Case 5 exists because of solar limb darkening. Cases 1 and 2 were found in honeycomb print through profile measurements; pages 10 and 20.

If each case is considered individually, the focal plane flux profiles vary drastically; Appendix B, page 8. The Sunflower analysis will be used later to predict the two meter performance. An important point to note is that the Sunflower analysis shows that the distribution of combined deviations, case 6, resembles a normal curve more than the other cases but does have a binodal shape to it. Therefore the receiver aperture can be smaller for a given concentration efficiency than it would be if the other distribution curves of cases 1, 2, 3 and 5 predominated. However these other cases do influence the case 6 Sunflower distribution curve by imposing the binodal shape onto the curve.

It is now appropriate to consider the types of deviations shown in Figure 16 as related to the two meter design. This is graphically presented with the help of CAD. Anticipated values based on available data were used in the ray traces in Figure 18. Focal point misses are shown. Two deviations cause the largest misses; those due to 1.) non parallel rays coming from the solar disc and 2.) the 3 milliradian slope error. The other three deviation types cause second order misses. The 1.68 inch receiver aperture is superposed on the ray traces in order to relate the magnitude of misses. If all five types are combined, the worst case miss is shown at 1.061 inch. This exceeds the 0.84 inch aperture radius.

The maximum ray deviation misses the aperture significantly. How badly does it affect concentration efficiency? This can be approximated by relating the combined miss above with the Sunflower results on page 9 Appendix B. Figure 19 is a copy and the two meter concentrator should be geometrically 98% efficient with reasonable probability. This indicates that if the surface deviations can be held to the maximums traced in Figure 18 and have the distribution curve predicted in the Sunflower analysis, then this geometric efficiency value can be achieved.

Based on the discussion to this point and inspection results on measured hardware, a surface deviation budget was established for the two meter concentrator sources of deviation. The budget is tabulated in Figure 20. Deviations are defined both by maximum values and by their distribution curves. The reference sources that allow the budgeting are also listed. Note that specular and on-orbit degradation are defined as degradation factors because of their complex geometric character.

### 3.2 PANEL CROSS SECTION ANALYSIS

The panel cross section must be capable of two things: 1) provide a light weight structure to efficiently reflect and focus the intercepted solar flux through the cavity receiver aperture, and 2) provide a structural capability of surviving launch, deployment and life on-orbit. The aluminum honeycomb sandwich construction can be optimized to meet these requirements, and a significant amount of work was done to analyze such factors as 1) core print thru on the reflective front face, 2) panel edge close-out integrity, and 3) thermoelastic properties.

#### 3.2.1 Core Print Thru Evaluation

Because of the stringent weight limits for space application hardware, the aluminum foils used in constructing the honeycomb sandwich cross section must be as thin as possible, Figure 21. Front face foils in the range of .003 to .016 inch thickness have been considered in previous work (Refs. 3,4,5,6,7) and during this 2 meter project. As discussed in Section 3.1.11 there are deviations from a true paraboloid due to honeycomb core print thru and also to panel edge construction. Both of these aspects were evaluated analytically and by fabricating many specimens with various cross sections and adhesive bonding procedures.

There are five factors which influence core print thru onto the front face foil:

1. Face foil thickness
2. Honeycomb core hex size
3. Adhesive formulation and properties
4. Adhesive fillet size
5. Process variables

Figure 22 shows the chronological sequence of specimens fabricated to evaluate core print thru and edge distortion. Unexpected results often required process changes and in some cases repeating a series of specimens. Nearly sixty specimens were made.

Figure 23 shows a cross section of the vacuum bag enclosure used for curing the adhesive. The fabrication is based on the commonly used aerospace technique whereby the metal and adhesive construction materials are held in intimate contact with a heated tool by a vacuum bag procedure. A full vacuum is maintained between front face and tool surface, while a reduced vacuum (for reasons to be discussed) is applied on the back face and core.

Selection of an adhesive was not part of the project work statement. Because of the special adhesive properties required, it is not easy to select candidate adhesives and can be a very time consuming task. The equipment at CSU/AMC was designed to allow vacuum bag processing at cure temperatures up to 375 degrees F. The properties of an ideal adhesive candidate are listed:

1. Zero cure shrinkage or expansion.
2. Coefficient of thermal expansion same as aluminum alloy.
3. Heat transfer coefficient similar to aluminum.
4. Glass transition temperature greater than 300 degrees F.
5. Toughness to maintain strength properties to -100 degree F.
6. Viscosity low enough to allow dip method of applying adhesive to core faces.
7. Adhesive and cohesive strength so that the aluminum core will fail before the adhesive bond fails when tensile tested.
8. Capable of withstanding vacuum, radiation and charged particle conditions in low earth orbit.

The first three properties are the most difficult to achieve, and to date have not been achieved. Two suppliers were provided by NASA and a third supplier was found by CSU/AMC. A discussion of Figure 22 now follows.

Specimens 1 through 5 were made with a regular "hardware store" epoxy adhesive to develop cleaning and lay-up procedures. Thereafter specimen fabrication proceeded on a one variable change per specimen basis. Specimens 6 through 23 were made to sort the five selected adhesives down to the best one for further evaluation. Various face thicknesses were also used in order to determine the optimum face thickness. Based on visual and profilometer measurements, the Advanced Polymer Sciences Resin X115(216), catalyst 245M91 adhesive was found slightly better than the Crest Products Corporation 471 and both were noticeably better than the three Theramic Engineering 250, 600 and 650 adhesives.

Unfortunately the face thickness evaluation had to be repeated because the back face 1.5 psig vacuum was too high and a core "bite thru" on the front face could be seen. Bite thru results because the face foil was thin enough so that the core begins to indent into it as a result of the bag pressure against the honeycomb core and onto the front face.

Specimens 24 through 30 were repeated with the APS and Crest 471 adhesives with a back face vacuum reduced to 0.25 psig. The "bite thru" was eliminated and profilometer measurements were performed on a NASA Sloan "Dektak II" machine. This machine is capable of measuring surface profile (and finish) in the Angstrom range and is very adequate for evaluating the very small surface slope errors caused by honeycomb print thru.

Figures 24, 25, 26 show three representative profile charts and the method of measuring surface slope errors for a given trace. Figure 24 is one scan taken on specimen 28, which has a .005 inch thick face foil, and the repetitive cyclic dimpling pattern due to core print thru is readily seen. The maximum angular slope error on the second cell from the left is 1.9 milliradians. Notice that the peaks of the four cells shown are not in a horizontal line, and the fifth peak is higher than the fourth by .000057 inch. This random peak-to-peak characteristic was noted in all of the initial specimens made. At first the random errors, which can be seen with the naked eye, was attributed to nonflatness of the aluminum plate used for specimen lay-ups. A steel plate with a special lapped surface was made and used for specimens 24 through 30, and the random error persisted as can be seen on these three figures. This type of error was evaluated further and is discussed later regarding specimens 41, 42 and 52.

It should be noted that maximum slope errors were determined for these profilometer measurements, and all other errors associated with a given profile scan vary from zero up to the maximum value. The depth of print thru dimpling is very slight at .000065 inch for Figure 25. However the slope errors are significant when related

to the design specification of 3 milliradians maximum. They are 1.9, 1.6, and 1.0 milliradians for the three figures.

Based on the deviation analysis of specimens 19 through 30, the APS epoxy adhesive was selected as having slightly less print thru than the Crest 471 epoxy adhesive. Visual inspection also showed slightly more print thru for the Crest 471.

Surface slope errors discussed up to this point have been maximum values for a given profile trace. Distribution curves for various surface deviation sources were discussed in Section 3.1.11, and it was noted that honeycomb print thru does not result in a normal distribution curve (Case 4, Figure 19) but is more like a  $\pi$  or a  $2\pi$  distribution (Cases 1 and 2). As Figure 19 shows these latter two cases can reduce concentrator geometric efficiency compared with the normal distribution case. The  $\pi$  case reduces efficiency more than the  $2\pi$  case. It is also apparent that the print thru on Figures 24, 25, and 26 tend toward the  $\pi$  case more than the  $2\pi$  case.

Figure 27A shows a smooth curve trace made thru the profile of Figure 25. Note that the peaks tend to be sharp and the valleys more rounded. The lower two curves Figures 27B and 27C approximate the  $\pi$  and  $2\pi$  cases as superposed on the Figure 25 profile. The similarity of the Figure 25 profile with the  $\pi$  case is apparent. Figure 28 compares the  $\pi$  and  $2\pi$  cases for the same dimpling depth and it shows that  $\theta_{\max}$  equals  $\theta_{\max}$  for both cases, but the  $\theta_{\max}$  slope error at radius R2 exists on an annular area twice as large as for the  $\theta_{\max}$  slope error at radius R1. The distribution curves for the normal  $\pi$  and  $2\pi$  cases are shown on Figure 29. The heavy bias of the  $\pi$  case toward  $\theta_{\max}$  explains why that case degrades concentration efficiency as much as it does in Figure 19.

Specimens thru number 30 were made with 3/16 honeycomb core, and Specimens 32, 33 and 34 were made with 3/8 hex, 1/4 hex and flexcore, respectively. This allowed evaluation of surface slope error versus cell hex size, Figure 30. The flexcore data is not presented because the surface slope errors were generally larger than the 3/8 hex core shown. It is noted again that the slope errors presented are the maximum values for each cell dimple profile evaluated. The max slope errors for the cell profiles evaluated vary considerably for the 3/8 hex, less so for the 1/4 hex and not much at all for the 3/16 hex. The curve was drawn thru the average max slope error values for each core size. The 3/8 hex size shows slope errors of between 0.5 to 1.6 milliradian, and the 1/4 hex size shows about 0.2 to 0.75 milliradian. These values are well above the allotted 0.3 milliradian maximum shown in Figure 20, while the 3/16 hex size shows max slope errors well within this maximum value.

Specimens 24-28 were made with 3/16 hex core but with face foil thickness as a variable (.003, .005, .008 and .012 inch). A second variable was aluminum alloy hardness. The 1145-0 condition is soft and 1145-H19 full hard. Figure 31 shows slope error versus face thickness and clearly shows that thicknesses below .008 inch result in large deviations. The .003 and .005 face thicknesses resulted in slope errors well above the 0.3 milliradian allotted. The hard aluminum alloy showed lower slope errors than the soft alloy. The hard alloy met the 0.3 maximum error at .008 face thickness while the soft alloy did not.

This difference was unexpected since the modulus of elasticity for both alloys is the same. The only explanation seems to be that the stress applied to the face foil directly beneath the adhesive fillet exceeds the 4000 psi yield strength of the 1145-0 but not the 26,000 psi of the 1145-H19. Thus the soft alloy has been strained into the plastic deformation region while the hard alloy has not. The aspect of selecting the aluminum alloy hardness will be discussed in Section 3.3.2.

Specimen 35 was prepared with a .002 inch thick layer of liquid adhesive over the entire front face sheet. This was done to simulate use of a .002 inch thick film adhesive in place of dipping the core into a .010 thick layer of adhesive as was done on all later specimens; and all 9 panels that were later fabricated. Use of a film adhesive would make panel lay-up a much easier task, but specimen 35 surface slope errors were significantly greater than specimen 26 which had the core dipped in .015 adhesive.

Specimens 36, 37 and 38 were processed with .015 fillet APS adhesive, .010 fillet APS and .010 fillet Crest 958 adhesive respectively. All had .008 (H19) alloy. The reduced size fillet was expected to reduce core print thru. Visual inspection showed little core print thru, and all three had no significant difference. However, the .010 fillet size was selected for panel fabrication because of the reduction in weight.

Specimen 39, 40 and 43 were fabricated to evaluate edge close out design as regards print thru distortion on the front face. Results will be discussed in Section 3.2.2.

Specimens 41, 42 and 52 were fabricated to evaluate techniques for reducing the random surface deviations mentioned previously. The honeycomb core is fly cut (Section 3.3.3) while in the HOBE form. It is speculated that when the HOBE is expanded into the honeycomb blanket, the nodes where cells have common sides are no longer perfectly planar. When the core becomes integral with the panel sandwich construction, this nonplanar condition could result in the random deviations noted. (Remember that peak-to-peak deviations are



very small, e.g. the .000057 inch noted on Figure 24, this is only 57 microinches).

Specimens 41 and 42 were bonded with a honeycomb core that was fly cut in the expanded condition. The core had to be stabilized by filling the cells over the top with a melt out wax (Rigidax) that is used for such purposes. Otherwise the .001 inch thick cell walls would collapse or tear badly from the intermittent fly cutting action. Two Rigidax waxes were tried.

Specimen 52 was bonded with a honeycomb core that had rows of saw cuts made on the back face side of the honeycomb. The intent was to reduce the "springback" of the core and force it to comply more readily to a planar condition on the front face nodes. Unfortunately this weakens the core and reduces the "web" strength of the sandwich construction. None of these specimens showed a reduction of the random deviations, and therefore the cause for the deviations is not clear. However, the combination of core print thru, random deviations and tool replication errors are within the allotted deviations for sources 2, 4 and 5 shown in Figure 20. This was determined by the panel optical inspection discussed in Section 3.4.2.

Specimens 50, 51 and 53 were fabricated in an attempt to further reduce core print thru. It was noticed that the adhesive fillet on the front face of previous specimens was usually larger than on the back face because some adhesive from the back face wicked by gravity action to the front face. Two process changes were tried to reduce the front face fillet size. Specimen 50 was cured with an adhesive fillet applied to the back face of the core only. The desired result would be a wicking to the front face but of reduced fillet size. This resulted in no wicking whatsoever and therefore no front face bond at all.

Specimen 51 was cured with the usual adhesive fillet on front and back faces of the core but with the tool upside down. In this orientation the front face adhesive tended to wick toward the back face and did result in a fillet size reduction. This would have required extensive additions to the full scale panel fabrication and was not implemented because of schedule/cost constraints. But the technique is recommended for further evaluation in any future process improvement work.

Specimen 53 was fabricated by a double dip method to reduce print thru effects. The procedure involved preparing a lay up, Figure 32, by applying a fillet to the front face only by placing the core on a Teflon surface and curing the adhesive. After cure, the core with the formed fillet easily separated from the Teflon. The fillet was cleaned by delicate grit blast, and the fillet then

dipped into a thin .002 inch thick layer of adhesive. A regular .010 adhesive dip was then applied to the back face. The objective was to end up with a full size fillet but with a reduced volume of adhesive in the final cure process. This would then result in reduced shrinkage of the adhesive at the front face and therefore reduced print thru. The process did not work, however, because the side movement of the core during dipping into the .002 adhesive layer could not be controlled. The applied adhesive fillet was larger than desired and resulted in more print thru.

Specimens 44 through 49 were prepared as a special series of tests as an evaluation of various aluminum surface preparation procedures before adhesive bonding. Samples of aluminum sandwich construction were being prepared for thermal gradient and thermal distortion testing at NASA Lewis, and one sample debonded badly. This of course signalled a breakdown in the aluminum clean and etch pretreatment process and must be guarded against by consistent in-process controls. A failure analysis indicated two possible causes, but at the same time, a thorough review of the clean and etch process was made. The results are discussed here. A large benefit resulting from this review because the latest improvements in adhesive bonding technology were uncovered.

The failure analysis revealed two possible causes 1) a can of "clean air" was used to speed up the drying of the larger than usual thermal distortion sample or 2) there was incomplete removal of the chemical paste used to clean and etch the aluminum prior to bonding. The latter is the most likely cause. As a result no "clean air" is permitted, and the rinsing procedures have been improved.

Figures 33 through 37 show the various surface preparation processes evaluated. Figure 33 is the classical sulfuric acid/sodium dichromate process used in the 1960's by the aerospace industry to prepare aluminum surfaces for adhesive bonding. It was this process that was used in fabricating panels for the 9.5 foot diameter antenna (Ref. 7). However it required a series of tank baths and spray rinses which involved hot and reactive chemicals (See page 6 in Appendix C). Two reasons prevented use of a similar facility at AMC. The cost to install the facility was not justified for making a limited number of panels, and the AMC building is not able to house the chemicals and treat the wastes from such a facility.

Figure 34 shows the alternate surface treatment process selected for specimen and panel fabrication on this project. It utilizes a paste type clean and etch material as a substitute for the liquid alkaline rinse and liquid acid/dichromate dips in Figure 33. It is this process that was changed as a result of the failure analysis.

Two techniques have been developed by the industry as improvements over those in Figures 33 and 34. Boeing Aircraft developed a phosphoric acid anodize step (Refs. 11-15), and was tried by adding it to the Figure 33 process as shown in Figure 35. The 3M Company also developed the use of Scotch Brite abrasion of the surface prior to anodization (Ref. 16) as in Figure 36. The final process selected for panel fabrication is shown in Figure 37, and its choice is now discussed by describing the specimens evaluated.

Specimen 44 (2 each 4" X 4") was prepared by adding the Scotch Brite abrasion step. These specimens were "finger peel" tested to gain confidence that good adhesion was once again attained. The results were positive. The next step was to prepare specimens 45, 47, 48 and 49 for tensile and shear testing and specimen 46 for retrieval at NASA Lewis. Figure 38 shows the types of specimens prepared and the clean and etch procedures used prior to adhesive bonding.

Figure 39 shows the lap shear test configuration per ASTM standard. The 1/16 inch stock was cleaned and etched prior to bonding as noted in Figure 38. Five specimens were made and tested for specimen lay ups, 47, 48 and 49; and the lap shear strengths are shown in Figure 40. Specimen 47 with Scotch Brite abrasion showed slightly better strength than specimen 48 with Scotch Brite abrasion plus phosphoric acid anodize. But 47 and 48 showed significantly higher strengths than the "standard" clean and etch procedure for specimen 49. The lap shear specimens failed as illustrated in Figure 39. The 1/16 pieces of stock show about 1/16 inch deformation, as shown, because the test jaws apply a slightly eccentric load into the bonded joint.

Figure 41 shows the honeycomb sandwich tensile test configuration. The faces of the 1.40 inch square specimens were adhesive bonded to the aluminum test adapters with a standard "tough" hardware store adhesive. Since the bond area between the specimen and adapters was much larger than the bond area between sandwich faces and the honeycomb fillets, the failure must occur in the honeycomb fillets. Five 1.40 inch square sandwich pieces per specimen lay up were tested, and tensile load strengths are shown in Figure 42. Scotch Brite abraded specimens showed a higher average bond capacity of 164 pounds. The Scotch Brite abraded plus phosphoric acid anodized specimens had a lower average at 135 pounds and a wider spread between high/low readings. The "standard" process specimens without abrasion or anodize had an average load capacity of 84 pounds, well below the other two. The clean and etch process selected for panel fabrication was therefore chosen to have Scotch Brite abrasion added. It had been anticipated that the phosphoric acid anodize would show higher load capacity than abrasion alone, but it did not consistently do that.

Specimen layup 46 (3 each 4 X 4) was used to run a repeat vacuum pump down cycle at NASA Lewis. These pieces did not exhibit any debonding as was experienced with the thermal distortion specimen that prompted this failure analysis.

Specimens 56 and 57 were special cases. The 4 inch square honeycomb sandwich pieces were cured on the panel stretch forming tool using stretched aluminum face foils. The pieces were then coated with EP-3 leveling layer epoxy. Profilometer readings were made before and after leveling layer application, and Figure 43 shows an example of the change in surface specularity. Figure 43A has a ragged profile that represents the as-received surface finish on the front face foil. Figure 43B shows the mirror-like finish that results and demonstrates that the leveling layer does mask out the undesirable surface roughness. The curvature of the traces occurs because the specimens have the shape of the paraboloidal curing tool. The various profiles made after leveling layer application suggest that the layer tends to "bridge" the random surface deviations discussed previously. But the work to demonstrate this would entail significant effort and was not done.

### 3.2.2 Edge Design

The radial and ID/OD edges received significant design and fabrication attention. There are two requirements for the edges 1.) that the construction not impose excessive surface deviations on the reflective front face and 2.) that the honeycomb sandwich not be exposed to excessive peel forces. Sandwich construction parts are susceptible to peel forces such as can be experienced during handling. However, changes in cross section along edges or seam joints can cause larger than desired surface deviations (Refs. 3, 4, 9). The design study (Ref. 1) incorporated tapered foam edge pieces with a zee close out from front to back faces, Figure 44. This zee close out joins the back face to the front face via the adhesive layers shown. The lower view shows how the edge pieces are assembled for cure. The foam is an open cell material with very low density at 6 lbs/cu ft (aluminum is 173 lbs/cu ft). This construction was successfully used on the 9.5 foot antenna (Ref. 7) where a thermal paint was applied on the front face, and the print thru was tolerable for the longer specified electromagnetic wavelengths. However, the print thru is discernible with the naked eye, and for the solar spectrum becomes significant. A review of the optical inspection data showed that angular surface deviations along the edges were 2 to 5 times larger than over the honeycomb sandwich cross section areas. Deviations just over 1 milliradian were measured. While this is probably tolerable for a 2000:1 concentration ratio, a reduction would be desirable to achieve higher concentration ratios for those space applications requiring higher absorber temperatures. When hinges and lock hardware is to

be bonded integral with the panels, print thru deviations will also be of concern. The panels fabricated included dummy corners on all four corners. These showed surface deviations on the same order as along the edges. The edge integrity can possibly be achieved without the use of a zee close-out piece by 1). providing a large adhesive fillet on the honeycomb 2). using a tough adhesive or 3). applying a polymer skin or foam as shown in Figure 45. Unfortunately the first action promotes more core print thru onto the front face, and the second action requires an adhesive with a coefficient of thermal expansion much greater than desired. Fine tuning the edge design will require additional engineering and fabrication considerations.

### 3.3 PANEL FABRICATION

#### 3.3.1 Concentrator Fabrication and Assembly

Because of funding limits, the project was devoted to only establishing panel fabrication capability, which is the most difficult aspect of overall concentrator fabrication and assembly. Confidence in the other aspects of the concentrator processing is high based on the experience gained in References 3 and 7. Reference 7 is particularly important because a 9.5 foot diameter antenna was fully qualified for flight, based on extensive tests on two engineering models. This section is therefore descriptive of the entire two meter concentrator process. However, the evidence that this fabrication technology is well developed is presented in Appendix C. The photographs are clear and self-descriptive, but additional details can be provided. The overall fabrication and assembly of a two meter concentrator is very nearly described by the pictorial process flow chart at the beginning of Appendix C, (pages 3-5) but there are some technical and some practical differences between the 9.5 foot antenna and the 2 meter concentrator processes:

- \* Stretch forming. The antenna stretch forming was done in a regular room atmosphere where airborne dirt particles between tool and aluminum stock caused slight scratches that did not affect antenna performance. But the same scratch depths cause significant performance degradation for the shorter solar energy wavelengths. A special clean room had to be used for the two meter panel stretching.
- \* Aluminum stock cleaning. Fund limitations precluded use of the large, occupationally safe series of cleaning tanks used to clean the 9.5 foot diameter antenna aluminum stock. Paste type clean and etch chemicals were used successfully on the 2 meter panels, although production panels would be produced

more reliably with the tank type facility.

\* Leveling layer. The 2 meter panels require a mirror-like finish with a high reflectance of solar energy. This necessitates application of a thin leveling layer in a clean atmosphere environment with a subsequent application of aluminum by vacuum evaporation. This particular process step was the most difficult in previous work (Refs. 3, 4 and 5), but it was even more so the second time around in the two meter work. This will be discussed later in section 3.3.7.

\* The 9.5 foot antenna was assembled on a large, expensive tool to facilitate production rates. The two meter concentrator assembly procedure would utilize a less costly modification by using the stretch forming tool as a major component. Production rates would be lower, however.

A step-by-step description of the entire 2 meter concentrator fabrication and assembly procedure is shown in Figure 46. It was prepared during the two meter design study (Ref. 1) and includes all major events along the overall processing path. Inspection events, which are critical to achieving reliable hardware, are shown in "rounded corner" rectangles. The sequence which describes what was done on the two meter project follows the "Fabricate Panel" line of events. While this represents the originally planned procedure, modifications were made during the fabrication of nine panels made on this project.

Documentation was emphasized from the start of fabrication of the first panel through to the ninth. Step by step procedures were recorded and altered as the process was developed. Each panel fabrication was recorded in detail by an Engineering Note (EN), a recorded document with originals on file. EN-1020, which records the ninth panel fabrication, is shown in Appendix G. It was important to make sure that each succeeding panel was made like the last, except where process improvements were deemed appropriate.

To thoroughly document the process, video tapes and process photos were taken during the fabrication of panel nine. The video tapes have been duplicated and are available for review. Selected process photos have been included in this report as figures referred to in this discussion.

A 25 ft. X 75 ft. area at AMC was dedicated to fabrication and several views are shown in Figures 47-50. Figure 47 views the panel adhesive bonding area in the far right with accessory benches in the foreground and left. The tool heater control console, tool temperature acquisition recorder/monitor and CAD plotter are in the center. The clean room for stretch forming is in the background. Figure 48 is a view 90 degrees to the Figure 47 view showing the aforementioned items plus the stock annealing oven to the right.

Figure 49 views the rear of the stretch forming room showing the motor/pump set for hydraulic actuation of the stretch jaws and the high efficiency air filter unit that blows clean, deionized air across the tool during the stretch operation.

Figure 50 views the fabrication area with the spray booth for application of the leveling layer to the left and the vented hood for cleaning and etching the aluminum face stock to the right.

Various tools and fixtures were designed and built, but the stretch forming tool is the centerpiece, Figure 51. It is used as the central feature in the following process steps:

1. Stretch forming
2. Panel adhesive bonding
3. Panel edge trim
4. Panel assembly to mounting ring
5. Panel tip position adjustment

Figure 51 shows the tool placed in the edge trimming jig. Steps 1-3 will be described later; while steps 4 and 5 were not performed on this project, and were discussed in Section 3.1.7.

The tool has to be heated quickly to the adhesive cure temperature of 300 degrees F, and so the entire undersurface was covered with thin, strip heaters as shown in Figure 52. The tool (drawing 9001003) is made of 2024-T351 aluminum alloy that was stress relieved at 375 degrees F for 11 hours prior to finish machining. The parabaloidal surface and drill bushing positioner holes were machined on a high accuracy 3 axis Bostomatic CNC milling machine. Inspection in a high accuracy 3 axis coordinate measuring machine showed that the resulting shape was within .003 inch band of a true parabaloidal surface, well within the .010 inch total form tolerance specified. Details of the tool fabrication and inspection are discussed in Appendix I.

Panel fabrication can be divided into three basic categories:

1. Prebond Fabrication.
2. Adhesive Bonding.
3. Postbond Fabrication.

All of these steps require special and often unique techniques developed specifically for this product. The adhesive bonding steps are especially unique because they are time constrained. The panel lay up and start of temperature heat up must be completed within one continuous 8 hour sequence for two reasons. The cleaned and etched aluminum stock oxidizes rapidly and can become contaminated if allowed to be exposed beyond an 8 hour period.

Secondly, the epoxy adhesive has a 4 hour pot life which means the panel assembly must be under vacuum bag and into heat up well within the 4 hour period after parts A and B of the adhesive are mixed. The large number of pieces to be carefully adhesive coated and assembled made it a challenge during lay-up of the first several panels, but became easily achieved as experience was gained. It should be noted that when the 9.5' antenna fabrication (Appendix C) was in mature production, it took 3 assemblers one 8 hour shift to lay-up and start the heat up of 2 panels (page 15, Appendix C).

The various fabrication steps will now be discussed in the sequence in which they are done.

### 3.3.2 Forming Aluminum Faces

The front and back aluminum faces that make up the "flanges" of the honeycomb sandwich cross section are formed in the same stretch process. Figures 53-55 show several views of the stock being stretched. Figure 53 was taken before the air shroud was put in place and shows the HEPA filter and ionization bar assembled in the back wall of the clean room. The objective is to wash the two pre-cleaned sheets of stock with clean, ionized laminar flow air to keep airborne particles from being trapped between the sheets and the tool. In spite of the meticulous care taken it was very difficult to prevent some scratching to occur. It took about 4 panel fabrications before good control was achieved, and even then only one of the final 5 panels was scratch free. The number of scratches on the other 4 were very minimal (perhaps 2 to 8). These scratches are only .0001's of an inch deep but do introduce slope type defects over a small area. The integrated area of these scratches is well within 1 percent of the total panel area and could be tolerated in actual flight hardware. But the visual appearance gives a negative aspect to the panel quality. The eye is very discerning. It is proposed, however that complete scratch control can be maintained with improvements to the clean room capability and in pre-stretch inspection methods.

The pre-stretch inspection for these panels took as long as 2 hours of viewing the stock while the room was darkened. A flash light was used to shine collimated light onto the stock and tool surfaces, all while the HEPA filter washed the area clean. This is the same effect noticed in a dark room when sunlight streams through a small opening and illuminates small airborne particles quite clearly. Particles attached to the tool or stock were gently brushed with an air wand, and they were then flushed away by the laminar flow clean air. The work area was carefully enclosed by an air shroud (Figure 54) to minimize entry of particles on either side of the tool. Side seals were used but are not shown in



position. Small smoke emitter devices were used to determine that air leakage into the clean area was not occurring.

Figure 55 is a good view looking endwise at the stock fully stretched over the tool. The 4 inch diameter hydraulic cylinders on either end have adjustable flow control valves in the inlet lines. This assures a slow, even stretching on both ends to minimize tearing of the stock before it was fully formed. In addition, the tool surface was spray coated with a thin Teflon coating to prevent bare aluminum to bare aluminum contact where minute weld-and-tear points would otherwise occur.

Some process difficulties did occur when attempting to stretch aluminum stock in the half to full hard condition. This is the preferred stock condition because of the greater resistance to wrinkle or "eyebrow" damage during stock handling and cleaning. However, the half and full hard stock would always tear at one of the jaws before full stretch could be achieved. It was very nearly achieved but not quite. Several ways were proposed to avoid tearing but were dropped because they entailed significant costs, and soft or quarter hard stock was successfully stretched.

It was important to keep the stretched stock in correct position on the tool, so the sides of the two sheets were temporarily taped to the tool. The end pieces were carefully trimmed just inward from the tool ends, and then were taped down also. The tool was then taken out of the clean room for further processing.

### 3.3.3 Core Preparation

The honeycomb core which forms the "web" of the sandwich construction requires special processing. In the first place it is somewhat difficult to handle because the .250 inch wide hexagonal cells are made of .001 inch thick aluminum foil. The as-received material requires additional processing, and Figures 56-59 show several process steps. The honeycomb is received from Hexcell Corporation in the HOBE (Honeycomb Before Expansion) form. It usually is received already expanded, but for solar concentrator fabrication it is required in HOBE form as will be explained.

Figure 56 is not clear and requires explanation, with the help of Figures 59A and 59B. HOBE is simply the precursor to the hexagonal form of the honeycomb. If an already expanded honeycomb blanket is squeezed in one of its length directions (it can not be squeezed in the other direction) it collapses to what appears like a solid piece of aluminum. This is the reverse of expanding HOBE into a honeycomb blanket. In Figure 56, an as-received .250" thick HOBE slice (60" long x approximately 2" wide) is being held. When expanded, the 2" dimension enlarges to 96", and because of a

"Poisson ratio" effect, the 60" length reduces to 40". The HOBE is manufactured as shown in Figure 59A. The aluminum foil feeds as a continuous length between rollers that apply strips of adhesive on the upper and lower surfaces. Sheets are cut at the end, and after every other one is rotated end-to-end, the sheets are stacked into a HOBE block and heat cured. HOBE slices are then cut to a customer's order. The HOBE slice expansion is shown pictorially in Figure 59B. The HOBE for making core for the panels is shown on the table between the two pull bars which are used to expand the HOBE into a core blanket. The pull bars are firmly attached to the ends of the HOBE with heavy duty double backed tape, and the HOBE is stretched into the partial and eventually full length as in Figures 57 and 58. It is not an easy procedure to achieve full opening of all cells and is the reason why honeycomb is usually received expanded.

When HOBE is ordered from Hexcell, it is cut from a large HOBE block with a bandsaw, Figure 59A. This leaves a rough finish on the faces of the HOBE which is normally of no consequence in most applications. But when used with the very thin face foils on concentrator panels the finish "prints through" to the reflective side as minute surface distortions. To avoid this, the HOBE is clamped in a fixture and is cleaned up with a special cutter in a milling machine as in Figure 60.

The truncated sector shape of the panel core is achieved by use of a "razor sharp" putty knife. The core blanket is placed over a pattern of the panel core shape, and the knife blade is guillotined through the .001" thick cell walls with little resistance. As in many of the panel fabrication steps, manual technique is important and requires practice before being fully successful. It has not been mentioned before, but all of the fabrication techniques in panel fabrication have been developed in-house because the experience just does not exist in available machine shops. Not that it could not be done elsewhere. But it has been found historically that it is more cost effective to train in-house personnel. This assures product uniformity and quality simply by using a limited number of qualified assemblers who are made available as needed. This was certainly contributory to the success in fabricating 2 engineering models and 4 flight models on the 9.5' antenna program (Ref. 7).

The honeycomb used for panel fabrication has a special surface treatment on the aluminum foil. It is an adhesion promoter because bare aluminum requires carefully controlled cleaning to ensure adhesion. The core was not precleaned before adhesive application as were the face foils. It is necessary, however, to avoid excessive handling prior to bonding. This was achieved by storing expanded core blankets in a protected container and then trimming

the core the day before lay up. Tensile tests on honeycomb specimens showed repeated high bond integrity at the adhesive fillet to core interface.

#### 3.3.4 Component Fabrication

The adhesive bonded honeycomb sandwich is the basic structure of the panel, but accessory components are required as shown in the Figure 61 close up and layed out on the work area table in Figure 62. These components provide the following panel properties:

1. Edge close outs to avoid handling damage.
2. Edge stiffeners to avoid local surface deviations.
3. And dummy corners simulate the hinge pieces and tip lock components shown in drawing 9001250-1.

Triangular cross section foam pieces are used as a transition technique to bond the .003" back face to the .012" front face. An exposed view of the edge construction is shown in Figure 44. A "Zee" close-out piece is placed on the edge and laps over the back and front faces as shown. Note the intermediate stiffener piece sandwiched between the Zee close-out and front face. This makes the edges more damage resistant.

The dummy corners are made of solid aluminum, not reduced weight sections as would be used in flight hardware. The objective of the dummy pieces is to simulate flight hardware while avoiding the significant costs of machining other part features required for flight. These dummy corners allow two objectives, to:

1. Evaluate the print through deviations on the front face due to the corner transition sections.
2. And provide tapped holes (in 3 corners) to handle and mount the panel for later process and inspection steps.

There are many special pieces of equipment tools and aids required for panel fabrication. They are layed out on a table ready for lay-up as shown in Figure 63.

#### 3.3.5 Cleaning Procedure

Cleaning and etching of the front and back faces are the most important steps in providing high integrity adhesive bonds. As previously discussed, the clean and etch procedure was modified from the preferred multiple tank method because of cost and facility limitations. The standard series of tank processes used to clean and etch the face foils for the 9.5' antenna are expensive

to duplicate and difficult to be made occupationally safe in the AMC facility. For these reasons the alternate method of using etch chemicals in a paste form was selected. This choice is not the best for higher production rates but is cost effective for prototype quantities.

The vented hood shown in Figure 50 was utilized to draw off fumes to the outside. It is shown in figure 64 in an earlier configuration used for cleaning and etching parts for small samples. There are two important features. The fan exhausted hood draws off fumes to the outside, and the large containers to either side are used to capture rinse water during the procedure. These tanks were periodically taken by CSU facility personnel for proper disposal.

The delicate nature of the thin faces necessitated use of handling fixtures during clean and etch. Remember that at this point in the process, the front and back faces are taped down to the tool. It was necessary to remove the back face from the front face in order to expose the bonding surfaces to clean and etch. A back face handling fixture (upper-right of Figure 62) allows removal of the thin .003" back face from the tool and provides backing to allow the clean and etch steps. The back face is removed from the tool by placing double back tape strips on the fixture and firmly pressing the fixture against the back face and lifting it off. The front face on the tool and the back face on the fixture are now ready for clean and etch. Figures 65-68 show the front and back faces during clean and etch.

Figure 65 shows the front face on the tool to the left of the hood and the back face on the fixture to the right. Figure 66 shows a close-up of the front face ready for processing. To prevent chemical damage to the tool, side and end dams were assembled to restrict the clean and rinse fluids to the front face only. Figures 67 and 68 show the back face being cleaned and etched. Figure 67 shows rinsing, while Figure 68 shows brush application of the etching paste.

After final water rinsing of the front and back faces, it was necessary to hot air dry the surfaces before bonding. Figures 69 and 70 show this set up. The back face, still attached to the handling fixture, is suspended several inches above the front face on the tool. The hot air guns force heated air between the wet surfaces, and temperature is monitored by thermocouples for the specified length of time.

### 3.3.6 Adhesive Bonding Procedure

The adhesive bonding lay-up must proceed in a timely fashion to make sure cure temperature heat-up begins well within the adhesive pot life. Many steps are involved and require a discipline to time management. One of the difficult aspects is to make sure the various pieces are being properly located, and this requires measuring locations without contaminating the cleaned and etched surfaces. Availability of the written fabrication procedure (Appendix G) is invaluable to ensure timely process control. Lay-up always involved three people; two as assemblers and one as procedure reader and note recorder. The earlier panel fabrication involved many in-process improvements where the recorded changes were later invaluable in preparing the next process procedure document. Fewer and fewer changes were eventually made, and the last panels were nearly identically processed.

While the panel construction is basically simple, the lay-up procedure requires a meticulously uniform approach. A verbal description alone can not easily describe it. While the following figures begin to describe it, the video tapes available for review are best for documenting the process steps. Figures 71-93 show sequential photos of the lay-up and cure procedure.

Figure 71 shows the tool in position for the lay-up. It is supported on three wooden posts in the framework of the specially fabricated curing oven. The objective of the oven is to provide the panel with as near to an isothermal environment as possible. Once the panel is under the vacuum bag, it is enclosed with thick blankets made of fiberglass insulation. At this point a full vacuum is being applied between the front face and the tool surface. A vacuum groove is machined into the tool surface [Figure 51] to facilitate uniform pulldown over the entire surface area. This vacuum is applied uninterrupted throughout the entire lay-up, cure and cool down procedure, approximately 30 hours, and is maintained when the panel is reheated and cooled two times as post-cure "stress relief" cycles.

At this point, the back face has been removed with the handling fixture, and teflon tape is applied along the edges to seal the front face to the tool, Figure 72. This photo also shows the aluminum stiffener pieces on all four edges. They are taped in place. It should be noted that from this sequence on, it is necessary to be very careful not to touch any surfaces that will have adhesive applied to them.

Figure 73 shows the foam edges and dummy corners in place. Adhesive was applied to the pieces before they were put in place. Hold down weights, shown in the foreground, are used temporarily to

keep the pieces positioned throughout the lay-up procedure. Teflon tape is used to hold various parts in place, Figure 74.

It is now time to put the honeycomb core in place, but adhesive has to be applied first. This is the most critical step, other than providing and maintaining ultraclean surfaces, in the lay-up procedure. The print through evaluation demonstrated that the fillet size must be minimized to avoid print through deviations on the front face. Adhesive is not applied in a continuous layer to the front face as is done in most honeycomb sandwich applications. Adhesive fillet size is controlled by dipping the core into a controlled thickness layer of adhesive, Figure 75. The adhesive dip layer is screeded to thickness, as in Figures 76 and 77, on a premachined aluminum tooling plate. Thickness is controlled by the two shim stock strips on either side as shown. Uniform dipping is aided by carefully tamping the entire core area with tongue depressors. The other side of the core is then dipped, after rescreeding the adhesive. Handling the core at this point is very critical and required developing delicate techniques.

The core is shown being assembled in Figure 78 and in place in Figure 79. This also requires delicate techniques. Honeycomb core tends to "saddle back" when it is formed over spherically curved surfaces. It was only a small amount for the large radius of curvature on the tool, but it was necessary to gently nudge the core down at various times from this point on.

The back face was then trimmed to shape, Figure 80. The face foil is shown nested in the handling fixture with the precleaned trim template in place. Trimming the .003 thick foil is easily achieved with a sharp, clean knife blade. The back face is then gently removed from the handling fixture and placed on the core, Figures 81 and 82. Care must again be taken to keep the back face located directly on top of the core, which as mentioned, continues to saddle back. The back face half of the Zee close-out section is then placed (no photos) to lay over the back face and the front face half of the Zee close-out piece previously assembled.

The pre-trimmed vacuum bag is then carefully placed over the lay-up, Figures 83, 84 and 85. A contoured handling fixture is used, as shown, to avoid shifting the loosely assembled parts. Sealing tape is applied around the entire panel periphery, Figure 84, before the bag is carefully adjusted to avoid wrinkles when the bag vacuum is applied, Figure 85. A partial vacuum is applied between the back side of the panel and the vacuum bag by a second vacuum pump. If a full vacuum is applied, the core will "bite" into the front face and cause print through deviations on the reflective side.

The vacuum bagged assembly is shown in Figures 86 and 87. The two vacuum manifold lines are shown running off the right of Figure 86. The close-up in Figure 87 shows how intimately the vacuum bag holds the assembly to the tool. It is important that this intimacy be maintained through out the cure cycle in order that the accurate shape of the tool be replicated. Note the white material just outside the periphery of the panel edges. This is a bleeder manifold made of a felt-like material that ensures uniform evacuation of air around the entire panel. Just outside the bleeder manifold is the vacuum manifold shaped in the form of a truncated pie shape made of 0.25 inch copper tube. The tubing has drilled holes all along the inside surface of the manifold. The sealing tape is located just outside of the manifold and must seal it entirely. This is a most difficult task because of the changing geometries around the panel, including bringing the manifold tube through the seal. Minute leaks cause immediate loss of vacuum, and usually takes about 30 minutes to find them all. This is achieved by listening for faint leaks and hand manipulation of the bag to tape seal. A "good bag" is judged visually by the intimate contact between bag and panel assembly and using a water manometer type gage.

The lay-up is now ready for enclosure in the curing oven, Figures 88 and 89. The portable wooden oven enclosure is being put in place in Figure 88. The four side pieces are hinged so they can be lifted for insertion of insulator pillows, Figure 89. Note the thermocouples attached to the tool in Figure 88. There are four thermocouples that control the four heater zones and one thermocouple for overtemperature protection. Note also the heater wires entering the mid section of the tool. They then attach to the strip heaters on the underside of the tool, Figure 52.

Figure 90 shows the lay-up "buttoned up" and the temperature controllers being set and turned on. The wooden enclosure is held closed with straps to prevent convective leak paths into the oven interior. It should be noted that all tooling, fixtures and process equipment were selected, designed, fabricated, assembled and de-bugged by CSU/AMC personnel. This process is so unique that it could not efficiently, cost and quality wise, be subcontracted out.

Monitor thermocouples are also used to record process temperatures through out heat up, cure, and cool-down. The acquisition unit is shown in the background of Figure 91. All panel cure cycles were recorded for quality control record purposes. The cool-down cycle is isothermally controlled by keeping the oven enclosure in place until room temperature is reached.

De-bagging is a carefully controlled process, Figures 92 and 93. There are yards of tape to be removed and they must be pulled gently from the various surfaces. As with most space application components, the panel is fragile and must be handled delicately. In some cases there is a slight bond between the two. Figure 94 shows the cured panel being removed from the tool. Handling screws are inserted in the dummy corners for this purpose. The vacuum groove imprint is apparent. The final trimmed panel edge is 0.625 inch inside this feature. Note the diffuse appearance of the surface because of the stretch forming operation. The panel is then rough trimmed just outside the vacuum groove, Figure 95. The panel is not trimmed to final size because the leveling layer has not yet been applied. Application of this layer results in a "drip bead" of material along the outer periphery. If the aluminum reflective layer were applied over this surface, there would be a significant surface slope error to deviate reflected solar flux. The leveling, reflective and protective layers are therefore applied before final trim.

### 3.3.7 Leveling Layer Application

#### 3.3.7.1 Purpose and Requirements

The Primary reason for building a concentrator is to reflect incoming solar radiation into a receiver. The ideal concentrator would have a surface texture similar to that of a glass mirror which reflects radiation specularly or at the same angle from the normal as it comes in.

Aluminum sheet stock used in the fabrication of concentrator panels has a surface texture which is primarily dictated by the finish of the mill rolls. Best finishes are in the one RMS range whereas standard commercial finishes can be in 10-20 RMS range. Stretch forming and surface treatments further reduce the quality of the surface texture to the point where a large percentage of the incoming radiation is diffusively reflected and would miss the receiver. Surface treatments like electrochemical polishing can improve the surface texture sufficiently for some application but not enough to be useful for a concentrator surface. Mechanical polishing leaves a great number of fine scratches which scatter the incoming radiation.

One proven method to mask the existing surface texture (Refs. 3, 4, 10) was to coat the reflection side of the panels with a thin layer of epoxy to produce a glass like surface texture as a substrate for the reflective coating.



The requirements for the coating material and the application process are formidable as described below.

- a) The coating must be applied uniformly and of sufficient thickness to mask all surface imperfections and the basic surface texture.
- b) The coating must produce a level, flat surface without holes, voids, ripples or wrinkles.
- c) The coating process must be controlled to minimize or eliminate inclusion of dust particles.
- d) The coating material must be compatible with the reflective coating.
- e) The coating material must adhere to the aluminum panel sufficiently to withstand stresses introduced by handling, trimming operation and thermal cycling.
- f) The curing temperature should be above the maximum operation temperature and below or equal to the curing temperature of the panel adhesive.
- g) The coating material, with a reflective and protective coating, must be compatible with the space environment for the mission duration.

#### 3.3.7.2 Spray Equipment

To meet the first three requirements, spray equipment was designed and built as shown in Figure 96. The equipment is of modular design and consists of three primary units; spray booth, traversing unit and the filter unit. The design for this effort followed the experience gained in the development of the spray application as reported in Reference 4. The spray booth is a standard 8 feet wide commercial unit which included the exhaust stack, fan and controls, a paint filter pressure differential gage and internal fluorescent lights. An observation window was added since the spray equipment is a closed system when in operation and the operation must be visually monitored. It is located next to the traversing unit for easy access to the spray gun controls. Interior modifications consisted of adding six 250 watt infrared lamps focussed on the area where the coated panel is located for a heated pre-cure of the epoxy. Also, a panel rotating fixture was installed on the spray booth table. The rotation was achieved through a drive shaft from the externally mounted D.C. motor with a variable speed controller. The heating lamps and the rotating fixture are shown in Figure 97. Rotating the freshly coated panel at the proper RPM prevents formation of runs or puddles on the panel and maintains the uniform thickness of the coating. To maintain cleanliness, the inside of the spray booth was covered with polyethylene sheets to catch the overspray. The covering was periodically replaced to prevent loose

epoxy particles from being blown around and possibly settling on the wet coating.

The heart of the spray equipment is the traversing unit. It was designed to hold two spray guns with a pressurized paint cup and to move them across the width of the spray booth while coating the panel. Controls on the outside permitted the adjustment of spray parameters as required. Traversing speed and air pressures to gun cylinder, nozzle and paint cup could be selected. The position of the spray guns was experimentally determined to obtain the proper coverage and overlap during spraying. The guns have individual adjustments to control needle movement and fan pattern. The traversing mechanism and the associated parts list are shown in Figures 98 and 99. The primary feature is a motor driven chain which is attached to a bearing platform. The bearing platform contains two open pillow block bushings which ride on two parallel bearing shafts. A mounting rod is attached to the bottom of the platform. Two spray gun mounting clamps are attached to the rod. The position of the mounting clamps can be varied to obtain the proper spacing of the spray guns. Limit switches (not shown) are at each end of the traversing mechanism to shut off the drive motor and the air supply to the guns at the end of the travel if these features are not controlled by the operator. The traversing unit is covered with stainless steel sheets, except for the areas matched to the spray booth and the filter unit, to prevent dust from entering the spray equipment. Casters on each leg permit moving the unit away from the spray booth.

One stainless steel end panel was fastened to the unit with a piano hinge to provide access to the spray guns without having to move the whole unit away from the spray booth. Figure number 100 shows a view of the mounted guns through the access door opening while the traversing unit was slightly moved away from the spray booth to show more detail of the inside. The last unit to make up the spray equipment is the filter unit which provides filtered air to the enclosed spray area. The unit is a standard 4' X 6' filter module meeting Federal Standard 209D, class 100 conditions with 2-1/3 HP blowers for positive air flow. The filtered air side is shown through the traversing unit in Figure number 101.

#### 3.7.7.3 Spray Evaluation

Not many coating materials are available as potential leveling coatings when evaluated against the previously stated requirements. Literature search and discussions with manufacturers quickly determined that commercially available materials suffer from a lack of physical data and application experience related to this application. The only exception being Emerson and Cumming's EP-3

which was successfully used as a solar concentrator leveling coating material in the 1960's and 1970's. The only reason one would not use it is its failure to space qualify because of its high outgassing rate. An experimental program to evaluate other candidate materials would have required a substantial effort and was considered to be unnecessary at this time. The development of spray parameters was therefore started using EP-3.

Solvent content of the coating mixture was varied between 10% and 40% of the epoxy. With each solvent-epoxy ratio other parameters had to be adjusted. The best combination consisted of the following:

Epoxy Mix: EP-3 Part A 100 volumes  
Part B 50 volumes  
Solvent 60 volumes  
Solvent consisted of 60% MIBK and 40% Toluene

Air Pressures: Main air supply 90 psi - static  
Gun Cylinder 45 psi flowing  
Gun Nozzle 45 psi flowing  
Fluid cup 5 psi flowing

Gun adjustments: Side part control (FAN) .114 inch  
Fluid adj. control .480 inch  
Fan pattern vertical  
Distance between guns 11.0 inch

Reference Figure number 96  
Gun Traversing time: 5 seconds  
(stop to stop)

Fixture rotation: 9 RPM

As the work proceeded to determine spray parameters several problems were encountered and had to be resolved.

One of the easiest problems to solve was the reaction between the coating material and adhesive backed tape. Invariably, the coating material pulled away from the tape used to fasten sample pieces to the back-up sheet of the rotating unit. Using metal clips or taping smaller pieces to a strap at the back solved this problem.

One of the most difficult problems encountered in the coating application was the appearance of voids. They consisted of circular areas up to approximately 1/4 inch in diameter where the coating material pulled away, leaving basically a hole in the coating except for a very thin film. Several items were either identified or speculated as potential causes for coating voids.

Physical evidence of foreign particles, either dirt or residue from the cleaning operation accounted for some voids. The particles were always found in the center of the void. Several corrective actions were implemented. To eliminate orange colored particles which were identified as residue from the acid etch paste, the brushing with a soap solution after etching was modified. For specifics see the cleaning procedure at the end of this section.

It should be noted that some foreign particles were completely covered with epoxy forming a raised defect. For this discussion these defects are treated as part of the dust problem. When attaching samples or panels to the rotating fixture, the traversing unit had to be pulled away, allowing air born particles to enter the spray booth. To eliminate this possibility, an access door was installed in the spray booth table between the rotating fixture and the overspray collection filter. Any particle entering this door, either air or person born, was downstream of the part to be coated. This access was used for loading, unloading and during final air blasting of the parts to remove any particles that may be on the surface.

Another area that received considerable attention was the cleanliness of the spray equipment. Guns, fittings and pressure cup were disassembled and twice solvent cleaned after each use. Prior to re-assembly, fluid passages were examined using a low power microscope and flushed with compressed air. Fluid lines connecting the pressure cup with the spray guns were used only once because they could not be cleaned sufficiently. Examination of the I.D. of the fluid lines revealed a thin film of a white substance which could be scraped off. Cleaning trials resulted in flushing the completely assembled spray system with solvent as the simplest method to remove this film. Throw-away polypropylene beakers used for mixing the epoxy also were solvent cleaned and air blasted prior to use.

Another source of dirt, within the spray booth, was noted when the air filter unit and the exhaust fan were shut off for an extended time period. Keeping the air filter unit on produced a positive pressure inside the spray booth and prevented dust from entering. Determining causes for voids which did not have a foreign particle as their origin provided quite a challenge. One supposition pertained to entrapped air bubbles which persisted long enough so that after bursting a void was retained. Although the spray system was using air for atomizing the epoxy and therefore did create a lot of small bubbles, observation indicated that these were not responsible for creating voids. These small bubbles readily migrated to the surface and disappeared especially when heat was applied. The attention then focused on entrained bubbles in the epoxy mixture. Degassing the epoxy under a partial vacuum did not

prove beneficial.

Another proposed cause was that local variations of surface tension could set into intricate motion an entire liquid film. These movements may result in voids or Benard's cells. This phenomenon is known as the Marangoni effect.

It was recommended to use at least one solvent in the mixture with the highest available surface tension because it would reduce or even eliminate the formation of Benard's cells. Unfortunately, useful solvents did not have surface tensions of sufficient variance to yield conclusive results.

During the course of these investigations and the determinations of spray parameters it was noted that the epoxy film was influenced by other parameters. At first it appeared that the aluminum alloy onto which the epoxy is sprayed is a variable. But, coating results of the same aluminum alloy but of different batch thickness as well as coating identical material before and after stretch forming, indicates that the alloy composition is not the problem. Eventually, it was determined that the surface condition is the primary reason for a non-uniform coating.

Various surface conditioning or preparation methods like solvent wipe, Scotch Brite polishing, degreasing, acid etching, soap washing and hot or cold rinses were tried individually or as part of an overall process. The most reliable and consistent process was patterned after the surface cleaning procedure previously discussed and used in preparation for adhesive bonding is listed below.

#### Aluminum Cleaning Procedure

1. Solvent Cleaning.
  - Wash 2 times with Toluene. Spray toluene liberally on panel in horizontal position. Wash with kimwipes. Dry with kimwipes.
  - Wash 2 times with methyl ethyl ketone. Same procedure.
2. Soap Cleaning.
  - Apply a mixture of 50% "CSP" cleaner (\*) and 50% tap water with brush. Brush in vertical, horizontal and diagonal; down to right and down to left with bristles forward. Rinse with hot (140-150 degree F) tap water.
3. Acid Cleaning.
  - Apply uniform coat of "PASA-JELL 105" (\*\*) with paint brush. Wait 1 hour and remove coating with hot tap water (140-150 degree F) spray and brush surface. Do not dry.

4. Soap Cleaning.
  - Same as 2 above except 2 applications.
5. Water Rinse.
  - Rinse liberally with distilled water of room temperature. With panel in vertical position, observe water break. Water should dry from top to bottom. If local dry spot appears, check for dirt particle. Remove with brush and rinse.
6. Solvent Rinse.
  - This was added for the EPON 826 coating based on recommendation by Shell Chemical Company to improve adhesion of coating to aluminum.
  - Spray panel in vertical position with acetone while in the spray booth.
  - \* Hillyard Chemical Company, St Joseph, Missouri 64502
  - \*\* Semco, Div. of Products Research and Chemical Company  
5454 San Feranando Road Glendale, CA
7. Drying.
  - Apply heat with heat lamps to remove moisture.

Summary:

The spray evaluation using EP-3 as the coating material proceeded to the point where an almost acceptable coating was produced by following a material cleaning procedure, keeping the equipment clean and following established spray parameters.

Following the established procedures, no perfect or defect free coating was produced since some dust particles were always present. It is believed that a spray system placed on a shop floor will never achieve a dust free internal environment. It is recommended that a spray system should be installed inside a clean room.

#### 3.3.7.4 Epoxy Evaluation

Concurrently with the spray evaluation, the ability of the coating to produce a flat and optically specular surface was evaluated. The only way to detect small imperfections is to coat the leveling layer with a reflective film. An aluminum evaporation fixture was built to fit inside a 2 foot diameter, 3 foot long vacuum chamber at the NASA Lewis Research Center. Samples as well as full size panels could be vacuum coated.

Prior experience with EP-3 was repeated as the reflective aluminum film showed a flat, specular surface. The satisfaction of being able to reproduce specular coatings did not last long because of the appearance of "blushing". This term is used to describe the

change from a specular to a diffuse reflecting surface. Blushing was sometimes present at the time the sample was removed from the vacuum chamber or it appeared at any time later. Some samples are over 6 months old and do not show any indications. Blushing was experienced with samples coated with aluminum at NASA and with samples coated with aluminum and silicon dioxide at a vendor. The diffuse reflectivity is caused by a change of the surface topography.

Microscopic viewing showed surfaces appearing as if they had been sandblasted to surfaces having undulations like sand dunes. These undulations could radiate from a center like the erosion pattern of a mountain [Figure 102] to a very orderly geometric pattern resembling a herringbone design (Figure 103).

Since these surface texture changes appeared after vacuum metalizing it was assumed that they are the result of a highly stressed aluminum film exerting a force on the epoxy. It can be visualized that a high compressive stress could buckle the surface to the point that the linear dimension is increased until the stress in the aluminum film is balanced by the resisting stress in the epoxy.

Scotch tape tests did not pull away aluminum particles indicating that there was no local separation between the aluminum film and the epoxy. Several tests were performed to find a method to either eliminate or reverse the blushing.

In one series of tests, blushed samples were exposed to a temperature of 225 degrees F for various time durations. This temperature represents the maximum curing temperature of EP-3 but is below a stress relief temperature for aluminum. At the elevated temperature, the blushing disappeared on some, partially or not at all on others. However, upon cooling, the blushing slowly reappeared.

In another experiment, the aluminum film was removed with NaOH, the surface cleaned and recoated with aluminum. The new film was somewhat milky in appearance suggesting a chemical reaction between the NaOH and the epoxy.

A major effort was then started to explore several epoxy curing cycles and aluminum evaporation rates in an attempt to possibly find process parameters which would not result in blushing. It was previously noted that coating cured at low temperatures were more immediately susceptible to blushing than those cured at the higher temperatures.

All coatings were initially cured overnight in the spray booth at about 110 degrees F to set the epoxy and to have a tack free surface. Final cures were performed on a 2' X 3' hot plate inside an insulated box. Heating was accomplished by 4 electric heating blankets individually controlled by a series 945 Watlow microprocessor-based auto-tuning controller.

Curing schedules varied at 185 degrees F, 225 degrees F or 250 degrees F and held at these temperatures for 2 to 3 hours, to stepped temperature increases of 15 degrees F to 25 degrees F followed by holds for 30 minutes to one hour at each step. Final temperatures were again 185 degrees F, 225 degrees F and 250 degrees F.

Of 84 cured samples which were aluminized, 20 were initially free of blushing but after 6 months only 3 survived unblemished. Most of the 20 samples were cured using a stepped cure schedule. These tests did not yield clear results favoring any specific curing schedule. Nine aluminum evaporation trials were conducted on small samples cut from one large coated sheet. The coating was step cured to a maximum temperature of 225 degrees F. In each of these trials two or three samples were positioned 15 inches to 27 inches from the filaments to explore any distance effect. No consistency was noted. New filaments were used for each evaporation to eliminate any variation due to remaining aluminum from the previous evaporation. Also, the aluminum weight of the charge was kept constant at .14 gram per filament.

The evaporation current was varied between 20 and 40 amps per filament. Two filaments were used in all evaporations. Evaporation was visually monitored to observe aluminum melting and evaporation. When most of the aluminum had evaporated, filament power was turned off.

Filaments were preheated at 12-15 amps until the aluminum melted. Power was then increased to the desired amperage. Evaporation times ranged from about two minutes at 20 amps to between 5 to 20 seconds at the 40 amp level. The best coatings were produced between 30-40 amps per filament with an evaporation time around 20 seconds. Of 12 samples from 4 evaporation trials which were originally acceptable only 3 remained unblemished. The other showed either blushing with time (4 months) or developed blushing as a result of pressure exerted on the surface during trimming experiments.

Although the evaporation experiments resulted in process parameters which yielded acceptable reflective coatings, the long term instability and susceptibility to damage from subsequent operations was unacceptable. During prior experience with EP-3 none of these



problems were encountered, and any attempt to resolve these problems with process variations failed. It was concluded that the epoxy must have changed. The manufacturer stated that the epoxy formulation had not changed. However, they now buy all the raw materials whereas they used to make them in house. It may be assumed then that the raw material may be different or may have been processed differently so that the final product performance makes it unacceptable for this application. Attention was then focused on finding a replacement for EP-3.

Shell Chemical Company recommended their Epon 826 resin, with curing agent Y. The coating can be cured at 300 degrees F for high temperature service.

The first experiments were conducted by using different solvents and mixing ratios. The coating was applied with a brush, cured and aluminized.

The following were tried:

1. No solvent
2. Xylene 10%, 20%, 30%
3. Glycol 10%
4. Toluene 10%
5. MIBK 10%
6. Alcohol 10%
7. Acetone 20%
8. 10% Toluene and 10% Glycol
9. 10% Xylene and 10% Toluene

All aluminum films were clear without any blushing or haze and remained that way after 4 months. Xylene and Acetone were selected as candidate solvents to lower the viscosity for spray application based on a visual comparison of the surface flatness.

Trimming experiments on some of the samples did not affect the quality of the coating.

The next step was to try spray coating with Xylene and Acetone separately and as combinations using different epoxy-solvent mixing ratios. The final selection was:

EPON 826	100 volumes
Curing Agent Y	25 volumes
Xylene	38 volumes
Acetone	25 volumes

Several of the trial spray coatings were aluminized in the NASA vacuum chamber. All reflective coatings were of excellent quality. Since the concentrator panels are scheduled to also have a protective SiO<sub>2</sub> coating over the aluminum, samples were sent to Denton Vacuum for aluminizing and application of SiO<sub>2</sub>. The NASA vacuum system did not have the capability to apply SiO<sub>2</sub>. Twenty samples with coatings prepared with different solvents and concentrations were coated by the electron beam evaporation process. All were excellent. This confirmed results obtained at the NASA facility even though the process was different and was done at a different facility.

Two problems however subdued the enthusiasm about this coating material. The first was the tendency to pull away from any foreign particles leaving a crater or very thin film around the particle. This problem was solved by the addition of 1% SR882 silicone resin as a flow promoter to the epoxy-solvent mixture. The product is made by the Silicone division of G.E.

The second problem has not been resolved. When cutting small samples from a big sheet with a knife, the epoxy coating separates from the aluminum sheet along the cut line. With only a slight pull, the epoxy coating can be completely removed indicating a very low adhesion. A quick fix type suggestion by Shell, spraying the surface with Acetone prior to spraying with the epoxy did not improve the adhesion. Further work on this problem is required.

Another Shell product was tried on a low effort basis. Epon 1001 resin and V-15-X-70 curing agent samples were provided by Shell for experimentation. The resin can also be used with curing agent Y like resin 826. Epon 1001 hardens fast, similar to lacquer, which reduces the wet time during which dust particles can be absorbed. The few samples prepared by brush application did not produce an acceptable surface.

In any spray application, air turbulence will carry a mist of the coating material to the back side of the part being coated. To keep the back side clean, it must be protected or shielded. A white strippable coating procured from Binks was tried. It can be applied by the spray or brush technique. When brushing, it almost behaves like rubber cement. After curing, it can easily be removed. Tests were conducted to determine its compatibility with epoxy solvents and curing temperature. No detrimental effects were noted.

#### 3.3.7.5 State of the Art and Recommendation

For the application of a uniform coat of leveling layer, a spray system was designed, built and put into operation with satisfactory results. Dust intrusion into the spray area appears to be a remaining determinant. It is believed that installing the spray system within a clean room will eliminate or reduce to an acceptable level this negative aspect. Acceptable highly specular coatings have been produced with Shell Epon 826 epoxy. Further work is required to improve its adhesion to aluminum. Tests should also be conducted to qualify this material for space application.

Other materials may or even should be evaluated to have ready alternates for the material that failed space qualifications.

#### 3.3.8 Reflective and Protective Coating

The leveling layer provides the specular surface required for controlled directional reflection, but the reflectance to the solar spectrum is too low. An aluminum coating is applied over the leveling layer to raise reflectivity. A silicon oxide final coating is applied to protect the aluminum during handling, cleaning and against oxidation. These two coatings were applied by a vacuum evaporation process by a subcontractor. While this process would preferably be done in-house, the facility requirements were well outside the project funding. Besides, there are several qualified subcontractors capable of applying space rated coatings. Previous coating work (References 3, 4, 5) was done in an in-house vacuum facility and the process is well defined (Reference 3).

The process involves heating pure aluminum and silicon oxide in separate crucibles wherein the material evaporates in straight line flight to the panel surface. The early work was done by evaporating the materials in electric resistance filaments, "boats" or crucibles. Technology has advanced and electron beam guns are also used to heat materials in crucibles, as was done for the present panel work.

Denton Vacuum Inc. was used for this project work and was qualified first by coating specimens mounted on a handling fixture, Figure 104. These specimens allow evaluation of coatings over various areas of the panel and are stored in protective containers for quality control records. Glass slides were also mounted on the fixture because these provide a reference surface for specular and spectral reflectance measurements on a "highest figure of merit" surface.

Each panel coated was accompanied by specimens mounted around the panel. These specimens were processed along with each panel, and represented the cleaning and leveling layer process that the specific panel experienced. These specimens are then used to visually rate the evaporation process and are also identified and stored for reference.

The vacuum evaporation requirements are defined in Process Specification PS-1006. The specified coatings are as follows:

1. Adhesion promotion layer  
1000-1500 Angstroms Silicon Oxide
2. Relective layer  
1000-1500 Angstroms Pure Aluminum
3. Protective layer  
1400-1800 Angstroms Silicon Dioxide

#### 3.3.9 Edge Trimming

The protective coating applied in Section 3.3.8 allows reasonable handling of the panel without damage to the aluminum reflective coating. The panel can be placed on the tool, as in Figure 105, without scratching the aluminum coating. The radial arm in Figures 106 and 107 show the high speed slitting saw mounted for trimming the radial edge. Figure 108 shows the slitting saw cutting the OD edge.

The slitting saw easily trimmed the edges. The difficult aspect was in making sure there were no minute surface slope errors introduced on the front reflective face. Many samples were cut before the final process parameters were established. Soft aluminum is not easy to cut, and the two inter layers of adhesive compounded the task. Good trimming could not be achieved without using a fine tooth cutting wheel (2"OD X .010" thick X 30 teeth per inch). But such fine teeth load up quickly. It was necessary to clean the wheel after each cut and make only six cuts per wheel. Lubrication was also important. A wax stick-type saw lubricant was applied to the wheel through out each cut. A single thickness layer of ordinary masking tape was also placed on the outer surface of the panel and helped greatly. The slight raised burr left after the cut was easily removed by filing off the corner manually, by delicate use of a new, sharp file.

### 3.4 INSPECTION

#### 3.4.1 Tool Accuracy

The stretch forming tool was fabricated at Tempcraft Corp, and the process from aluminum blank to final inspection was controlled with great care. As has been noted, the tool is the primary component that provides the final high concentration efficiency in reflecting the solar flux through the receiver aperture. The tool accuracy required was comfortably met by machining on a 3 axis CNC milling machine and Appendix I details the fabrication process. Several visits with Tempcraft resulted in establishing the 17 step procedure to ensure tool accuracy. Since improperly heat treated aluminum can change shape, the rough blank stock was stress relief aged at 375 degrees F for 11 hours.

The tool was inspected on a high accuracy 3 coordinate measuring machine, Figures 7-11, Appendix I. Thirteen inspection paths, as in Figure 6, were recorded. The data is recorded in both graphic and tabular form, and the paraboloidal surface was within .0033 inch of a true surface (well within the .010 tolerance specified).

Two procedures were used for the final inspection. One used the same mathematical program used in machining the tool surface so the inspection recorded deviations from that program. This resulted in the extensive inspection noted above. A second inspection was made at selected points, Figure 13, by a program independent from the machining program. The cross check indicated there had been no error made in preparing the machining program.

The flatness of the tool base was also measured and recorded as shown in Figure 13. This was done primarily to allow a later measurement after several panels were heat cured on the tool, and any tool shape change would be detected. The first measurement when the tool was machined showed the base flat within .0015 inch. Nine months later, after panels were fabricated at 300 degrees F, the flatness was still within .0015 inch. No significant shape change.

#### 3.4.2 Panel Optical Inspection

Optical inspection of solar concentrator surfaces for space applications is difficult because of the light weight, flexible nature of the panels. For instance, a panel of the 9.5 foot antenna (Ref. 7) was held in a cantilevered manner at the ID end. A deflection was measured at the OD tip when the panel was positioned concave side up and the concave side down. The analysis showed a one g deflection of close to 0.080 inch. This is an order of magnitude greater than the errors allowed in manufacture for a

solar concentrator panel. Therefore the panels must be positioned in the most rigid direction relative to the Earth's one g field. This is done by placing the panel length horizontal and the concave surface sideways.

The panel inspection rig is shown schematically in Figure 109 and photographically in Figures 110-113. The most rigid section modulus of the panel is placed as in Figure 109. A small filament, high intensity lamp illuminates the panel, like a searchlight. The reflected rays are nominally parallel, for a perfect surface, and pass through the steel grid and cast a shadow on the plastic target. If a deviation exists on the panel surface, the reflected rays have a bias error that causes the shadow to be displaced from the plastic target grid. These displacements can then be analyzed at each node of the shadow pattern.

Figures 110-113 show several views of the rig. The panel is discernable in the upper right of Figure 112, and the steel grid is to the left. The plastic target grid is shown to the left of Figure 111. Photographic paper is placed behind the target grid and held firmly in place with a back-up panel. This is all done in a dark room, and when the light source is turned on for a controlled time, the shadow is recorded relative to the target grid as in Figures 114 and 115 (65% and 150% scale respectively). These reproduced copies are not as clear as the original, and the analysis is done with the aid of a 7 power binocular microscope.

Displacement of the center of a shadow node can be measured relative to the target grid in the circumferential and radial directions. A total of 232 points were measured for panel number 6 (Appendix H) and resulted in the histograms in Figures 116 and 117. The distribution of deviations obviously have a normal Gaussian distribution shape. The calculated normal curves are shown superposed on the histograms. The statistical data is as follows:

Radial deviations

1 Sigma = 0.32 milliradian  
3 Sigma = 0.97 milliradian  
Median = +.05 milliradian

Circumferential deviations

1 Sigma = 0.42 milliradian  
3 Sigma = 1.26 milliradian  
Median = -0.13 milliradian

The significant result is that the 3 sigma deviations (maximums) are close to the 1 milliradian desired for the panel surface deviations. Note that the design spec, Figure 15, requires a 3 sigma value of 3 milliradians. As discussed in Section 3.1.11, the remainder of the design spec deviations are allotted to deviation sources 1 and 6 through 9 in Figure 20.

Note that the mean deviations for Figure 116 and 117 are not zero. This is an indication that the panel could be better aligned in the test rig.

A definite advantage to this inspection method is that it graphically shows the panel condition quickly. Deviations become immediately apparent. A disadvantage is that the finite size of the light source makes it impossible to measure deviations smaller than about .01 milliradian. If the plastic target is moved much farther than 50 inches from the steel grid, the shadow edges become fuzzy and measurement imprecise.

The geometric relationship between deviations measured at the target grid and surface slope errors on the panel is shown in Figure 118. A surface slope deviation  $\theta$  at the panel surface reflects as a  $2\theta$  deviation from theoretical as shown. For the geometry selected at 50 inches between grid and target, a shadow displacement of .100 inch at the target results in a  $2\theta = 2$  milliradian deviation of the ray coming to the target and a  $\theta = 1$  milliradian at the panel surface. Evaluation of the 232 shadow deviation points were made to a resolution of .010 inch which allows identifying deviations to the nearest 0.1 milliradian. The shadow projection method is therefore just able to measure surface deviations pertinent to solar concentrator technology requirements.

#### 3.4.3 Panel Weight

Panel number six weighed 0.771 pound and intercepts 1.92 square feet of solar flux. The panel specific weight is therefore 0.40 lb/ft<sup>2</sup>. This includes the following items:

1. Front face (.012 thick alum)
2. Back face (.003 thick alum)
3. Adhesive (.010 fillet)
4. Leveling layer (.002 epoxy)
5. Foam edge close outs
6. Edge Zee close out pieces
7. Four dummy corners (Alum.)

The honeycomb sandwich construction by itself has the following items and specific weights:

	lb/ft 2	%
1. Front face (.012)	.173	60
2. Back face (.003)	.043	15
3. Adhesive (.010 fillet)	.063	22
4. Leveling layer (.002)	<u>.010</u>	<u>3</u>
	.287	100

Therefore items 5, 6 and 7 have a specific weight of  $0.400 - .288 = 0.111$  lb/ft 2. For larger diameter concentrators, the same items become a smaller percentage of the total weight, and the panel specific weight would become lower. A specific weight closer to 0.35 lb/ft 2 is considered achievable on larger panels. The design specification of 0.2 - 0.4 lb/ft 2 is considered achieved.

### 3.5 Two Panel Test Rig

The qualification of the 9.5 foot antenna for flight (Ref.7) demonstrated the reliable performance of the panel actuator and positioner hardware. Many deployment tests were also made with zero g simulators attached. This demonstrated the kinematic and kinetic ability to reliably deploy without structural interferences or damage. However, the antennna requirements are less stringent than for solar concentrators, and the need for interpanel locking after deployment is required on solar concentrators. Locks between panels at midspan and at the tip were designed (Ref 1) as shown on sheet 3, Appendix E. Demonstration of lock hardware performance is minimal (Ref. 3). Therefore one project task on the 2 meter concentrator was to design and build a test rig to evaluate lock performance. Because of project priorities and fund limitations, a two panel test rig was designed but not built. All details are available however if this task should be restarted. Appendix E shows the 3 sheet assembly drawing and parts list. The panel hardware is identical to that shown on the 2 meter concentrator assembly drawing, but the mounting ring is simplified into a single mounting block base to reduce costs.



#### 4. Recommendations

The results obtained from the fabrication effort demonstrate that the capability to build panels meeting specification is available. Process refinements will further improve performance for space applications that require higher absorber temperatures. Additional work that is considered necessary to progress toward flight hardware is as follows:

1. Continue evaluation of space compatibility of the selected adhesive and leveling layer formulations.
2. Continue evaluation of cyclic temperature fluctuations on honeycomb sandwich shape stability.
3. Continue evaluation of thermal gradients on the deployed concentrator shape control.
4. Continue design evaluation of panel locking devices to provide structural stiffness to the deployed concentrator.
5. Consider a flight experiment of a Sunflower type structure to obtain data for correlation with analytical codes. The flux profile in the focal region and surface shape control data are needed.

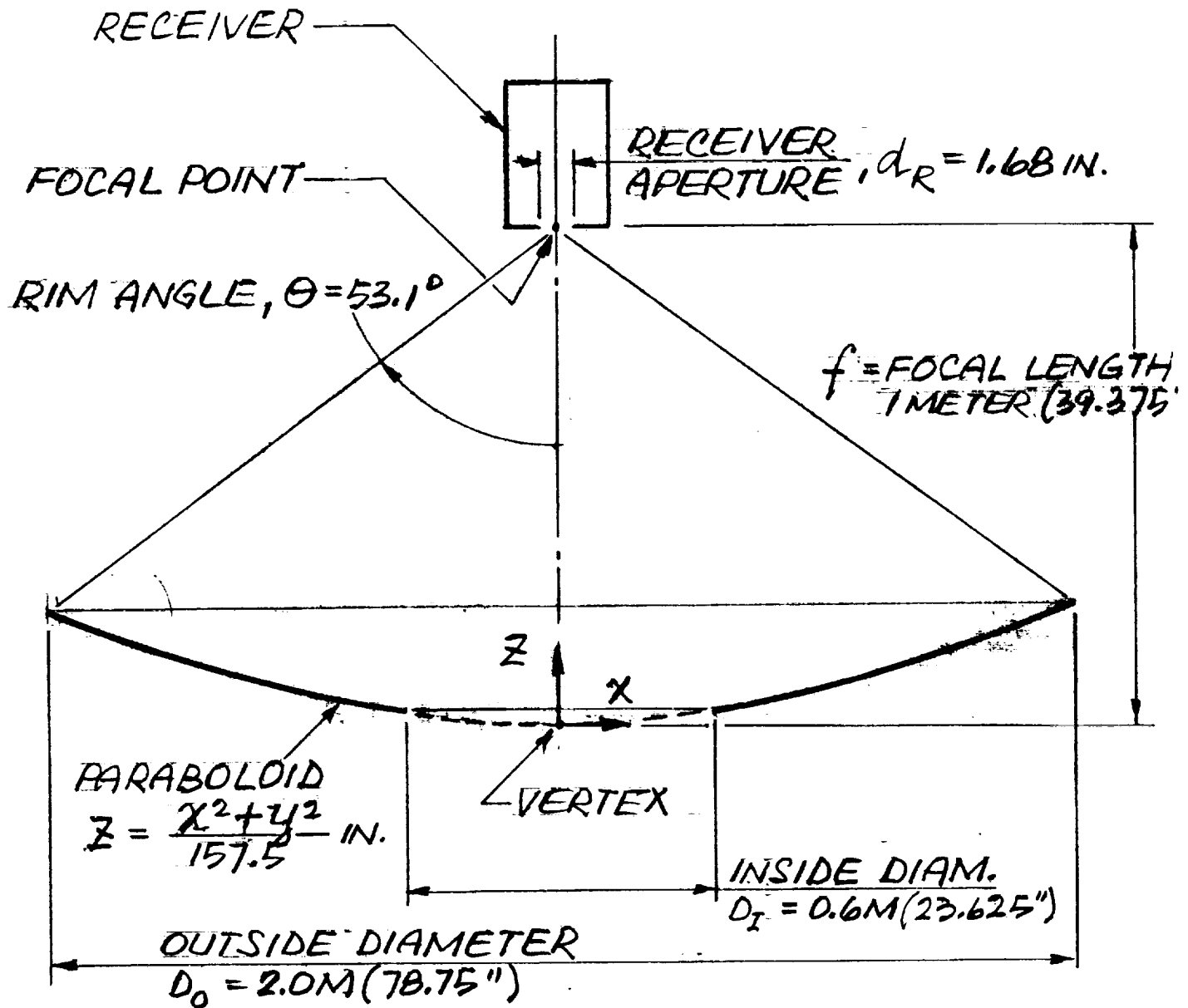
## Appendixes

- A. Selected Five Foot Diameter Concentrator Data
- B. Selected Sunflower Concentrator Data
- C. Selected 9.5 Foot Diameter Antenna Photographs
- D. Two Panel Test Rig
- E. Two Meter Concentrator Assembly Dwg. 9001250
- F. Two Meter Concentrator Panel Dwg. 9001250-1
- G. EN-1020 "Panel Fabrication Procedure"
- H. EN-1022 "Slope Error Deviations of Panel No. 6"
- I. EN-1001 "Fabrication of Stretch Forming Tool"

## References

1. "Two Meter Auto-Deployable Prototype Concentrator", A. Pintz et al, Cleveland State University/AMC Report February 1989
2. "Design of an Auto-Deployable Technology Demonstration Solar Concentrator", A. Pintz et al, IECEC conf., August 1989
3. "Sunflower Solar Concentrator", TRW Inc, NASA CR-46, May 1964
4. "Stretch Formed Aluminum Concentrator", TRW Inc, NASA CR-66069, 1964
5. "Binary Rankine Cycle Energy Conversion", TRW Inc, Air Force Report APL-TDR-64-5
6. "Brayton Cycle Solar Collector Design Study", TRW Inc, NASA CR 54118, March 1964
7. Flight Qualified 9.5 Foot Diameter Deployable Antenna, 1967
8. "Review of Solar Concentrator Technology", A. Heath Jr., et al, IECEC Conf., September 1966
9. "Calorimetric, Optical and Vibration Investigations of Stretch Formed Aluminum Solar Concentrators:", M. Rhodes et al, NASA TN D-4889, November 1968
10. "Polymer film Coating of Magnesium for Paraboloidal Mirrors", T. Mroz, NASA TN D-4734, August 1968
11. "PABST: New Reliability for Adhesive Bonding" Machine Design, Apr. 78, pp 20-25
12. "Phosphoric Acid Anodizing of Aluminum for Structural Adhesive Bonding" J.C. McMillan, et al SAMPE Quarterly, Apr. 76, pp 13-17
13. Aerospace Recommended Practice, ARP-1524, SAE
14. Boeing Process Spec BAC 5555
15. Boeing Process Spec BAC 5514
16. "Development of Oxide Films on Aluminum with the Phosphoric Acid Anodization Process", J.S. Ahern et al, contained in "Specialized Cleaning, Finishing and Coating Processes", ASM, Materials Park, OH

# TWO METER CONCENTRATOR GEOMETRY



$$\text{AREA CONCENTRATION RATIO} = \frac{(D_O)^2 - (D_I)^2}{(d_R)^2}$$

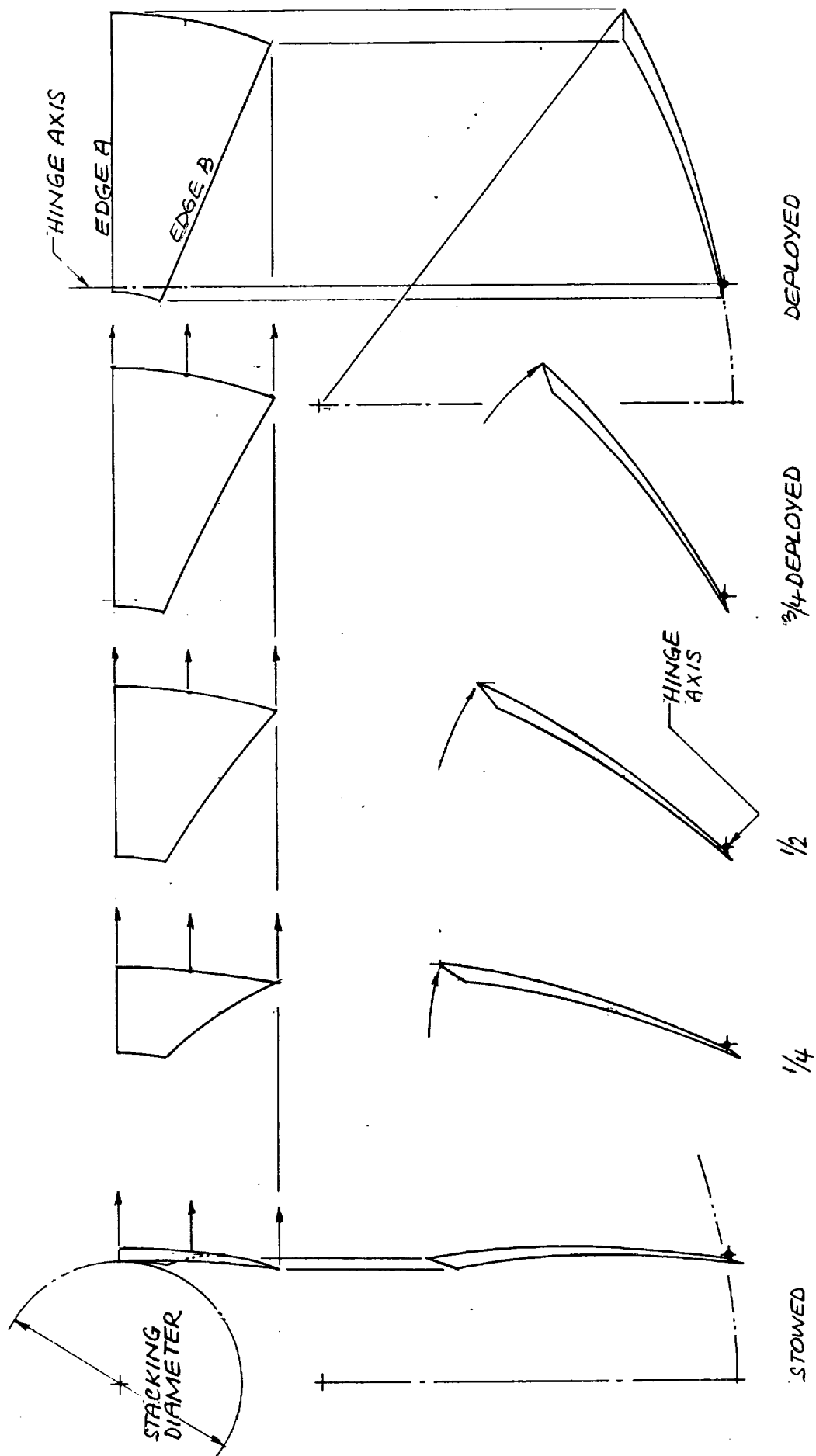
FIGURE 1

## REQUIREMENTS FOR A DEMONSTRATOR SOLAR CONCENTRATOR MIRROR

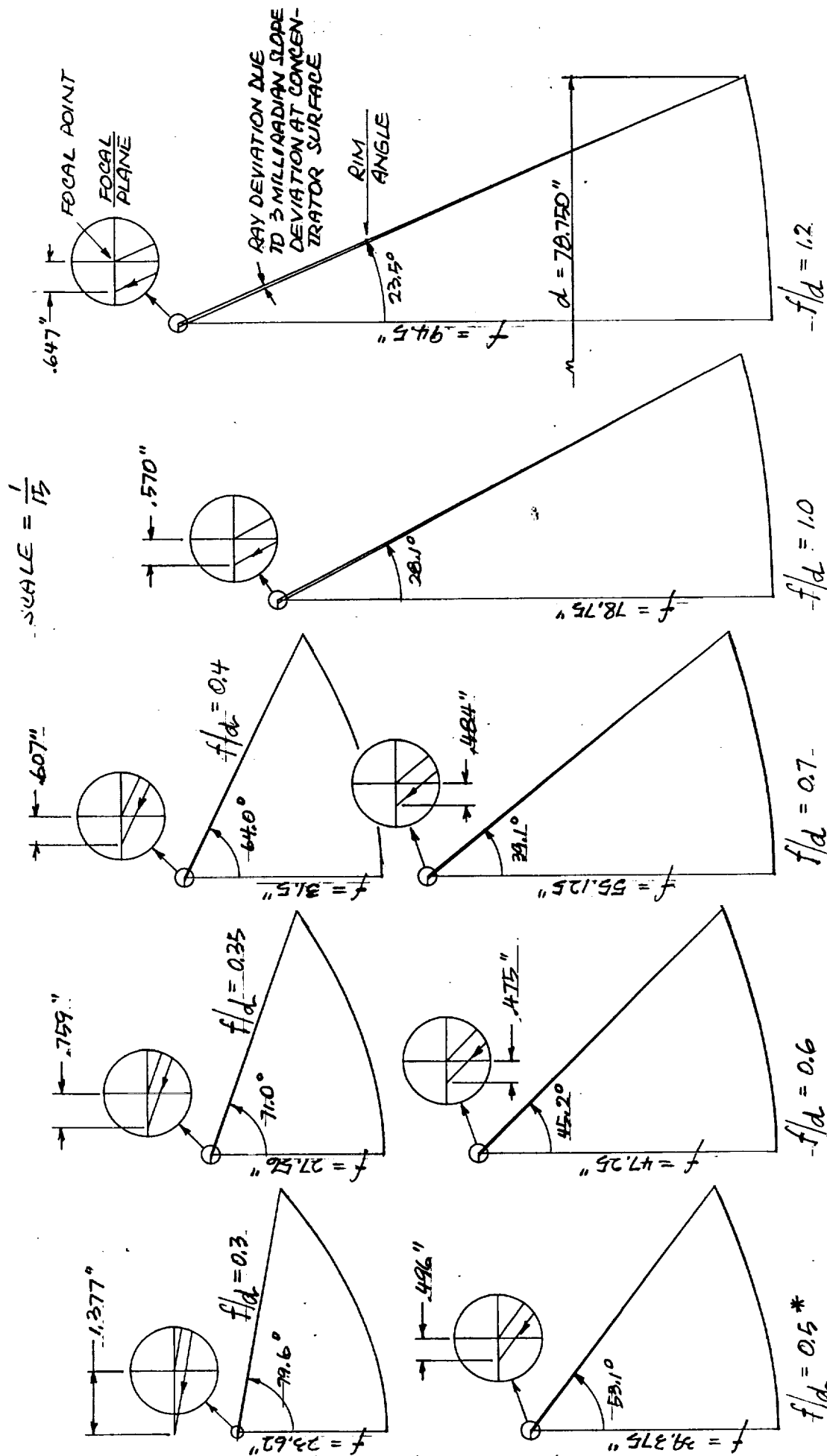
CONCENTRATION RATIO ——— > 2000:1  
SURFACE ERROR ————— 1 MILLIRAD MAX. (1 SIGMA)  
DEPLOYMENT ————— AUTO-DEPLOYABLE  
POINTING ACCURACY ————— 1 MILLIRAD MAX.  
SURFACE REFLECTIVITY ——— > 88%  
STOWABILITY ————— MANUAL  
PROTECTION ————— TERRESTRIAL HANDLING  
WEIGHT ————— 1-2 KG/M<sup>2</sup> (.2-.4 LB/FT<sup>2</sup>)  
CONCENTRATOR DIAMETER — 2 METERS (78.75")

### OBJECTIVE:

DEMONSTRATE PRESENT STATE OF THE ART IN  
DEPLOYABLE SOLAR CONCENTRATORS FOR SOLAR  
DYNAMIC SPACE POWER SYSTEM APPLICATION



PANEL DEPLOYMENT GRAPHICS      FIGURE 3

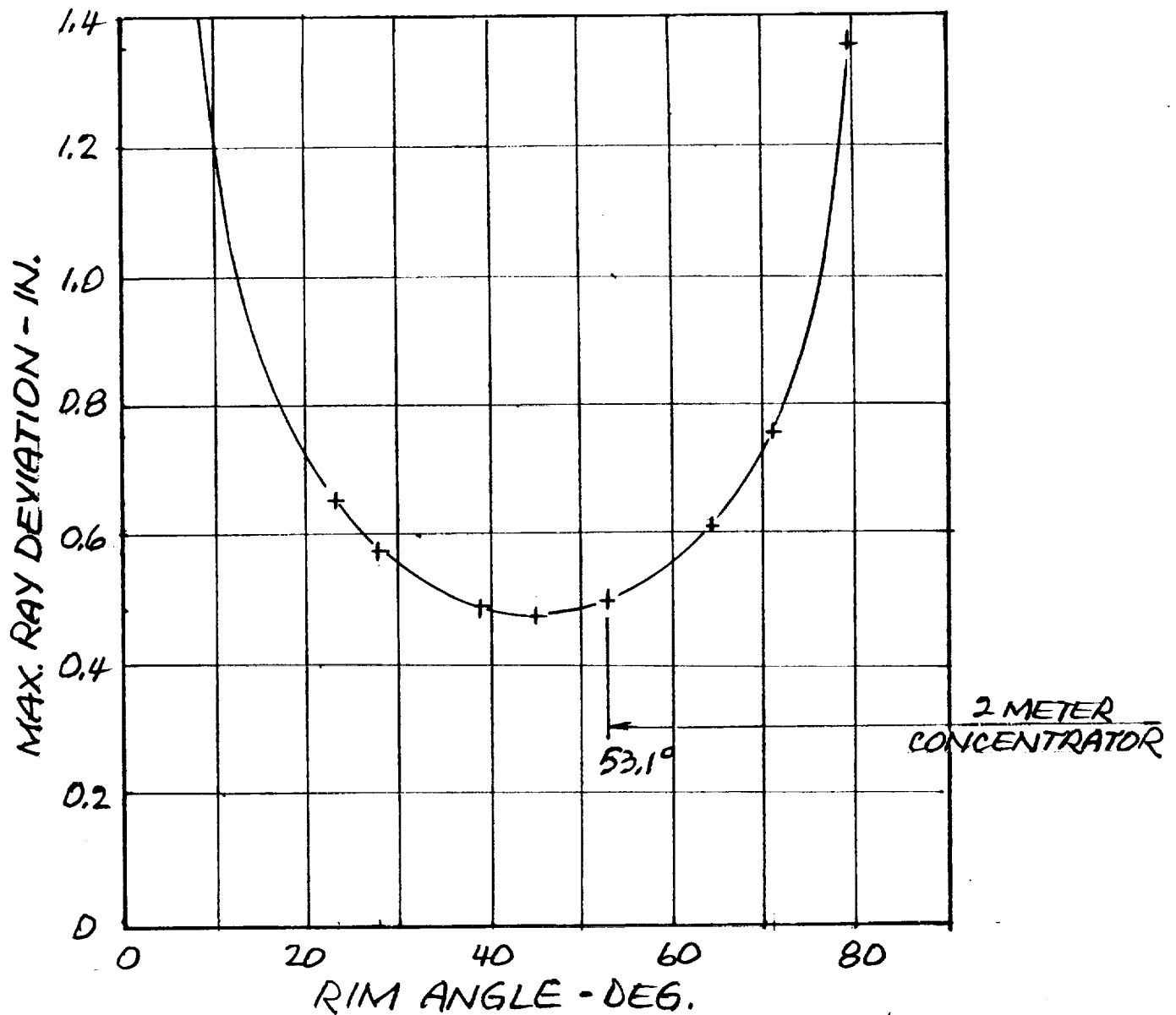


\* 2 METER CONCENTRATOR

RIM ANGLE VERSUS F/D RATIO

FIGURE 4

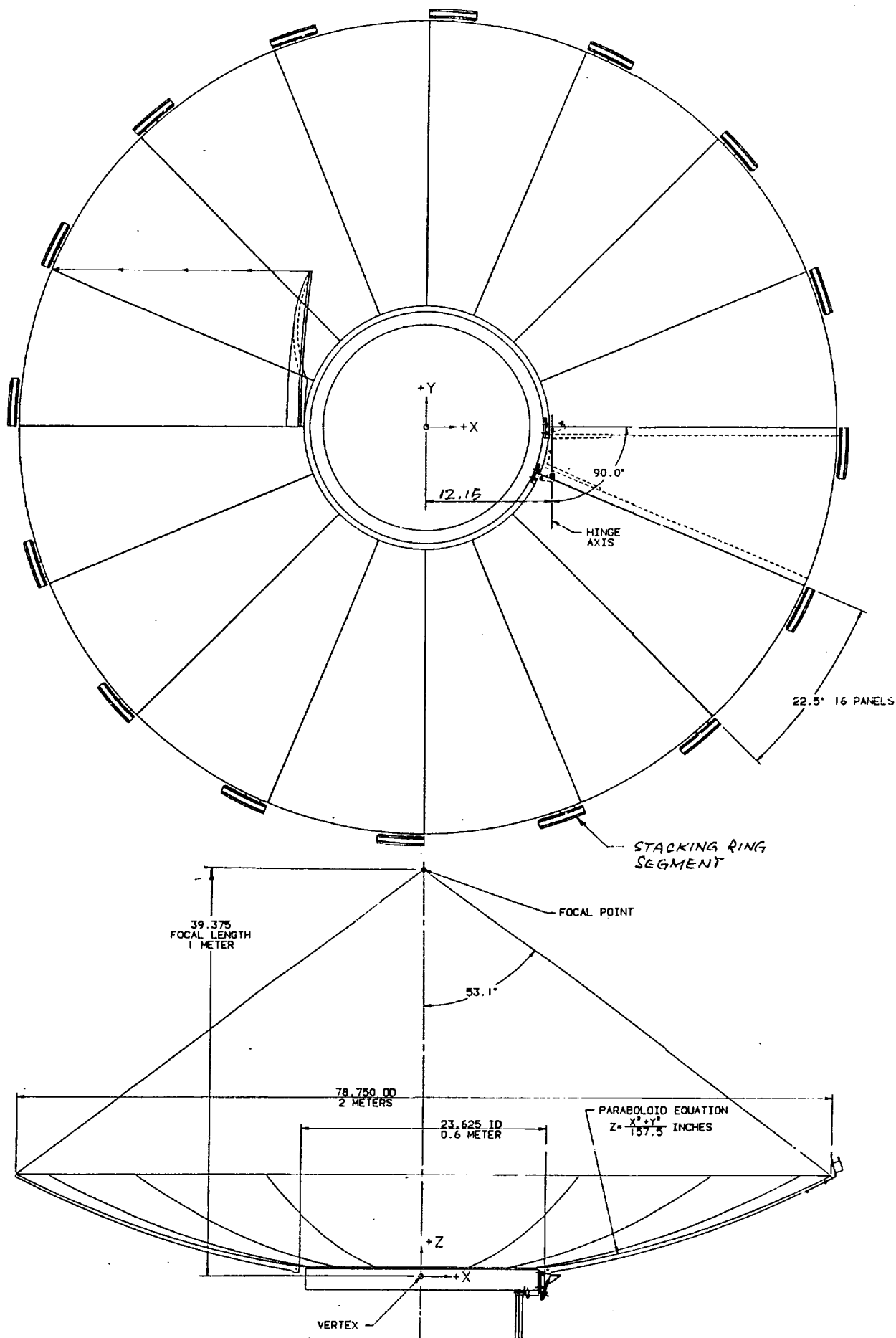
# RAY DEVIATION VERSUS RIM ANGLE



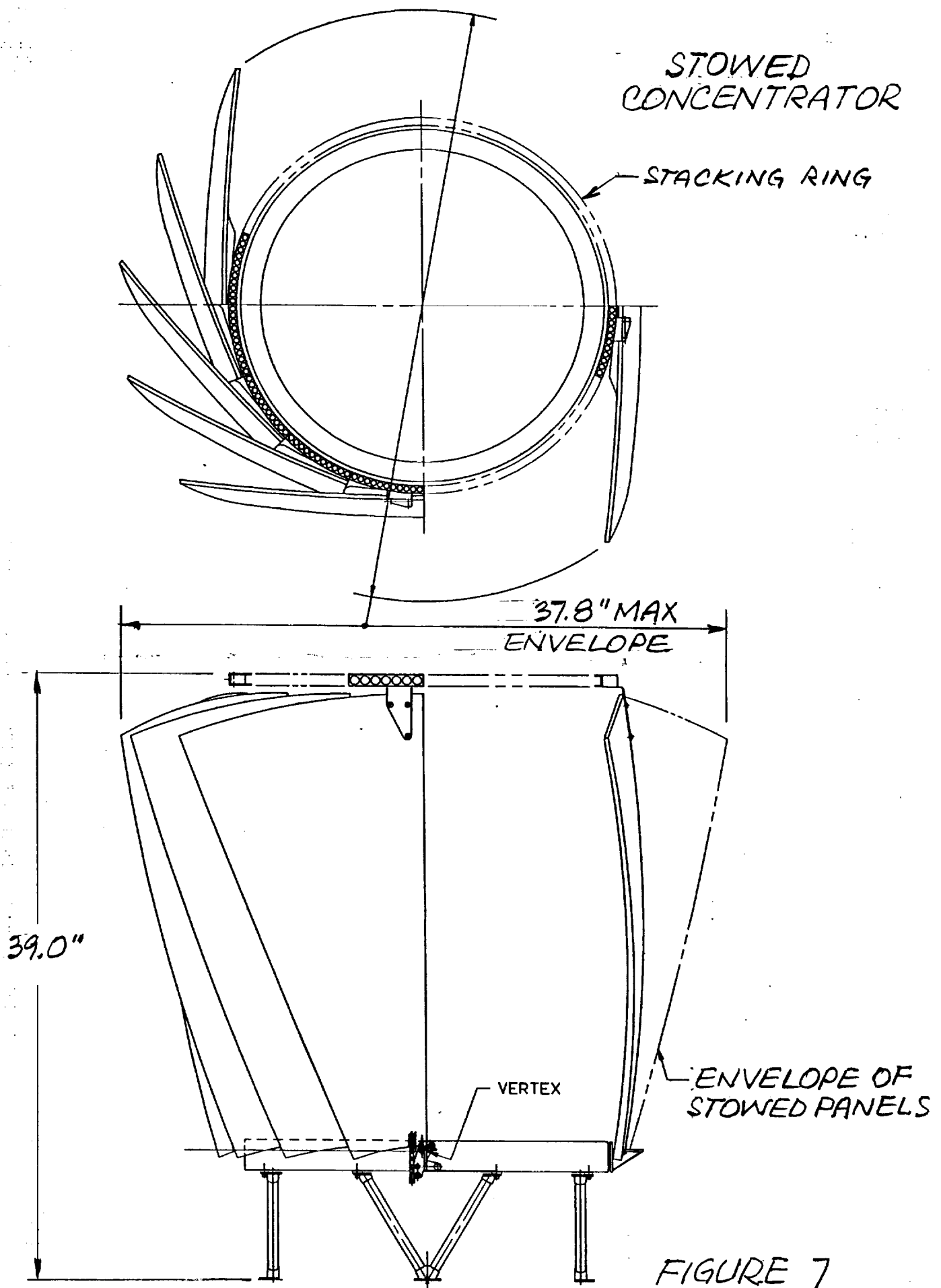
REF: FIGURE 4

FIGURE 5





DEPLOYED CONCENTRATOR FIGURE 6



# PANEL HINGE GEOMETRY

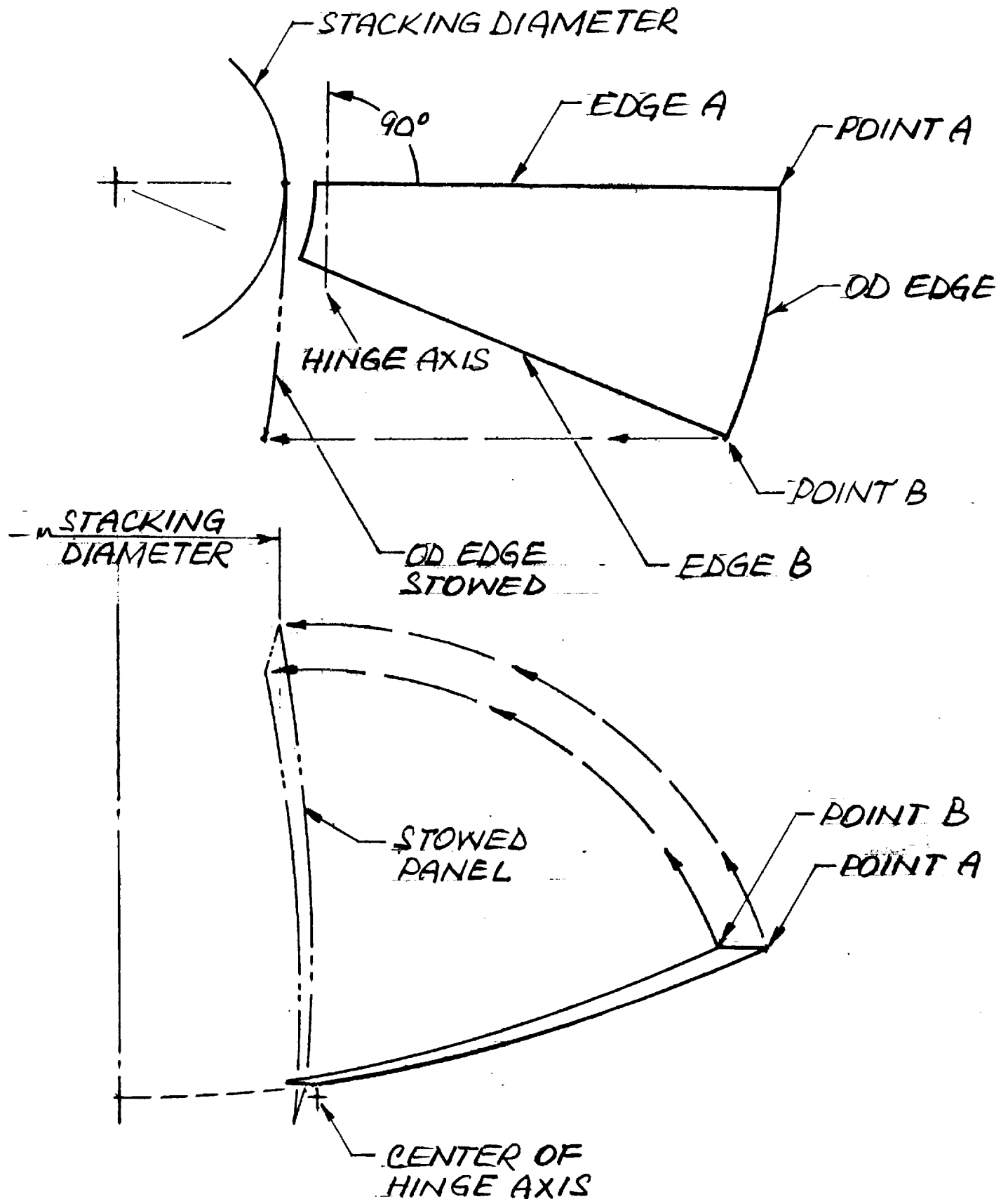
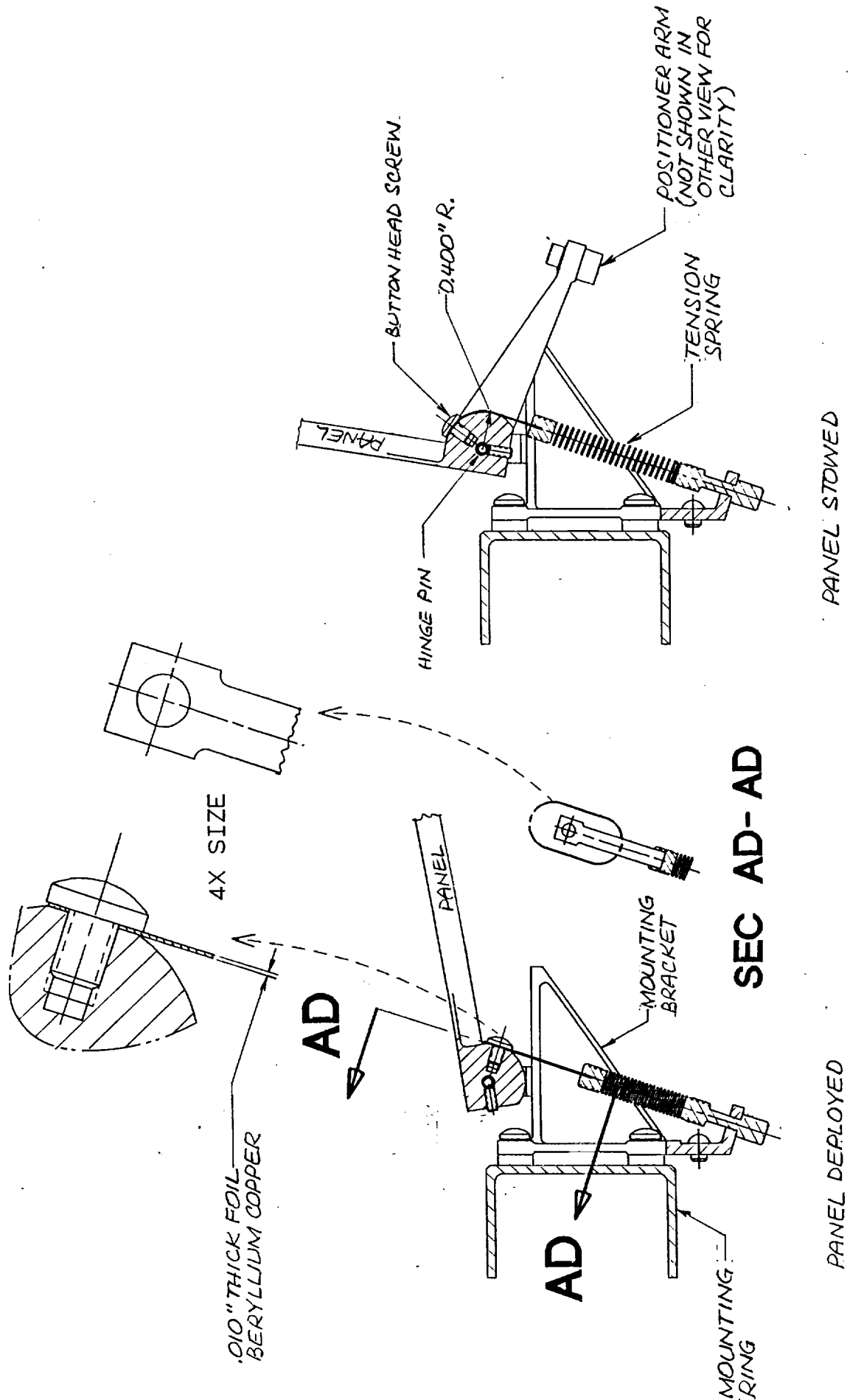
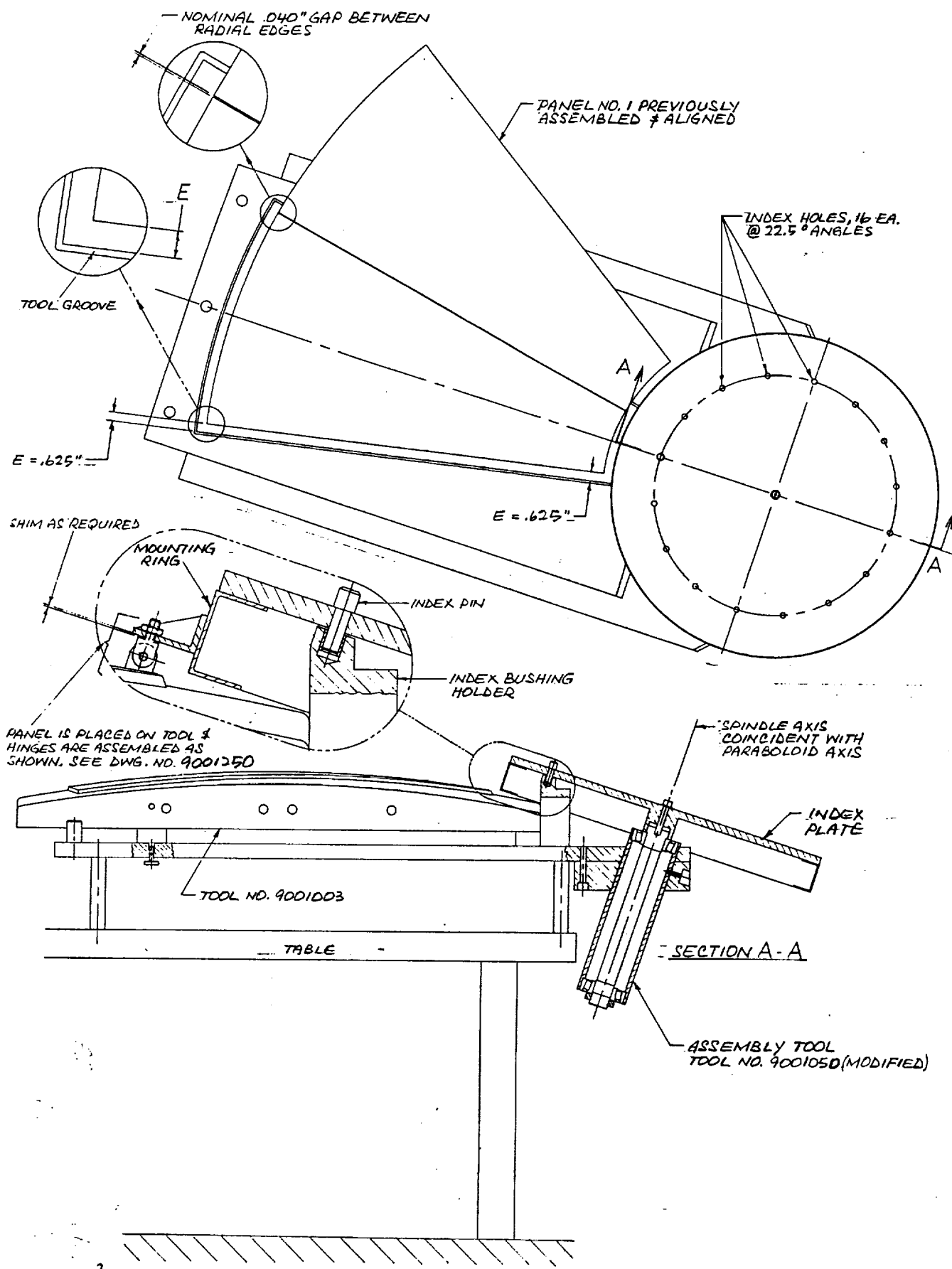


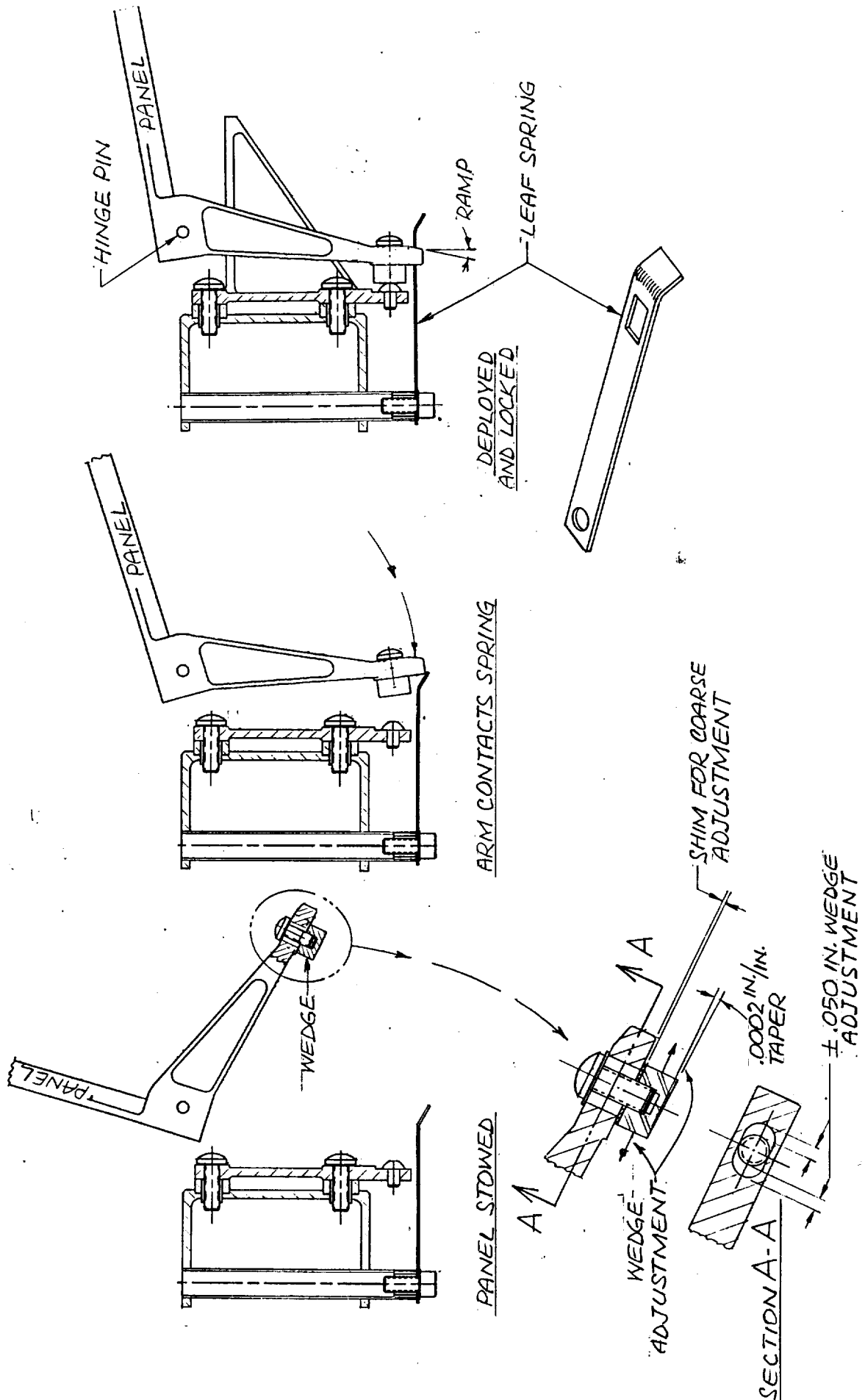
FIGURE 8.



PANEL DEPLOYMENT ACTUATOR      FIGURE 9

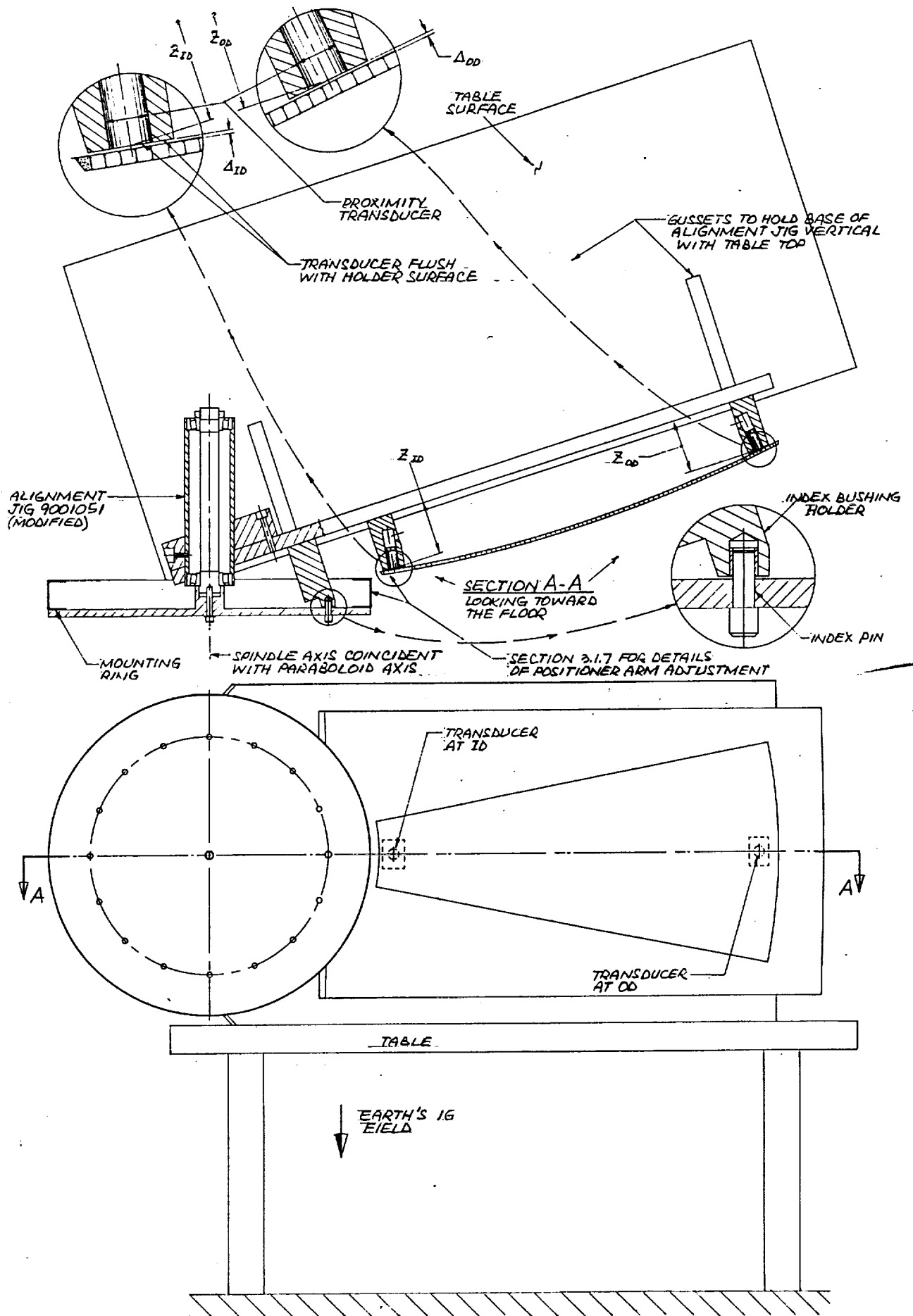


ASSMBLY JIG FIGURE 10



PANEL POSITIONER

FIGURE 11



POSITIONER JIG FIGURE 12

# TEMPERATURE GRADIENTS LOW EARTH ORBIT

## CONCENTRATOR SURFACE TEMPERATURES

HEAT TRANSFER SIMULATION FOR LEO

FRONT FACE EMISSIVITY, .04 BACK FACE EMISSIVITY 0.2

FRONT FACE ABSORPTIVITY 0.1

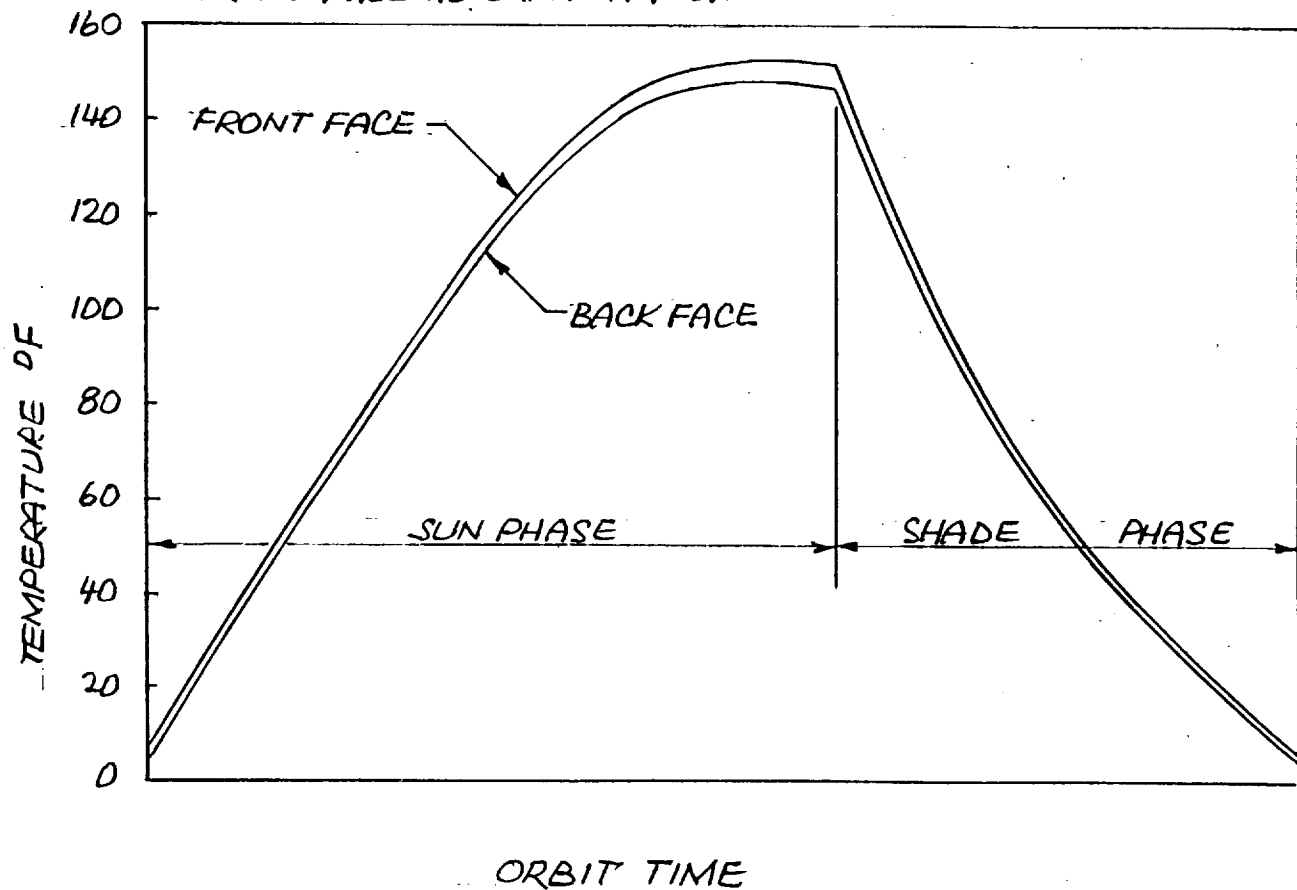
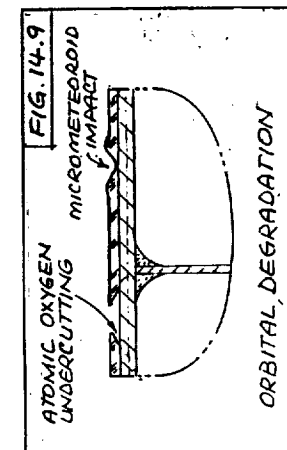
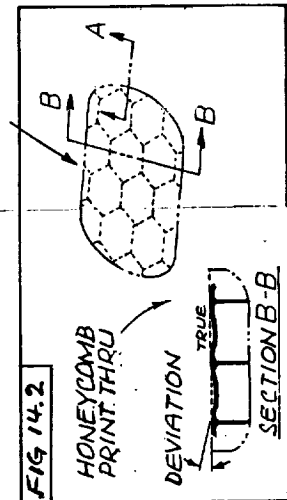
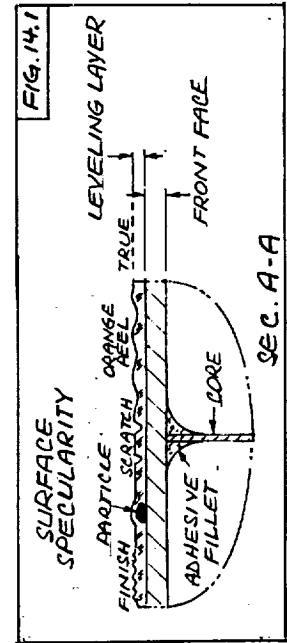
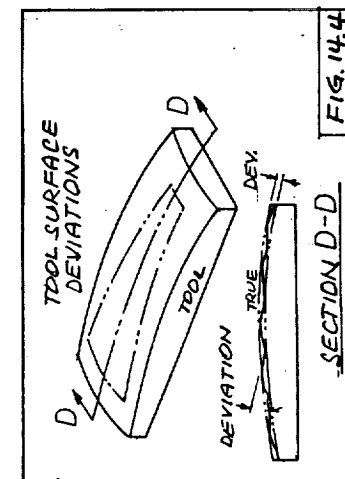
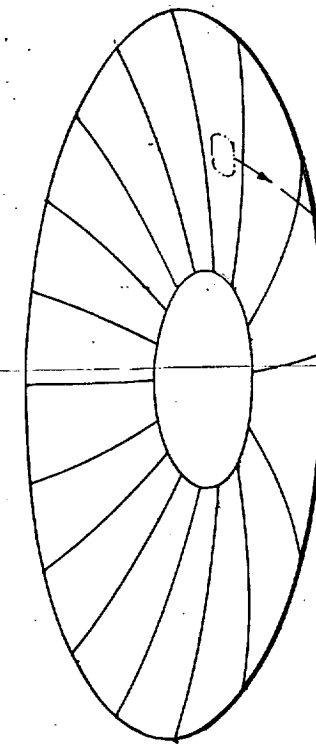
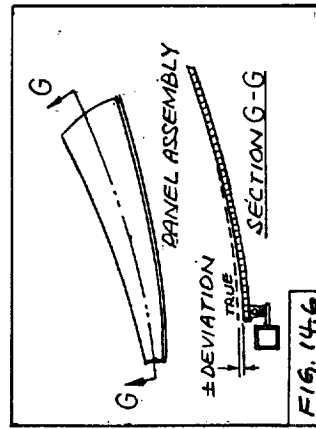
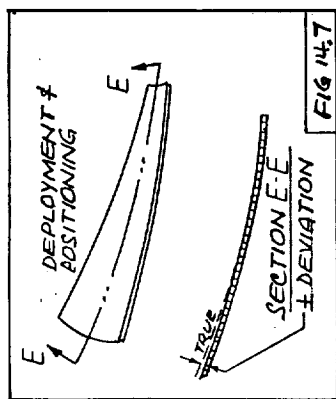
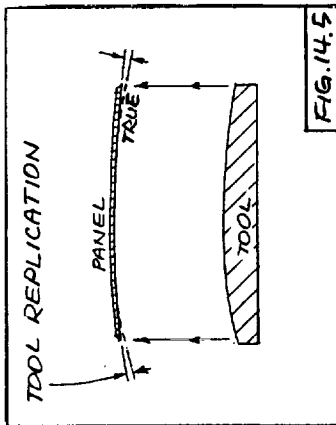
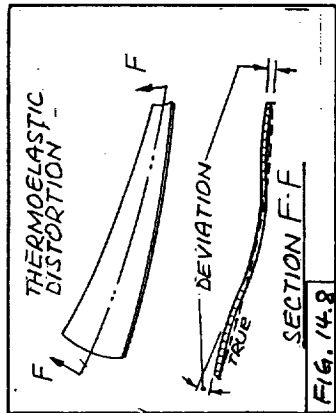
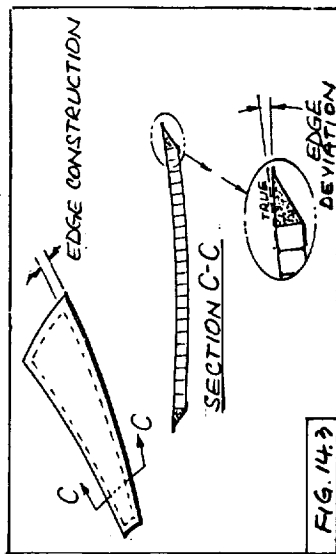


FIGURE 13





SOURCES OF SURFACE DEVIATIONS

# SPECIFIED SURFACE DEVIATIONS FOR TWO METER SOLAR CONCENTRATOR

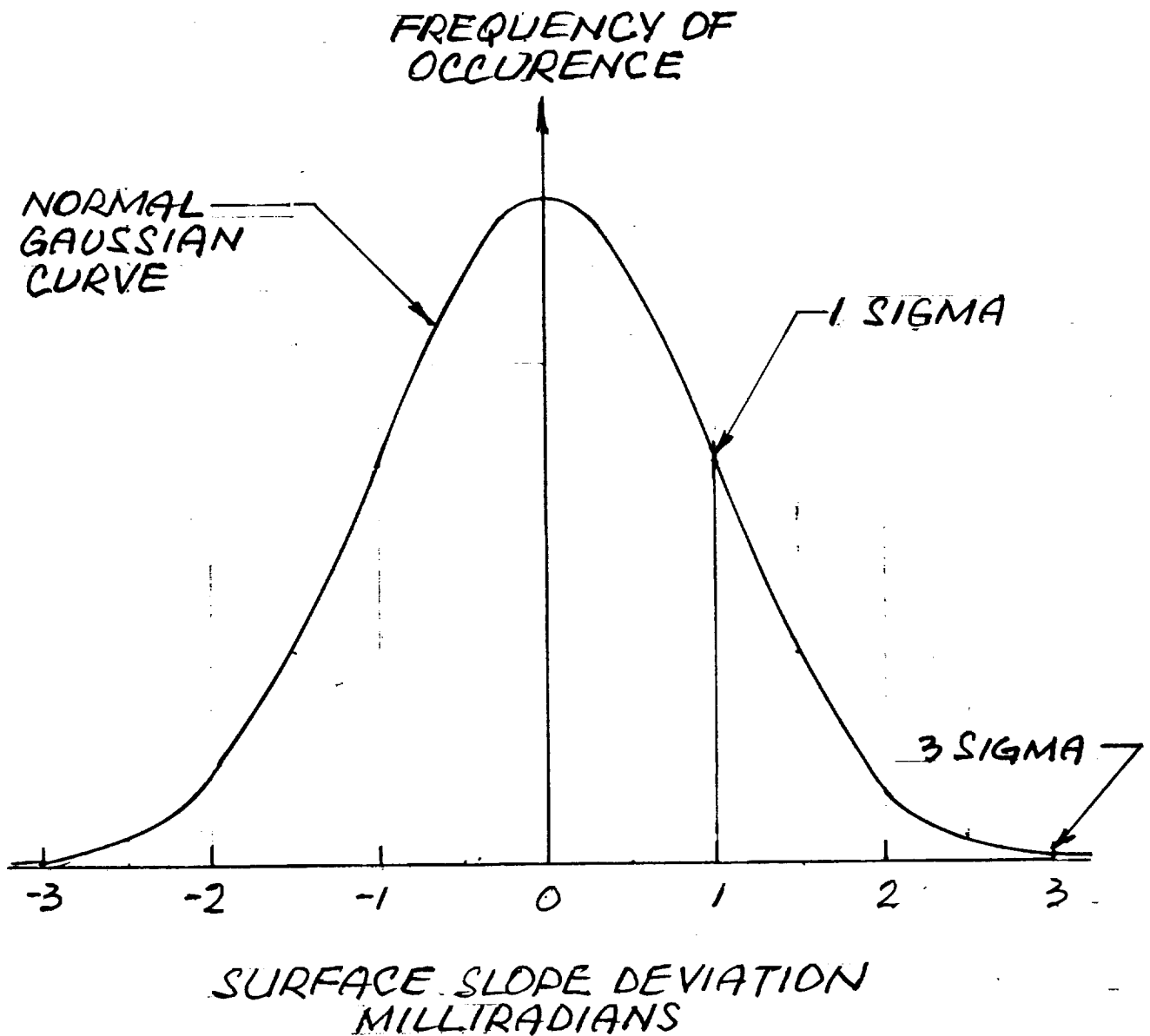
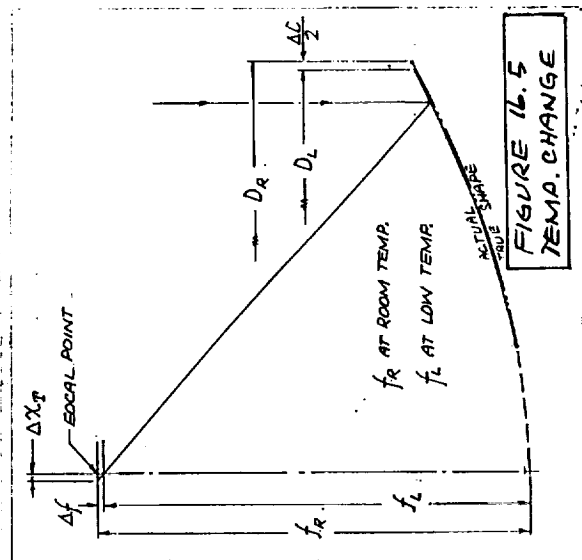
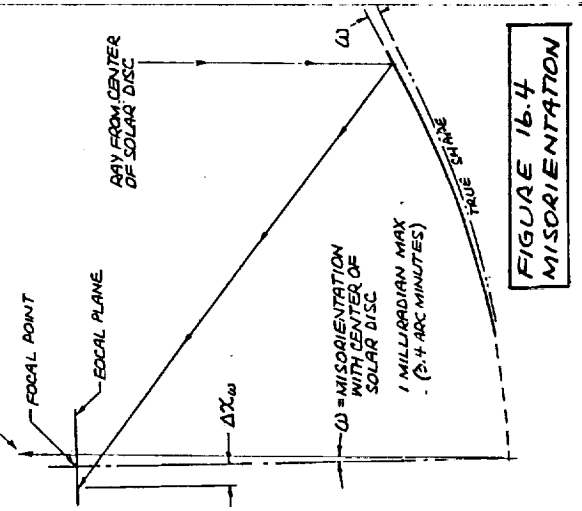
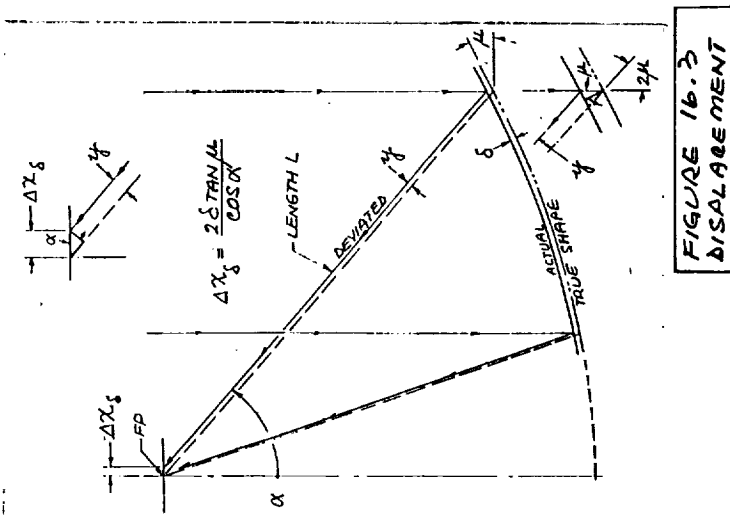
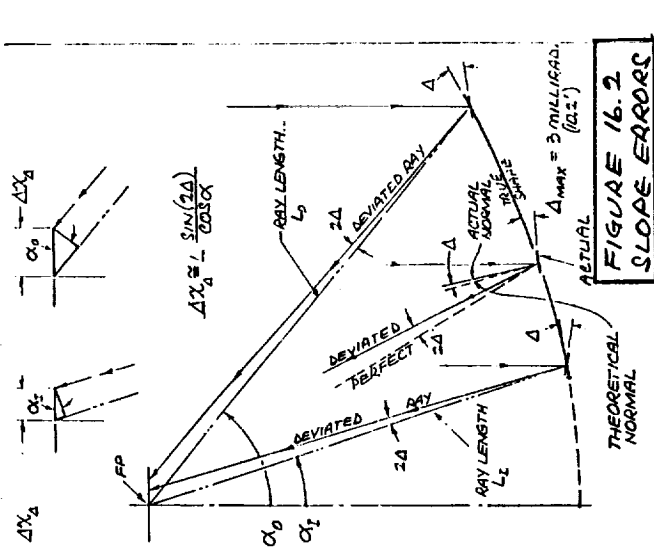
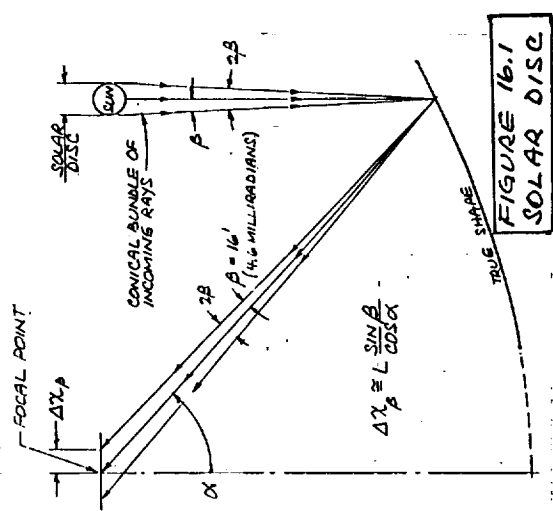
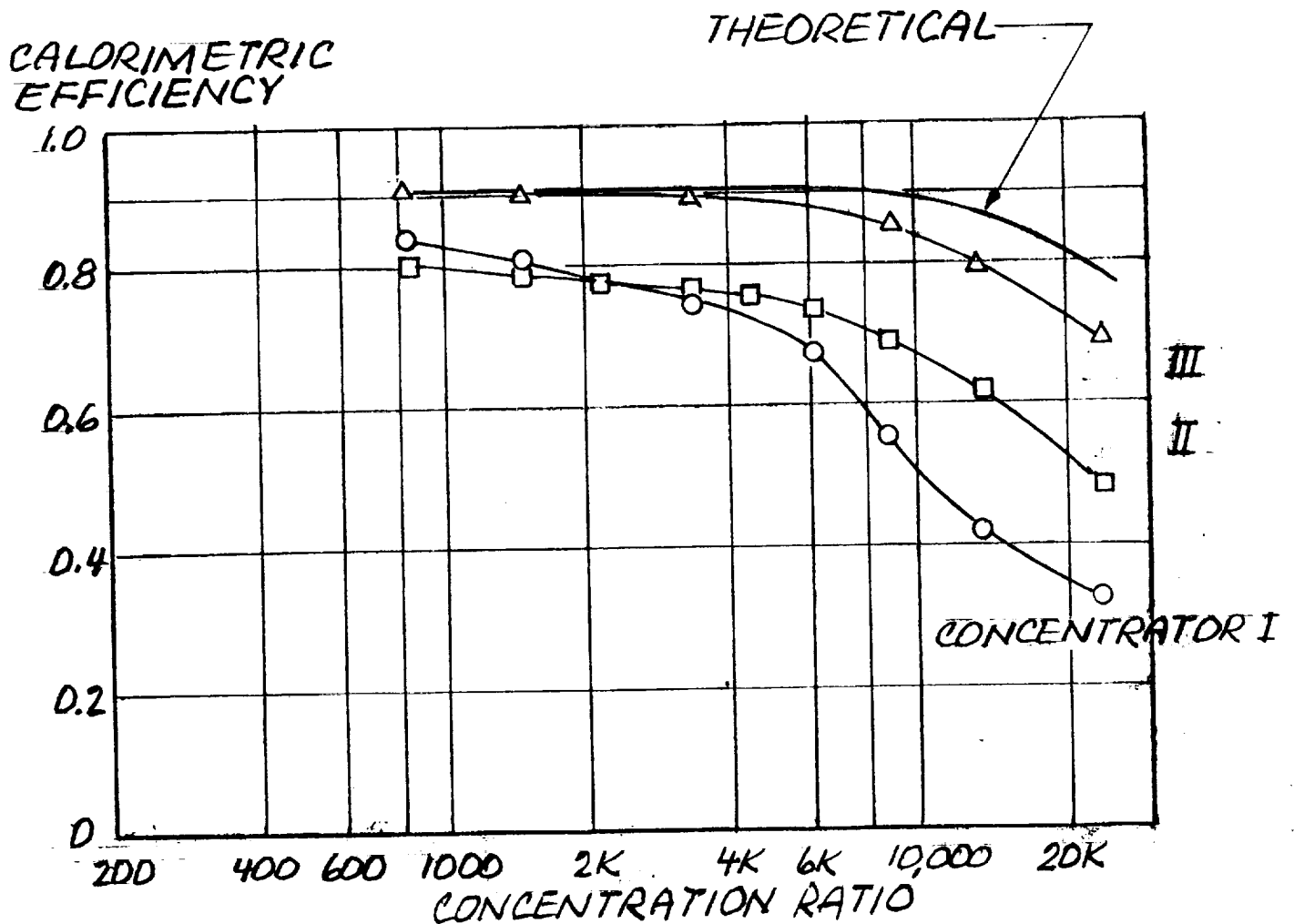


FIGURE 15



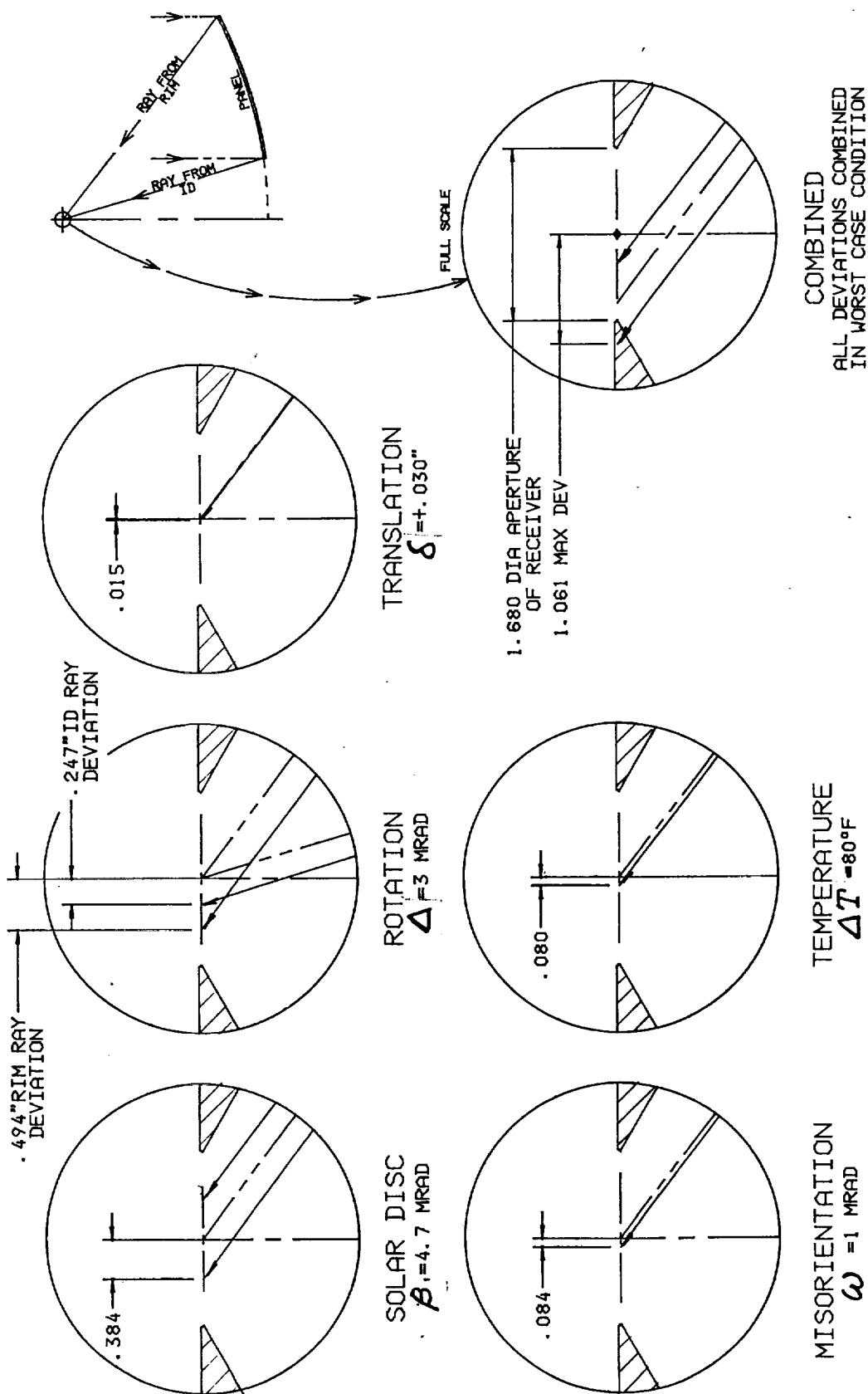
# CALORIMETRIC EFFICIENCY OF 5 FT DIAMETER FIXED DISH SOLAR CONCENTRATOR



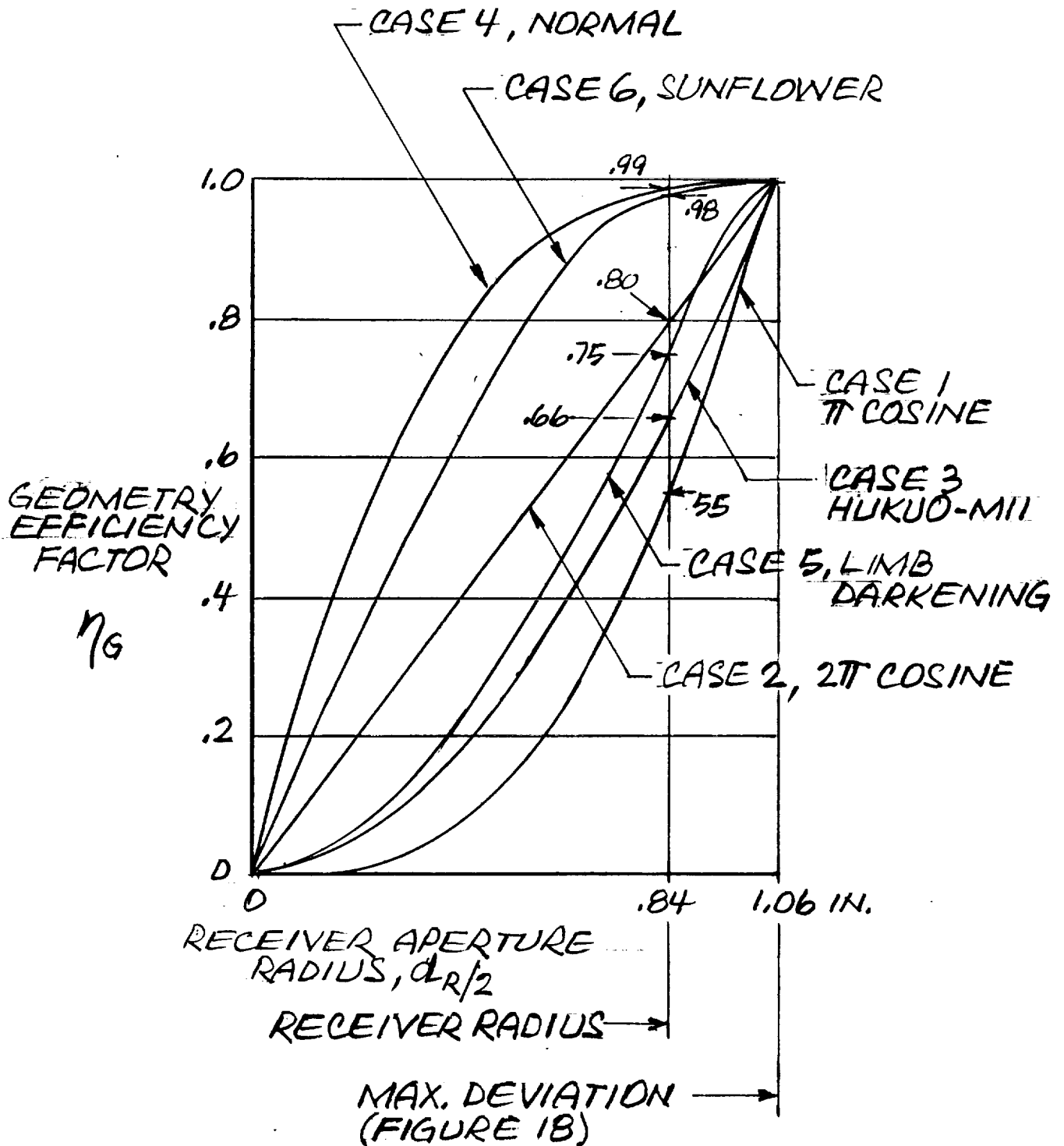
REF: REVIEW OF SOLAR CONCENTRATOR  
TECHNOLOGY, A. HEATH; E. HOFFMAN  
NASA LANGLEY, IECEC CONF. 1966  
FIGURE 2

FIGURE 17

# RAY TRACE RESULTS FOR TWO METER SOLAR CONCENTRATOR (FULL SCALE)



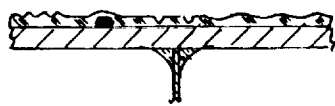
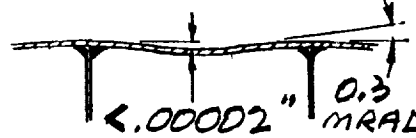
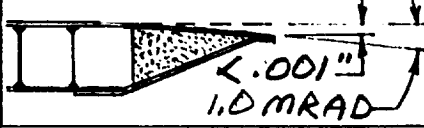
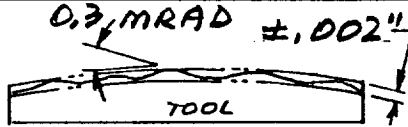
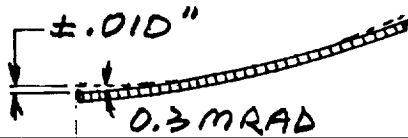
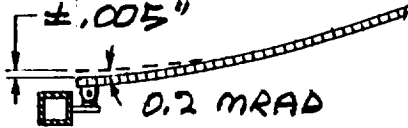
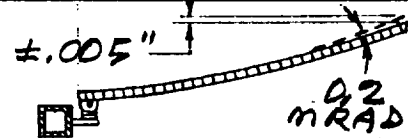
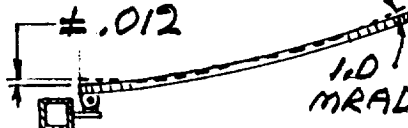
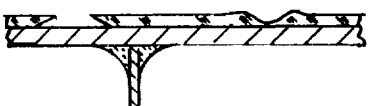

# PROBABLE GEOMETRIC EFFICIENCY TWO METER CONCENTRATOR



REF. 3, FIG 4.1-5

FIGURE 19

# BUDGET OF SURFACE DEVIATIONS FOR TWO METER SOLAR CONCENTRATOR

SOURCE OF * DEVIATION	DEVIATION		REFERENCE SOURCE
	MAXIMUM VALUE	DISTRIB. CURVE	
1 SPECULARITY		$< 2\%$ LOSS DUE TO $\eta_4$ FACTOR	REF. 4
2 HONEYCOMB PRINT THRU	 $< .00002"$ $0.3$ MRAD	$2\pi$ COSINE	REF. 3 AND 2 METER PROJECT
3 EDGE CONSTRUCTION	 $< .001"$ $1.0$ MRAD	SYSTEMATIC	REF. 4
4 CURE TOOL SHAPE	 $0.3$ MRAD $\pm .002"$ TOOL	NORMAL	2 METER
5 PANEL REPLICATION OF TOOL	 $\pm .010"$ $0.3$ MRAD	NORMAL	REF. 7 AND 2 METER PROJECT
6 ASSEMBLY ACCURACY	 $\pm .005"$ $0.2$ MRAD	SYSTEMATIC	REF. 7
7 POSITION CONTROL	 $\pm .005"$ $0.2$ MRAD	SYSTEMATIC	REF. 7
8 THERMOELASTIC DISTORTION	 $\pm .012$ $1.0$ MRAD	SYSTEMATIC	REF. 3
9 ON-ORBIT DEGRADATION		$< 5\%$ LOSS DUE TO $\eta_8$ FACTOR	
COMBINED DEVIATIONS	 $\pm .030"$ $3$ MRAD	CASE 6	REF. 3 (APPEN. B, PG. 6)

\* SEE FIGURE 14

FIGURE 20

# PANEL HONEYCOMB CROSS SECTION

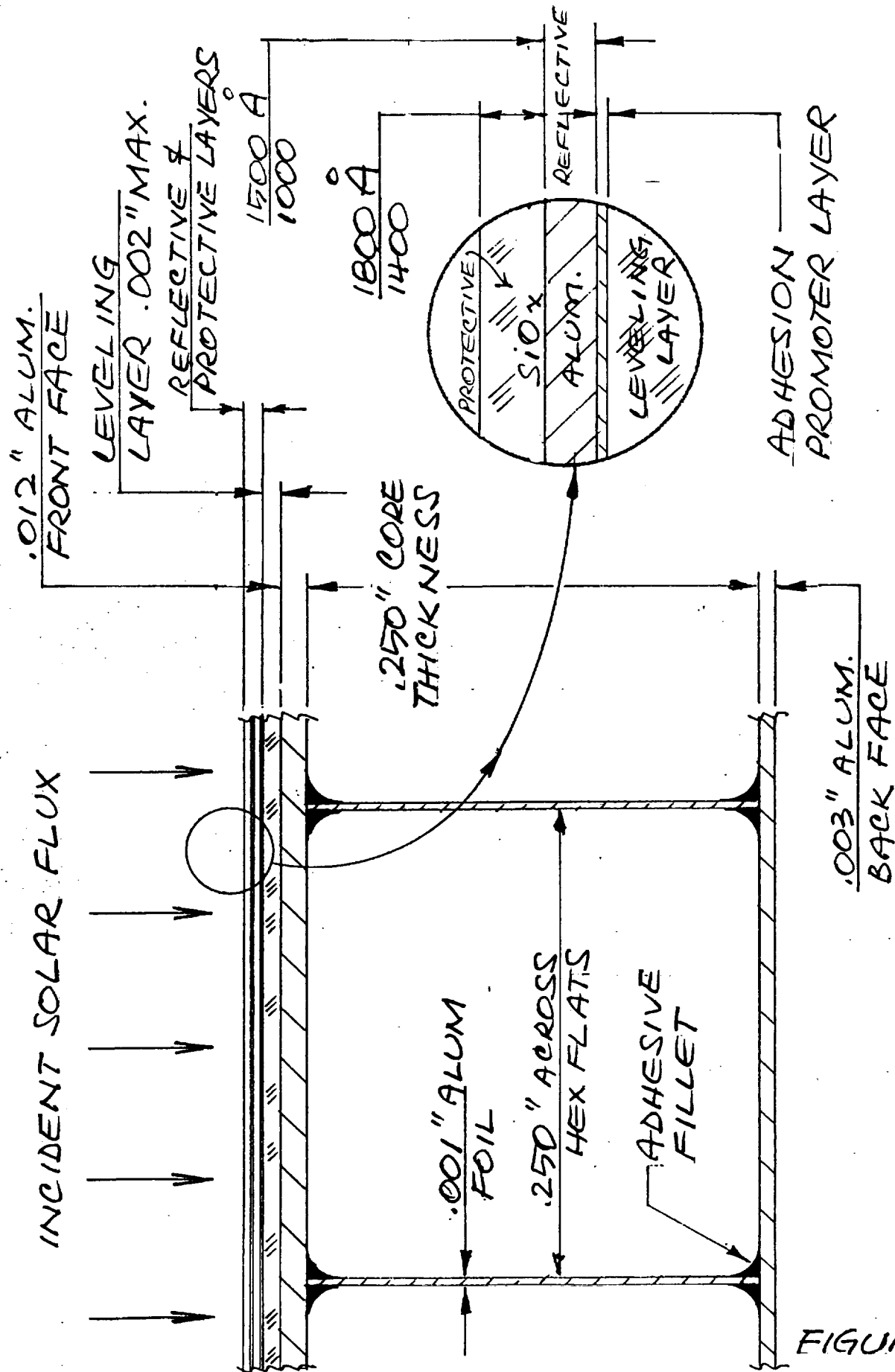


FIGURE 21



1-5 LAYUP PRACTICE

6 THERMATIC 250 ADHES 7 THERMATIC 250 ADHES 11 THERMATIC 250 ADHES

8 THERMATIC 800 ADHES 9 THERMATIC 800 ADHES

10 THERMATIC 850 ADHES

ADHESIVE EVAL

20 .005(HI 9) 23 .008(HI 9)

24 .003(O) 25 .008(O) 26 .008(HI 9)

27 .012(HI 9) 28 .005(HI 9)

29 .012(HI 9) 30 .008(HI 9)

CREST 471 3/16 HEX

12 .003(O) 13 .003(O) 14 .005(HI 9)

15 .008(O) 17 .008(O) 18 .008(HI 9)

21 .012(HI 9) 22 .012(HI 9)

AP9 ADHES 3/16 HEX

32 3/8 HEX 33 1/4 HEX 34 FLEX CORE

CORE SIZE

35 .002 ADHESIVE

36 APS .015 37 APS .010 38 .010 CREST 958

FILLET SIZE

40 TRACKS 43 ADHESIVE DISPENSER

EDGE DISTORTION

41 CORE FLYCUT EXPANDED 42 CORE FLYCUT EXPANDED

44 FINGER PEEL 45 TENSILE TEST 46 NSSR VACUUM TANK

47 TENSILE TEST 48 TENSILE TEST 49 TENSILE TEST

50 ADHESIVE BACK FACE ONLY 51 TOOL UPSIDE DOWN 53 DOUBLE FILLET DIP 55 FILLER IN ADHESIVE

PRINT THRU REDUCTION

56 EP-3 57 EP-3

LEVELING LAYER APPLIED

52 CORE CUT HALF WAY

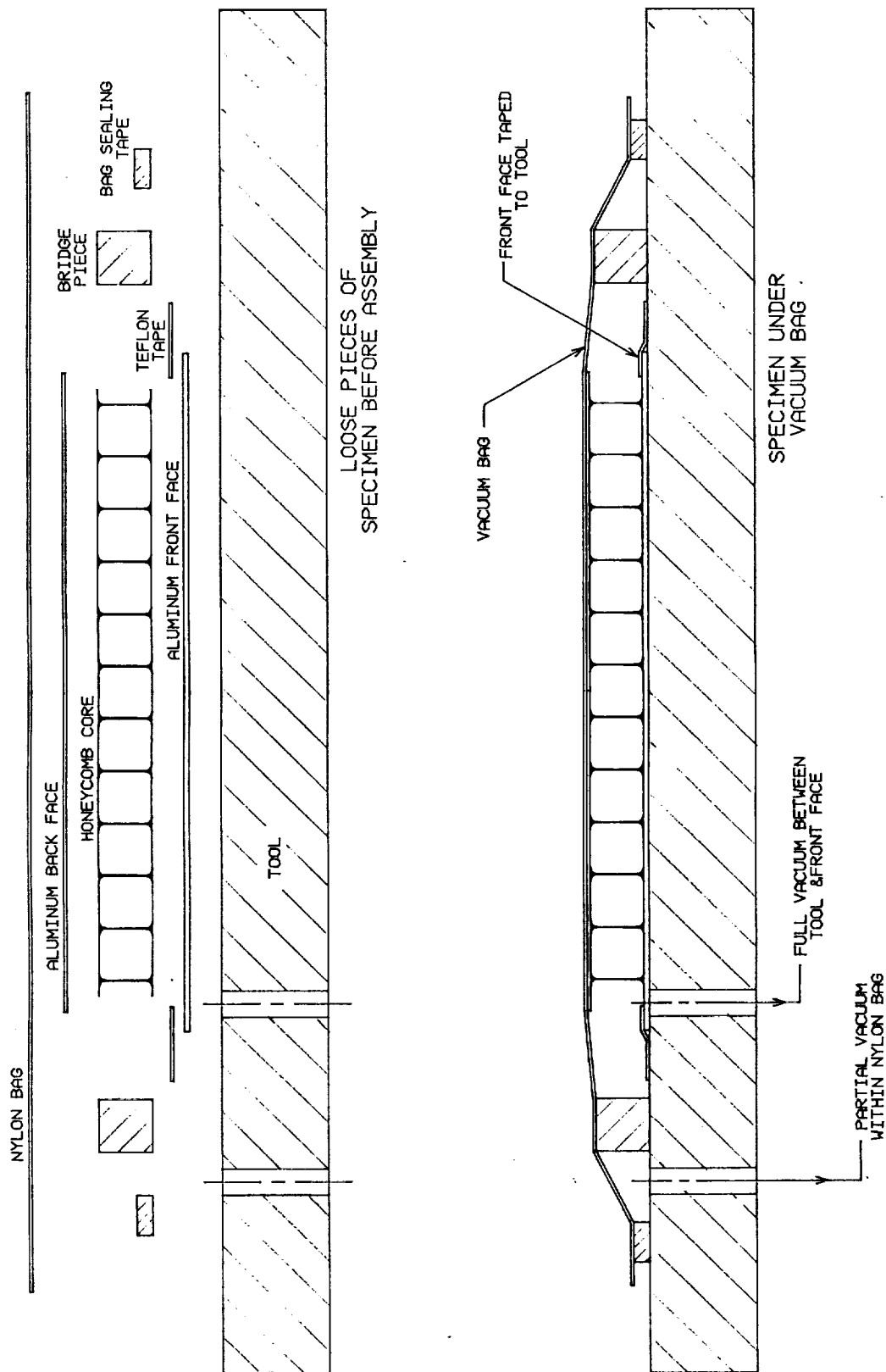
CORE DISTORTION

ADHESIVE STRENGTH

2 EA 4"X30 6 EA 1.40"X30 1 EA 4"X30 3 EA 4"X30 2 EA 1.40"X30 5 EA LAP SHEAR 5 EA 1.40"X30 1 EA 4"X30 5 EA 1.40"X30 5 EA LAP SHEAR 1 EA 4"X30

FIGURE 22

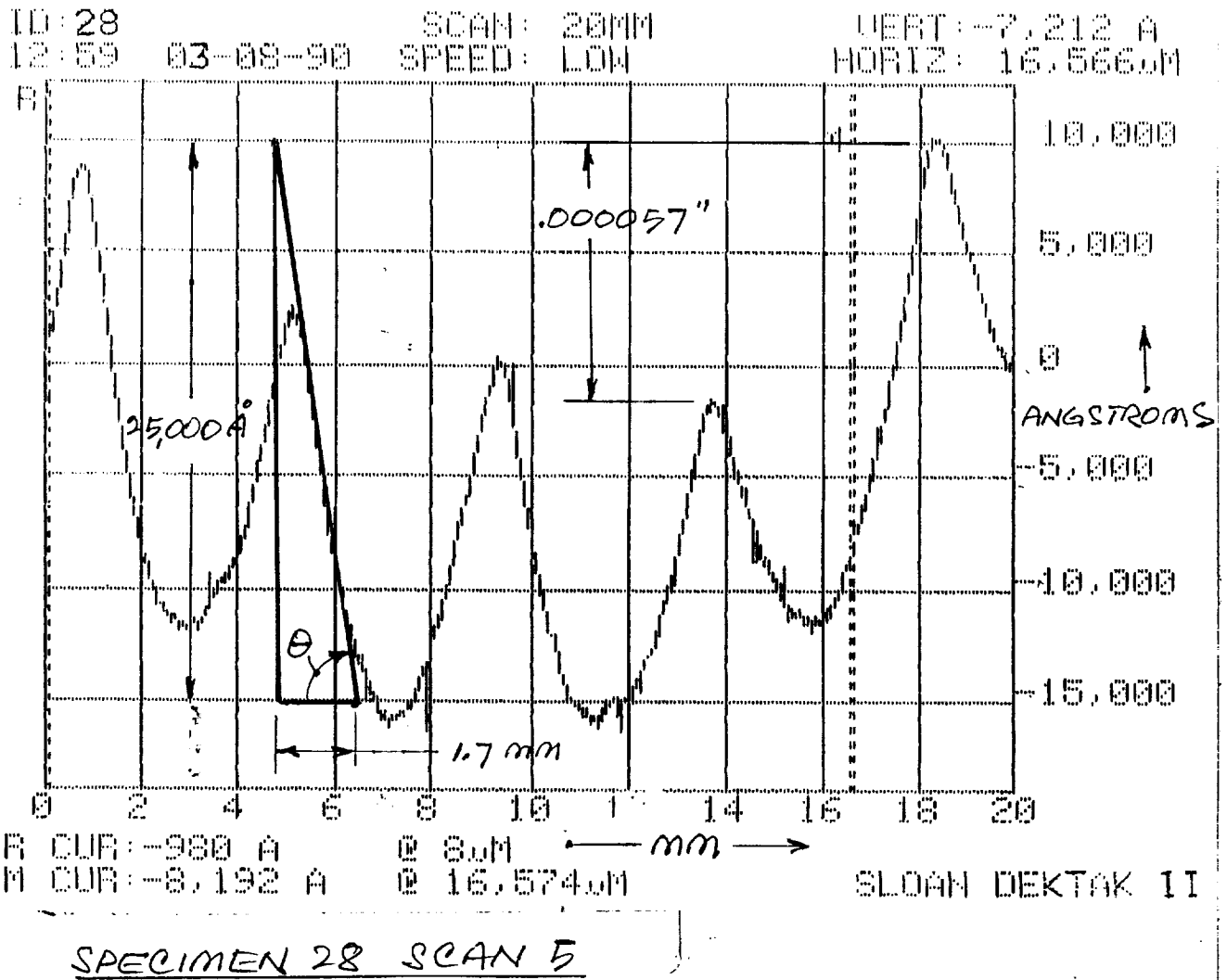
# VACUUM BAG CURING OF HONEYCOMB SPECIMEN



VACUUM BAG CURING SET-UP

FIGURE 23

# PROFILOMETER CHART



$$\theta = \frac{25,000 \text{ Å}}{1.7 \text{ mm}} = \frac{.000125''}{.067''} = .0019 \text{ Radian}$$

FIGURE 24

# 

ID: 30

03:00

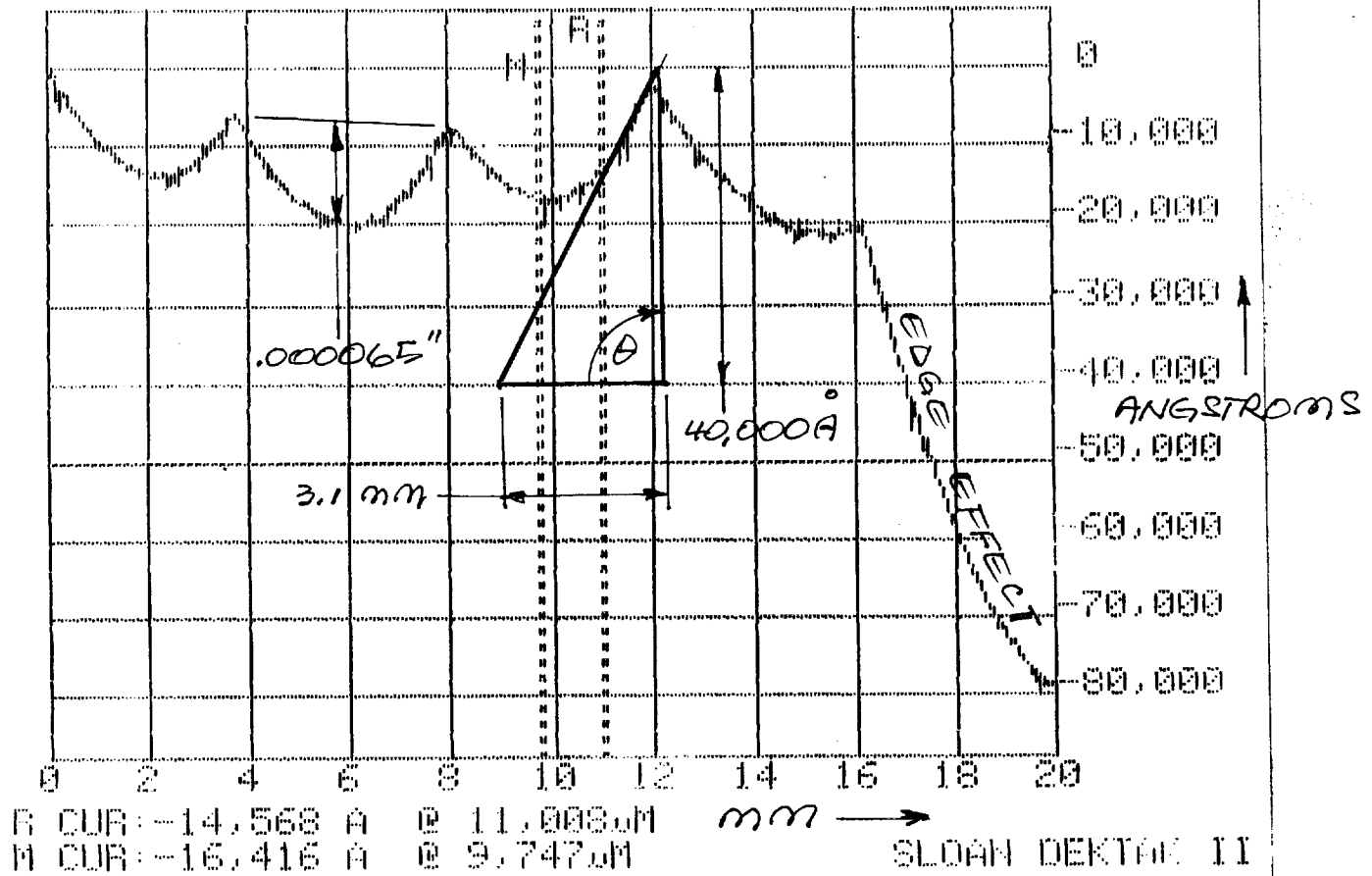
03-27-90

SCAN: 20MM

SPEED: LOW

VERT: -1.849 A

HORIZ: -1.261 μm

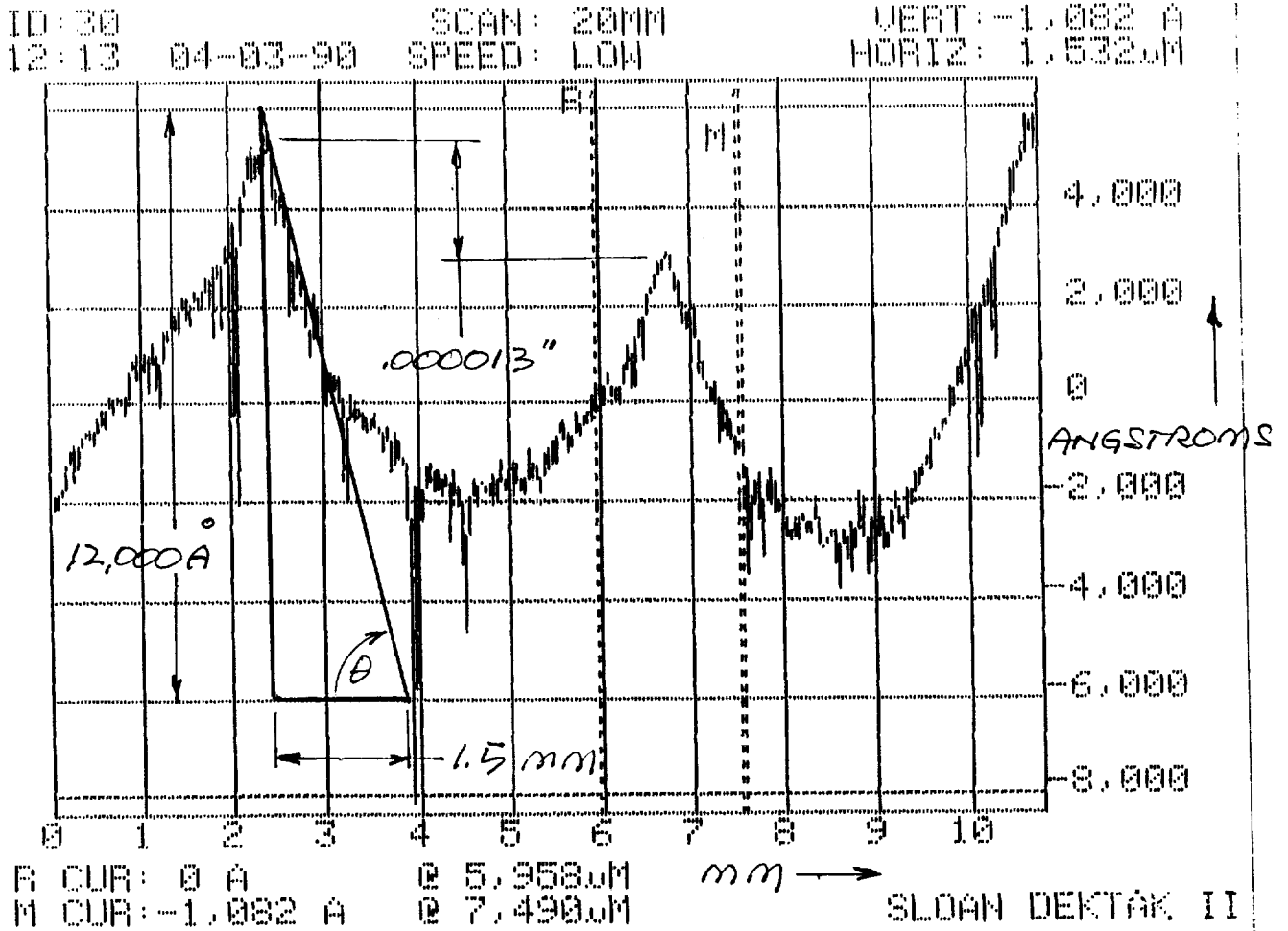


SPECIMEN 30 SCAN 1A

$$\theta = \frac{40,000 \text{ Å}}{3.1 \text{ mm}} = \frac{.0002''}{.122''} = .0016 \text{ RADIANS}$$

FIGURE 25

# 



SPECIMEN 30 SCAN 3B

$$\theta = \frac{12,000 \text{ Å}}{1.5 \text{ mm}} = \frac{.00006}{.059} = .0010 \text{ RADIANT}$$

FIGURE 26

# SPECIMEN 30 SCAN 1A

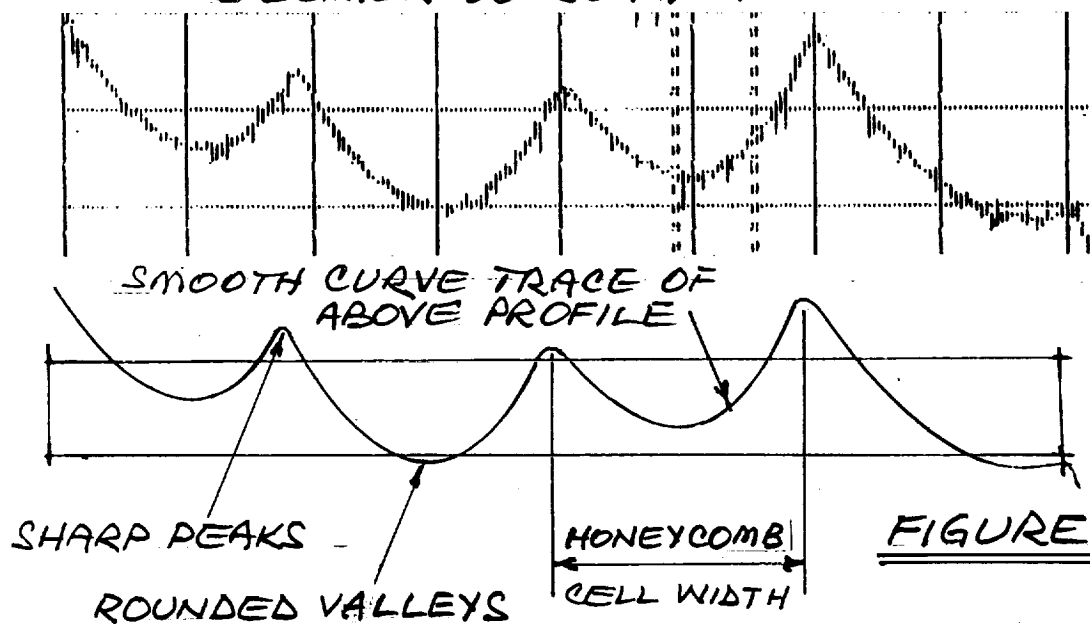


FIGURE 27A

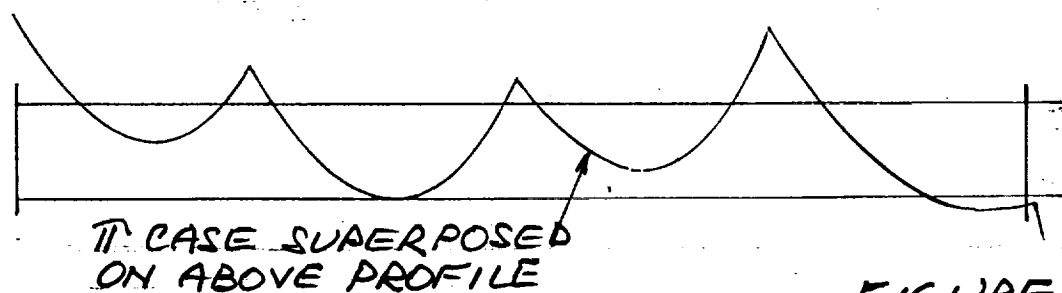


FIGURE 27B

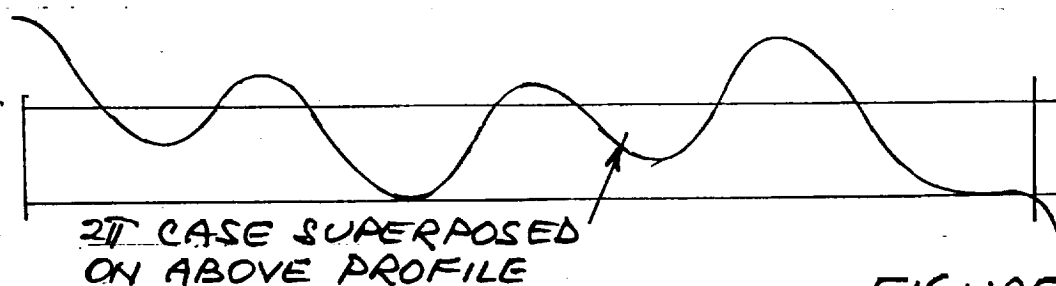
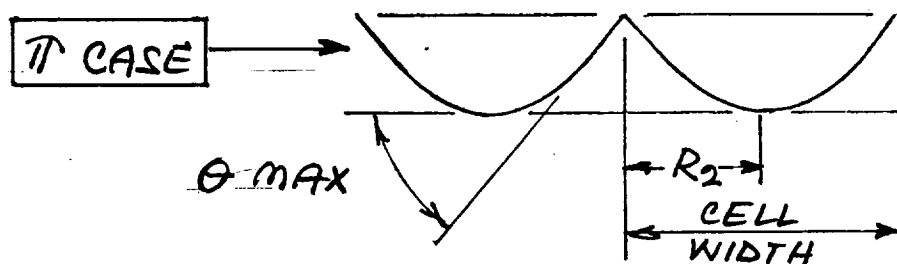


FIGURE 27C

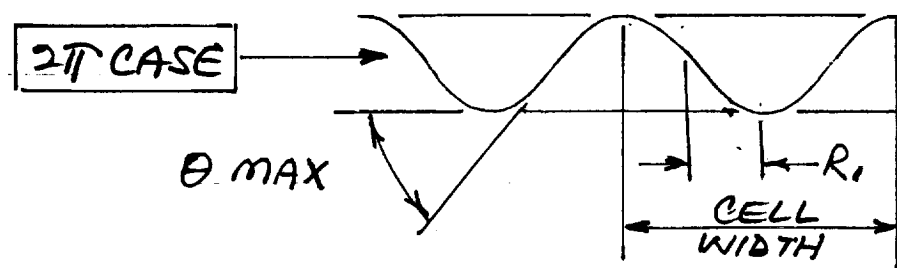


FIGURE 27

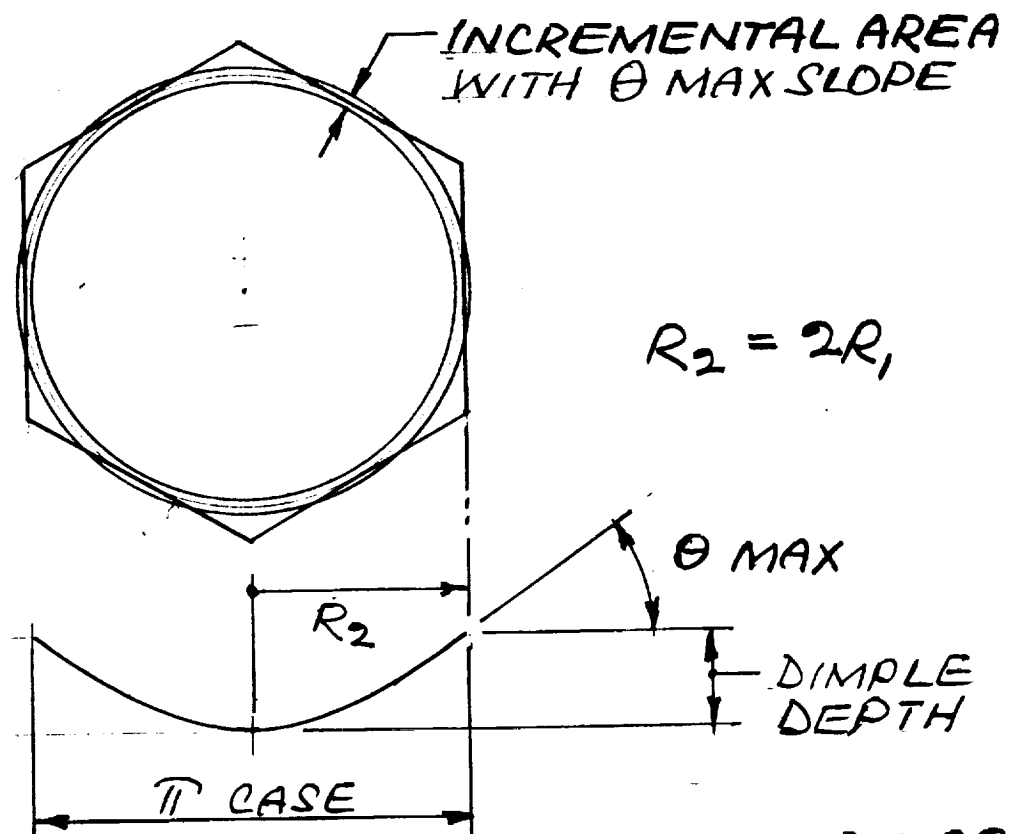
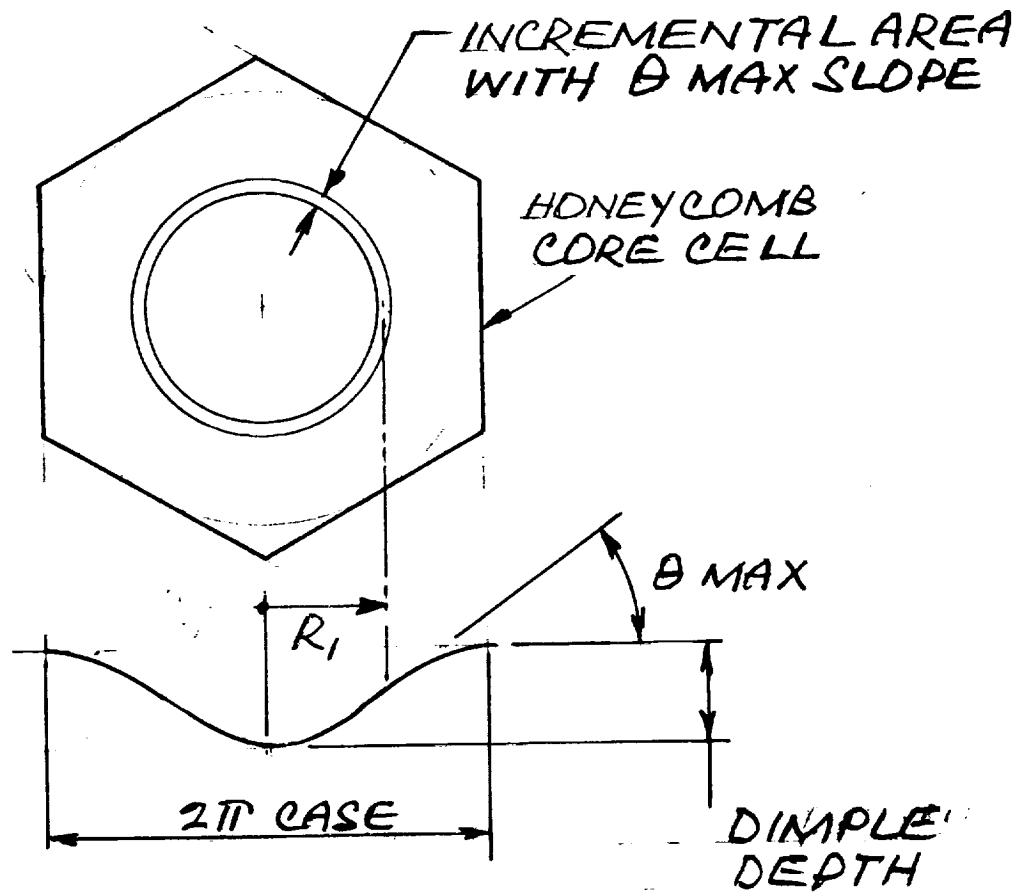
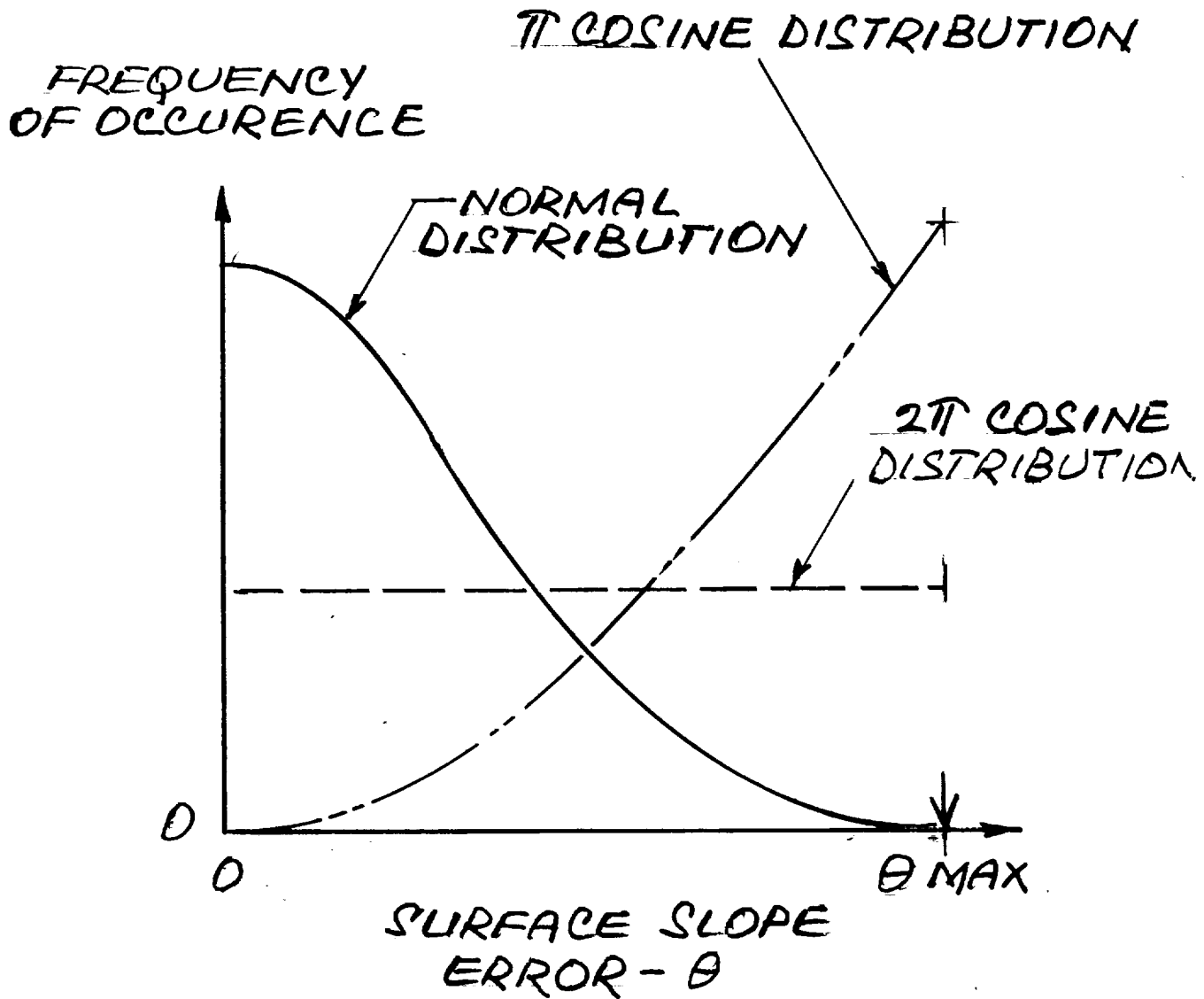


FIGURE 28

# SURFACE DEVIATION DISTRIBUTION CURVES



REF. 3, FIG 4.1.2

FIGURE 29



# SURFACE SLOPE ERROR\* VS CORE HEX SIZE

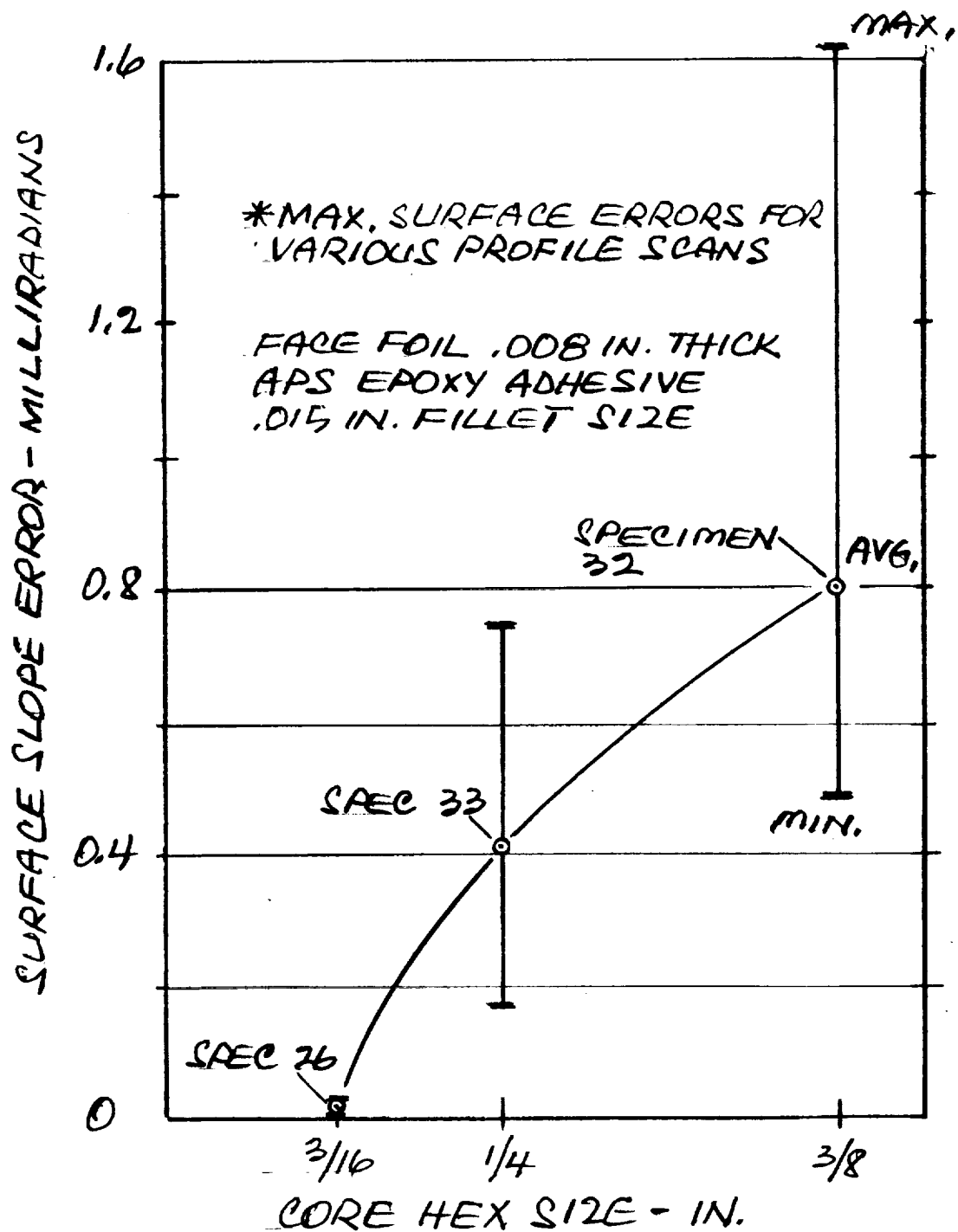


FIGURE 30

# SURFACE SLOPE ERROR\* VERSUS FACE THICKNESS

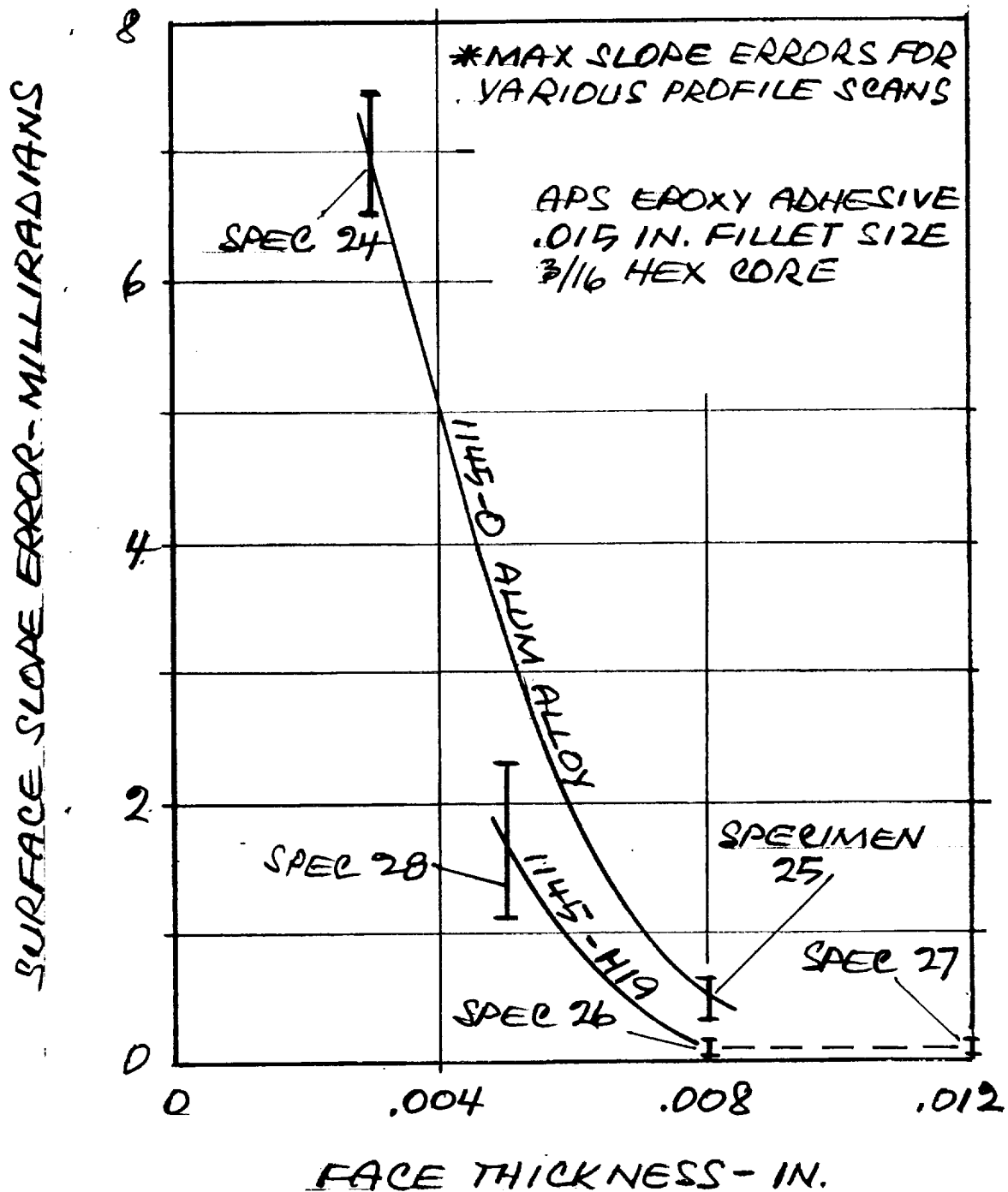
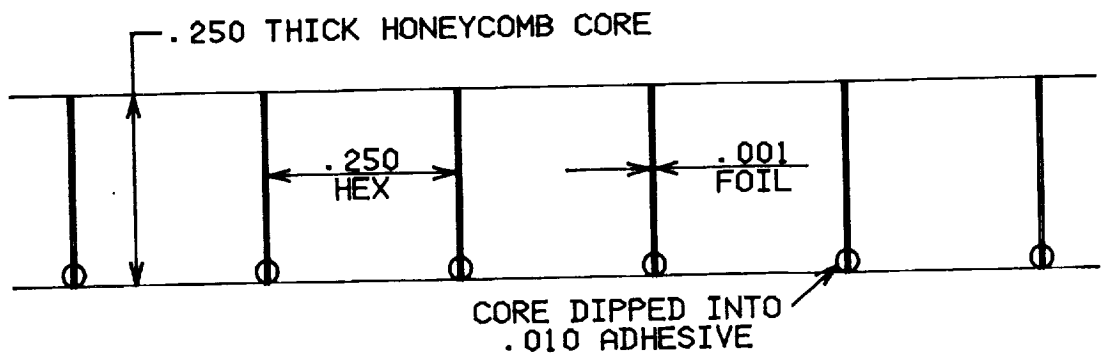


FIGURE 31

# DOUBLE DIP ADHESIVE FILLET PROCESS



STEP 1

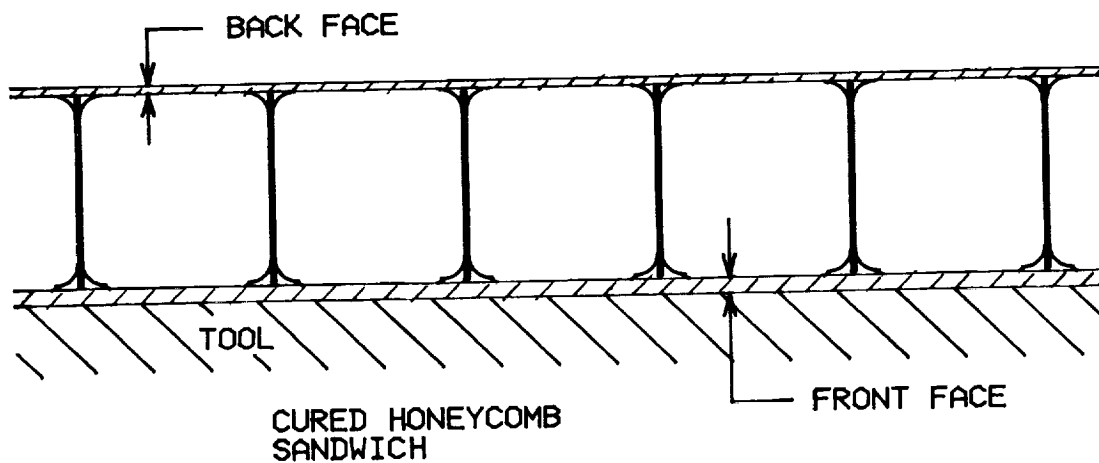
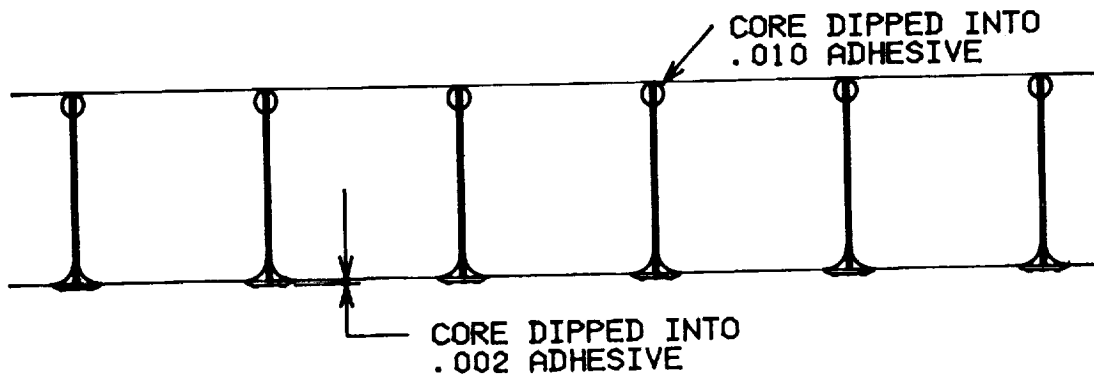
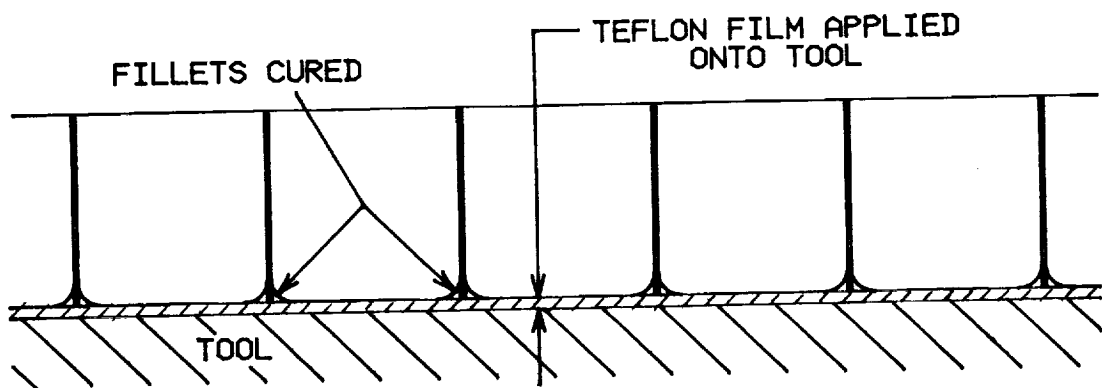


FIGURE 32

# CLASSICAL SULFURIC ACID/SODIUM DICHROMATE CLEAN & ETCH PROCESS

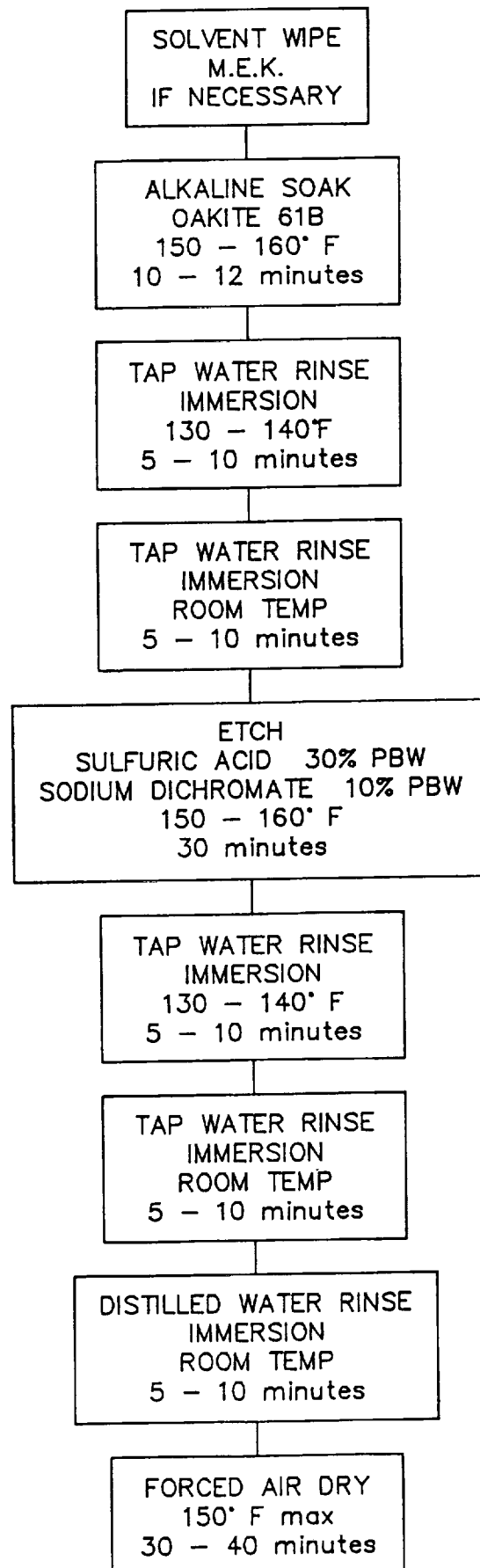
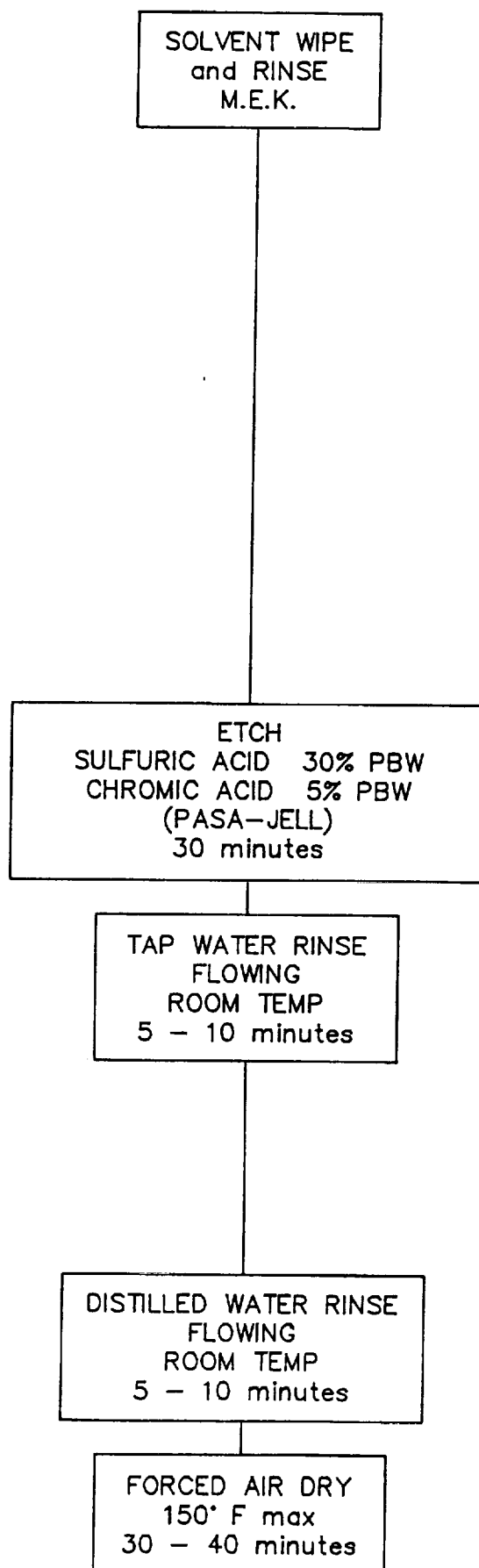


FIGURE 33

# PASTE CLEAN & ETCH PROCESS



C-2.

FIGURE 34

## PROCESS EVALUATION NO. 1 - ANODIZE

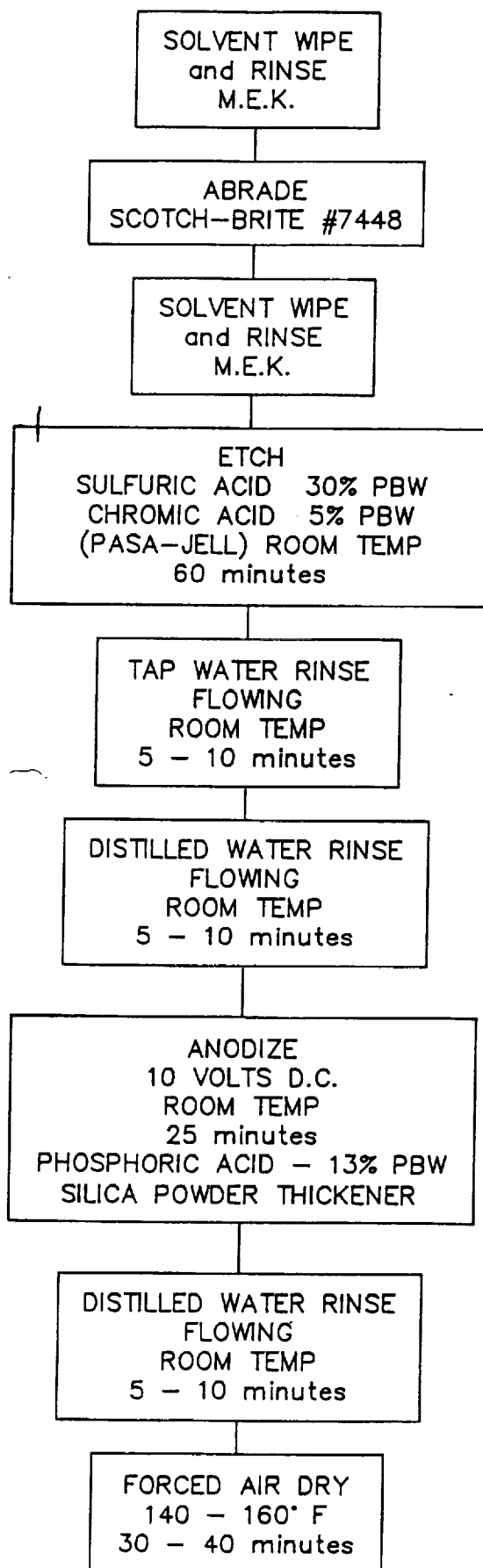


FIGURE 35

## PROCESS EVALUATION NO. 2 - ABRASION

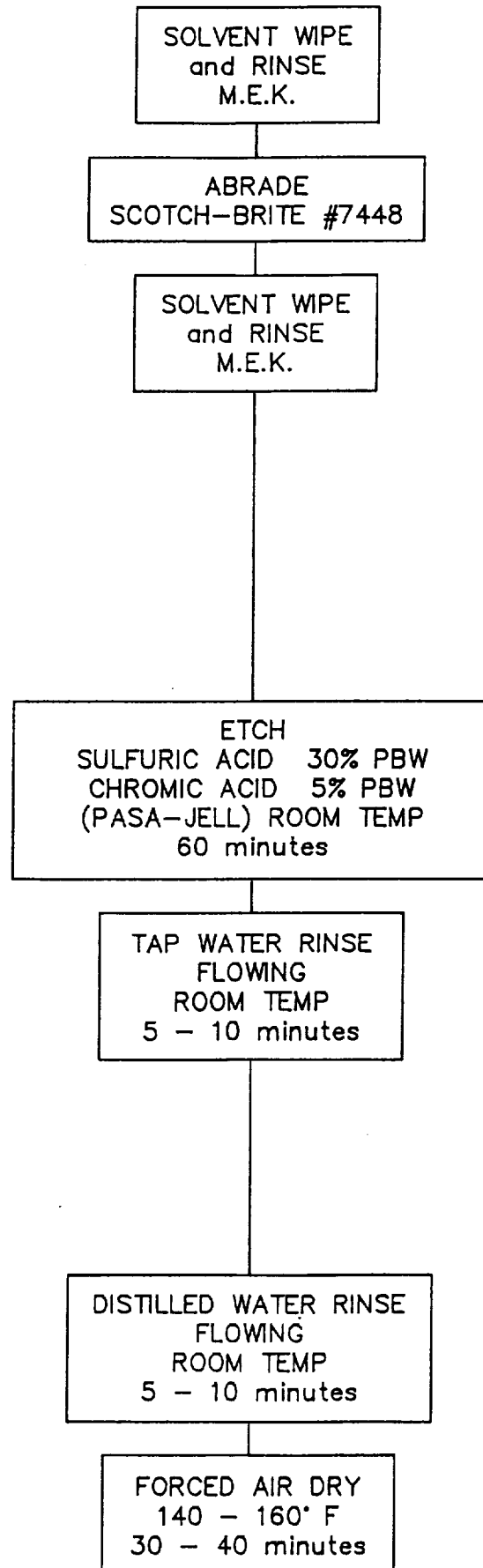


FIGURE 36

# PREFERRED CLEAN & ETCH PROCESS

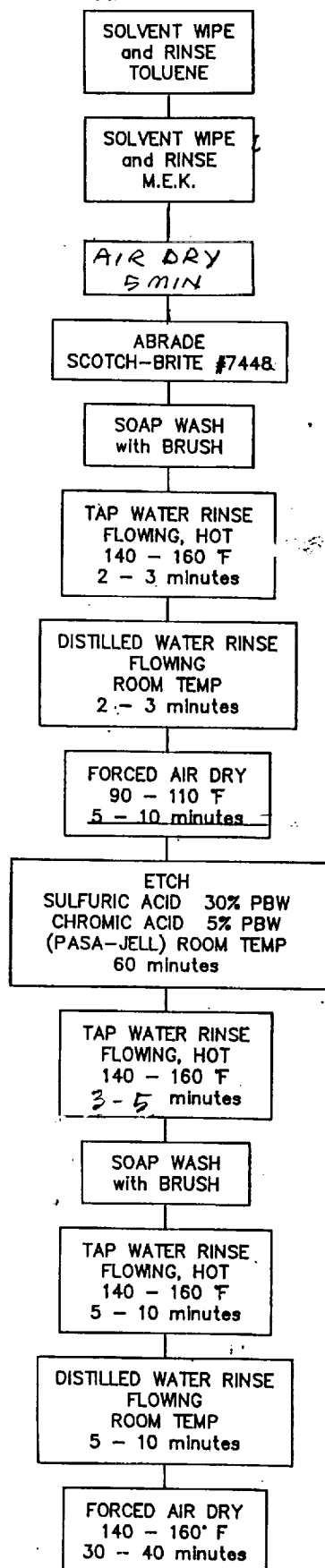


FIGURE 37



SPECIMENS PREPARED  
FOR  
STRENGTH EVALUATION

SPEC NO	NO OF SPECIMENS PREPARED	SURFACE CLEANING PROCEDURE
44	2 EA 4" SQ HONEYCOMB	PER FIGURE 36 (SCOTCH BRITE ABRAID)
45	5 EA 1.40" SQUARE HONEYCOMB SANDWICH 1 EA 4" SQ HONEYCOMB	PER FIGURE 36 (SCOTCH BRITE ABRAID)
46	3 EA 4" SQ HONEYCOMB	PER FIGURE 36 (SCOTCH BRITE ABRAID)
47	5 EA 1.40" SQ HONEYCOMB 5 EA LAP SHEAR 1 EA 4" SQ	PER FIGURE 36 (SCOTCH BRITE ABRAID)
48	5 EA 1.40" SQ HONEYCOMB 5 EA LAP SHEAR 1 EA 4" SQ	PER FIGURE 35 (SCOTCH BRITE ABRAID PLUS PHOSPHORIC ACID ANODIZE)
49	5 EA 1.40" SQ HONEYCOMB 5 EA LAP SHEAR 1 EA 4" SQ	PER FIGURE 34 (CLEANING PROCEDURE USED PRIOR TO FAILURE OF DISTORTION TEST SPECIMEN)

FIGURE 38

# LAP SHEAR TEST SPECIMEN

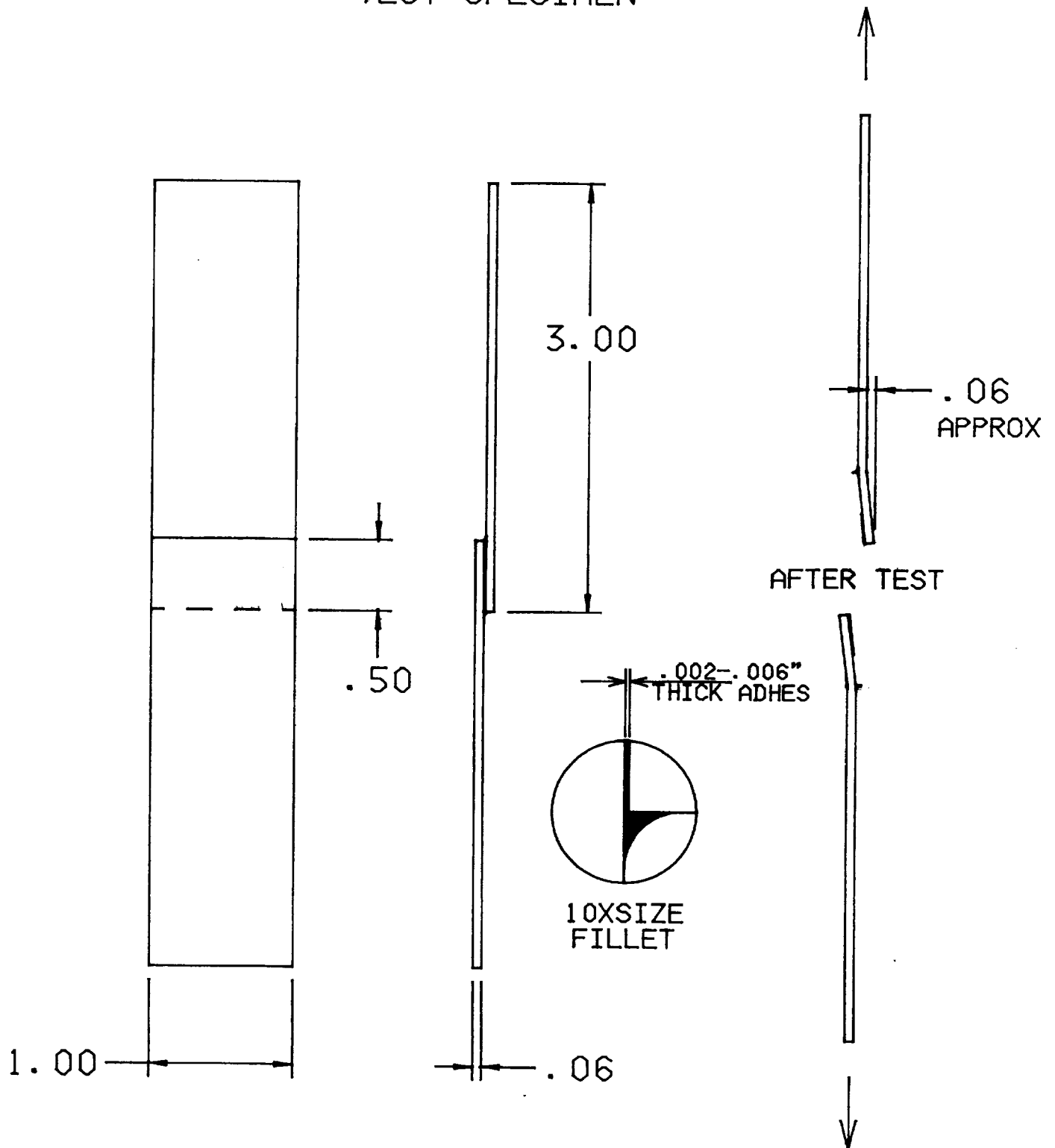


FIGURE 39

## LAP SHEAR TEST RESULTS

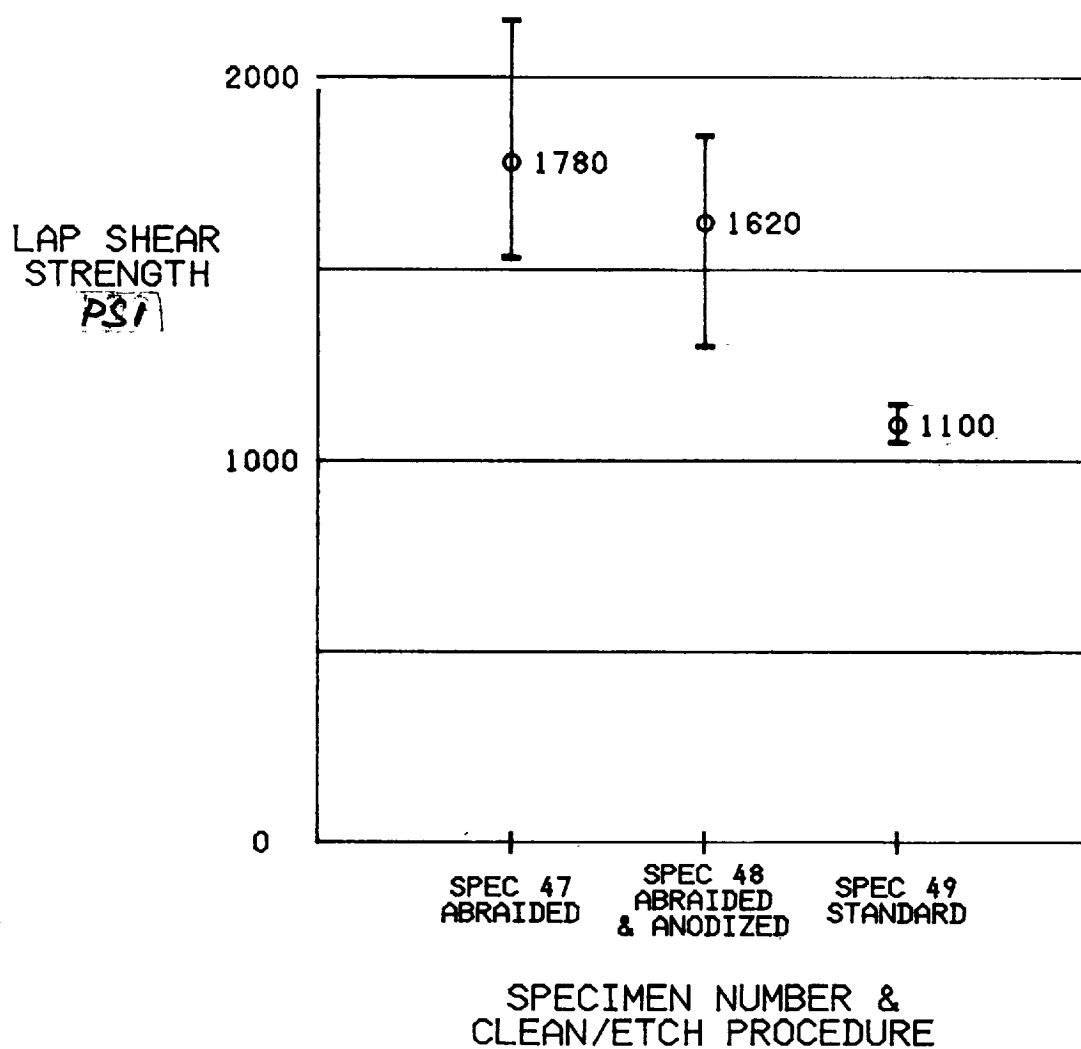


FIGURE 40

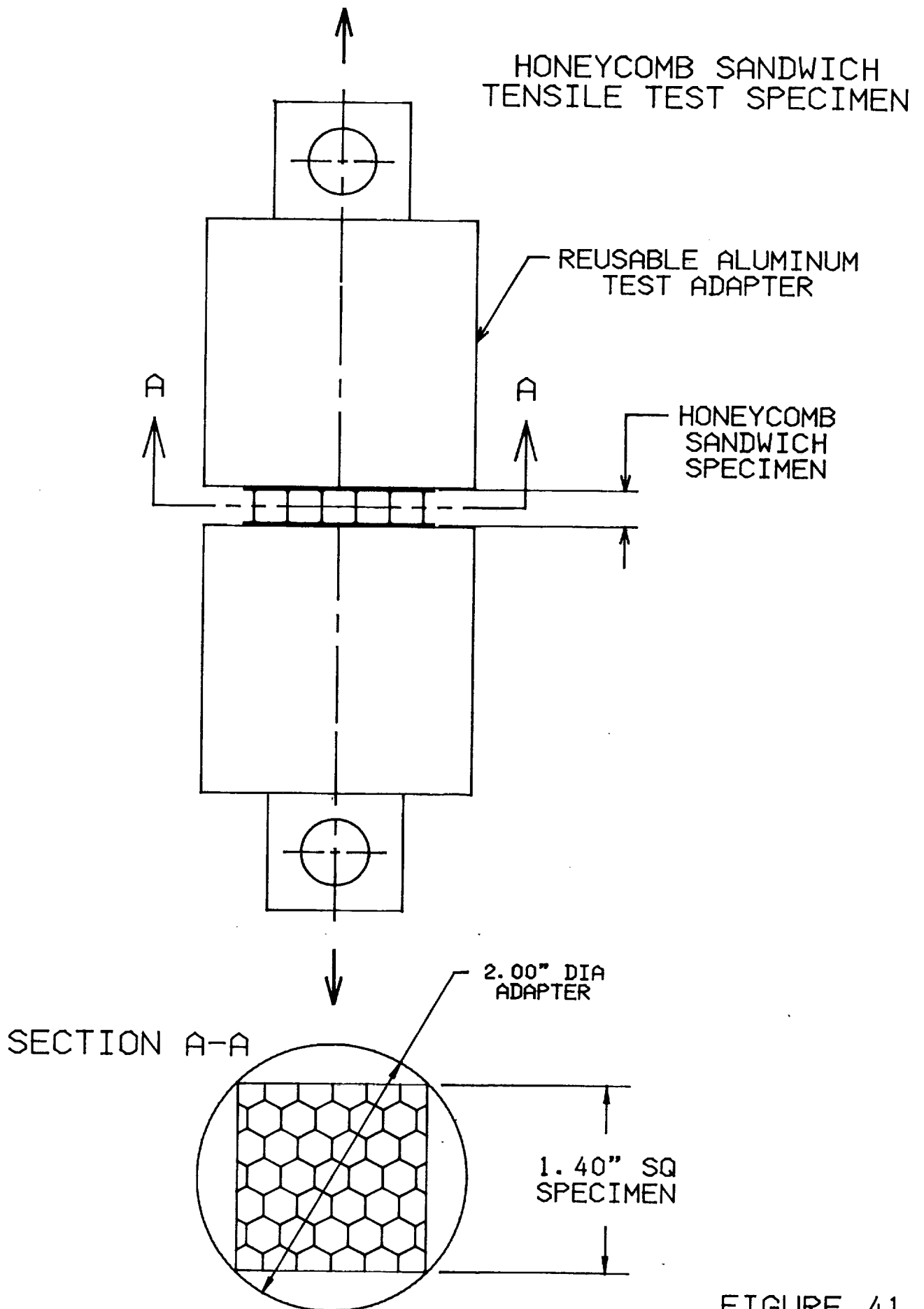


FIGURE 41

# HONEYCOMB SANDWICH TENSILE STRENGTH TEST RESULTS

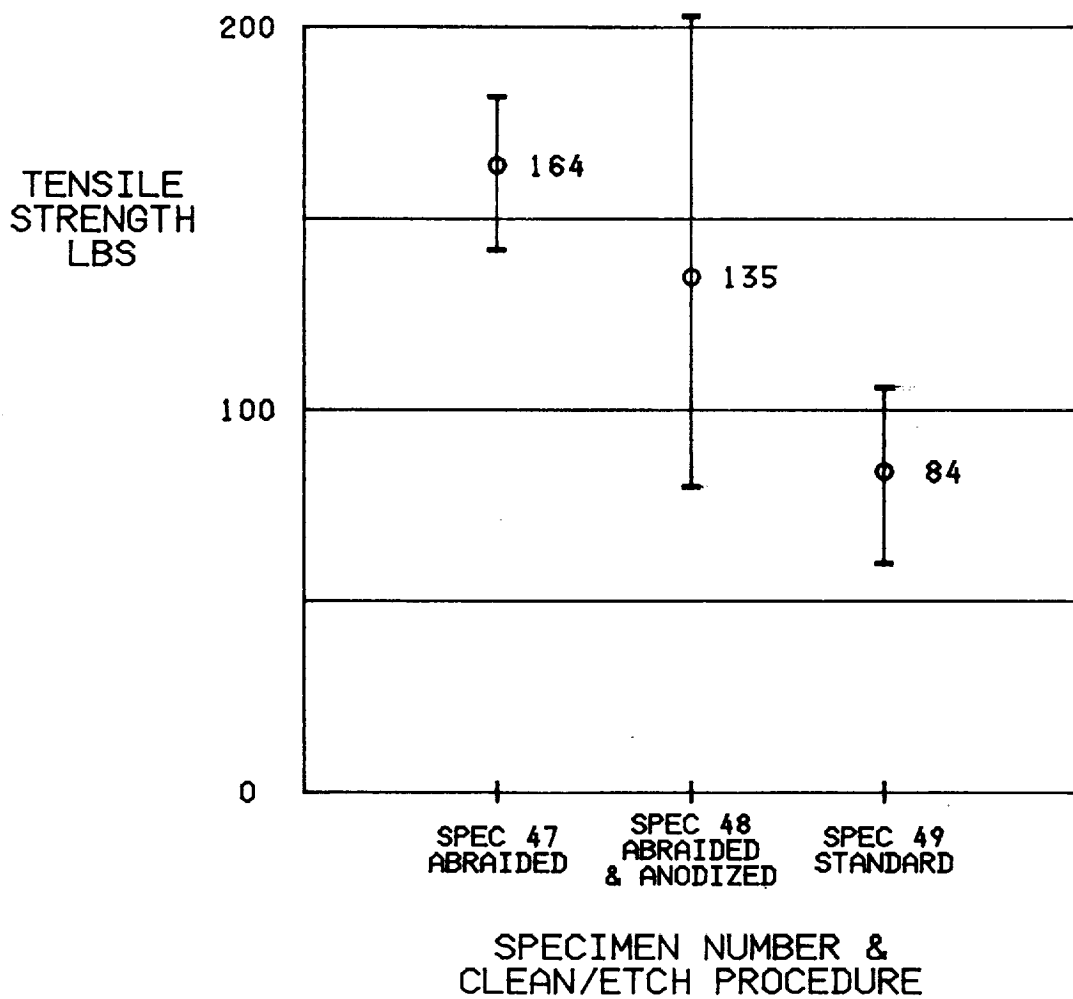


FIGURE 42

# EFFECT OF LEVELING LAYER ON SURFACE SPECULARITY

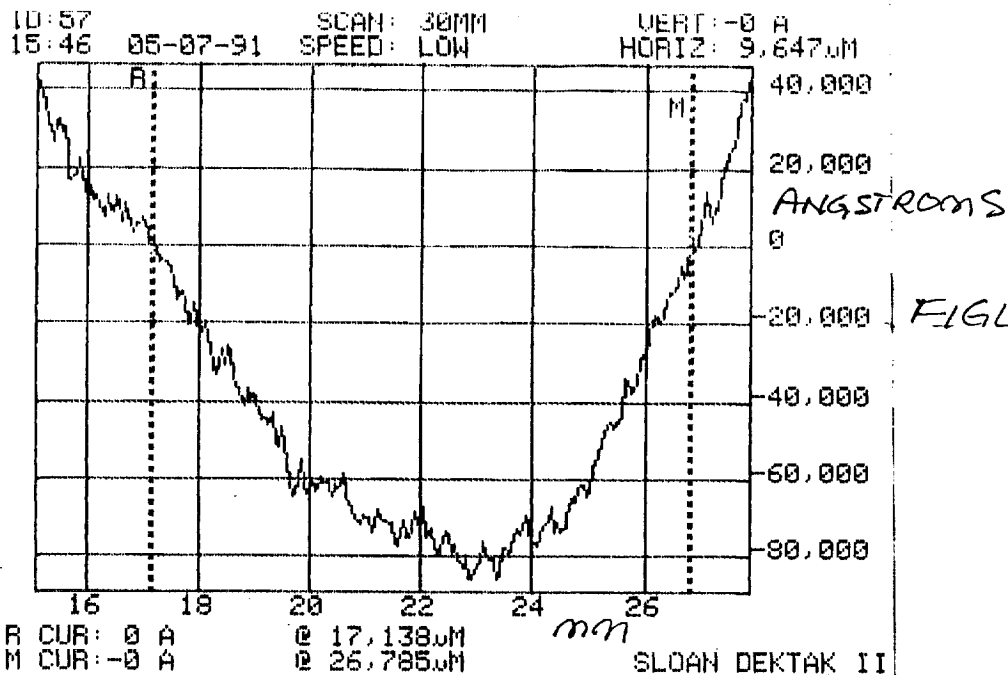


FIGURE 43A

SAEC. 57 BEFORE EP-3 LAYER

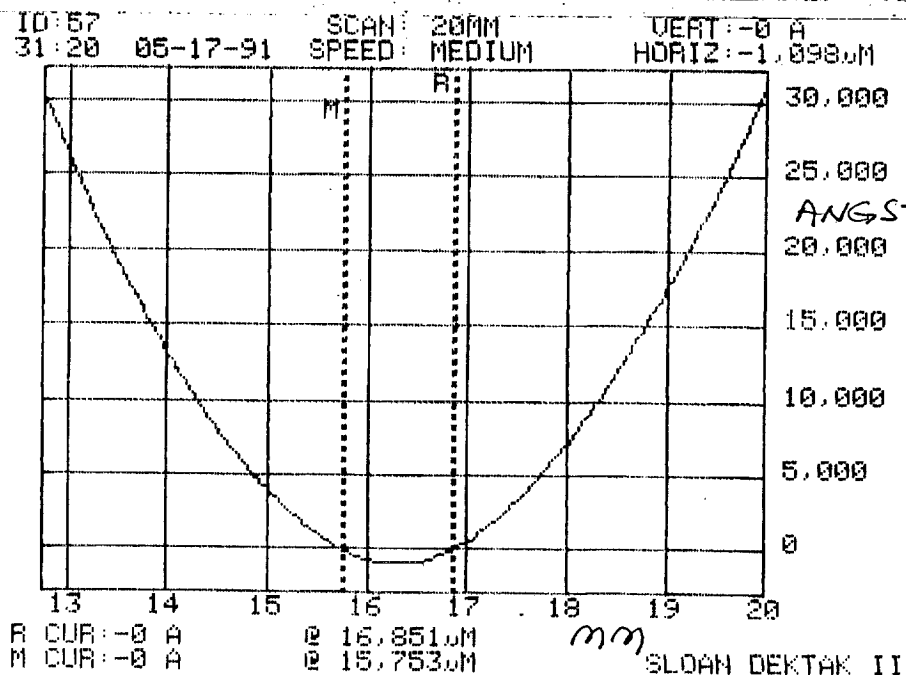
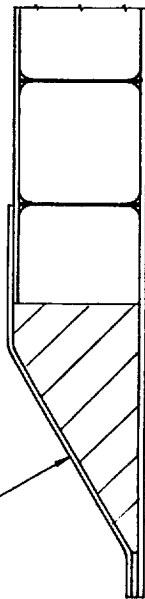


FIGURE 43B

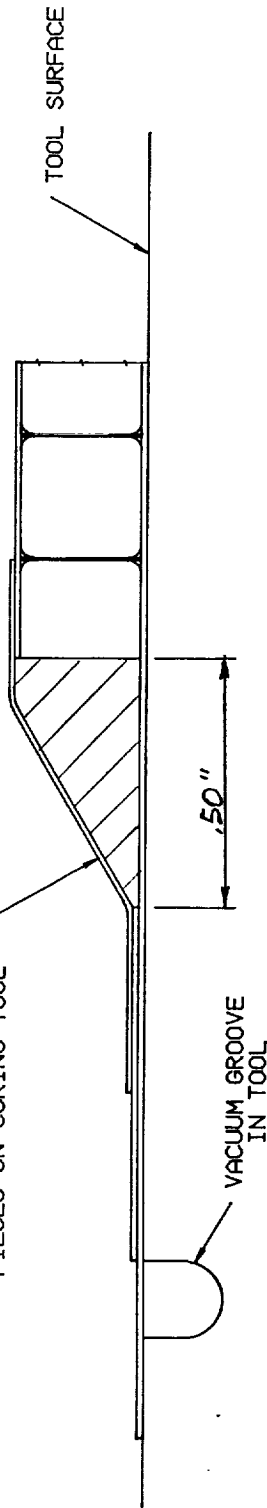
SAEC 57 AFTER EP-3 LAYER

# RADIAL EDGE CLOSE-OUT DETAIL

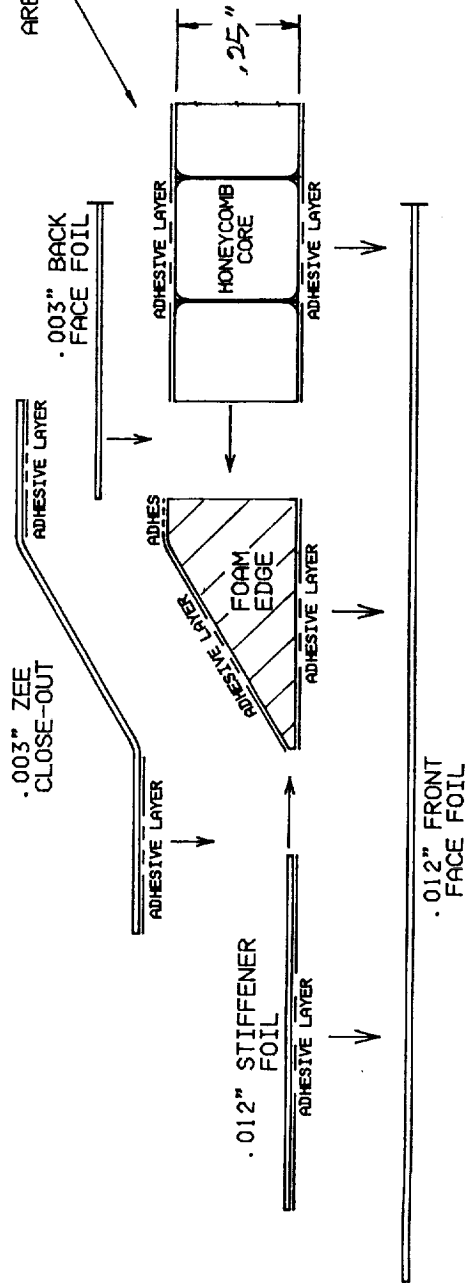
EDGE AFTER REMOVAL  
FROM TOOL AND TIMMED



LAY-UP OF EDGE CLOSE-OUT  
PIECES ON CURING TOOL



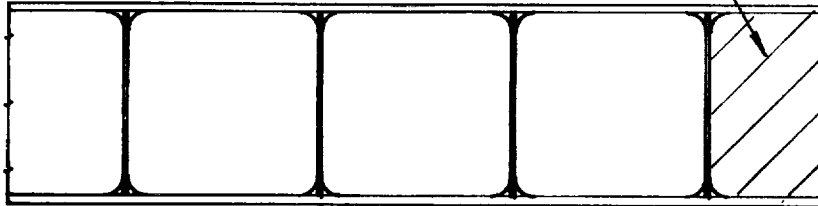
EDGE PIECES AS THEY  
ARE ASSEMBLED FOR CURING



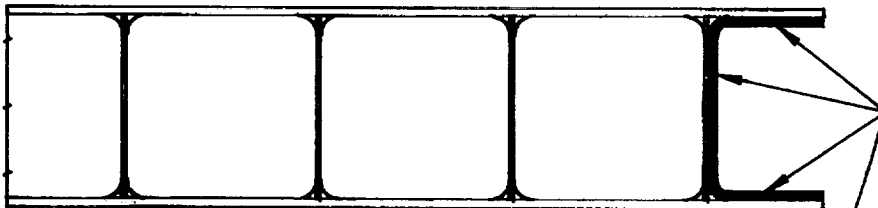
RADIAL EDGE CLOSE-OUT DETAIL

# POTENTIAL EDGE CLOSE-OUT DESIGN

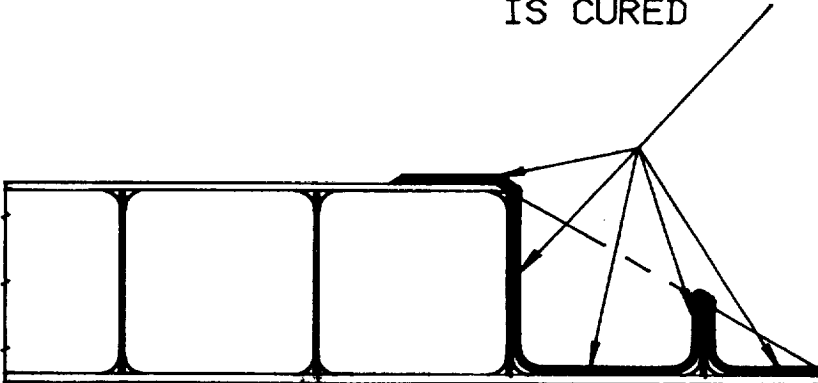
FOAMED EDGE AFTER  
PANEL IS CURED



STRAIGHT EDGE  
CONFIGURATION



CONTINUOUS SKIN POLYMER  
APPLIED AFTER PANEL  
IS CURED



BEVELED EDGE  
CONFIGURATION

FIGURE 45

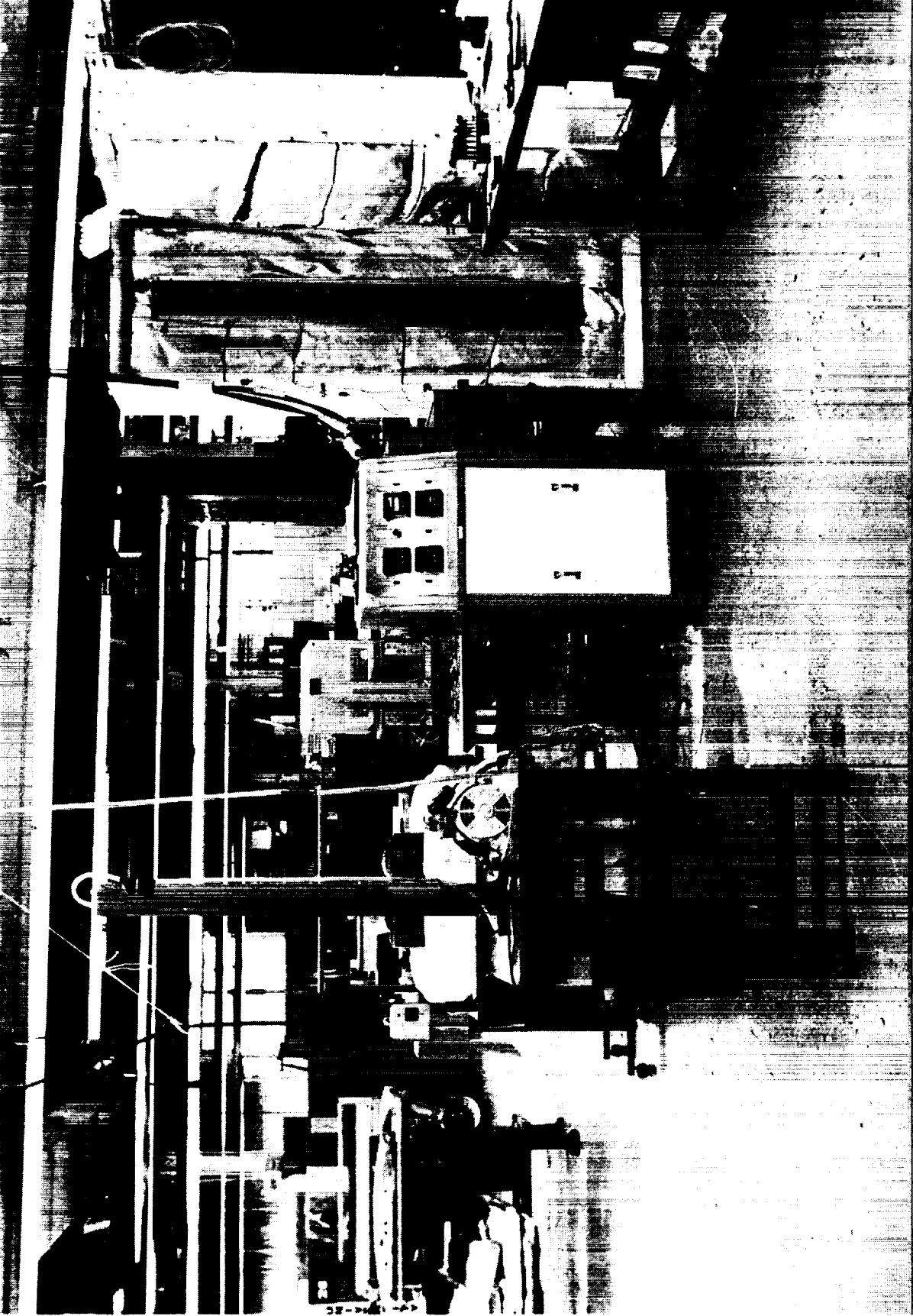






*Panel Fabrication Area*

*Figure 47*



*Panel Fabrication Area*

*Figure 48*



Figure 50

Panel Fabrication Area

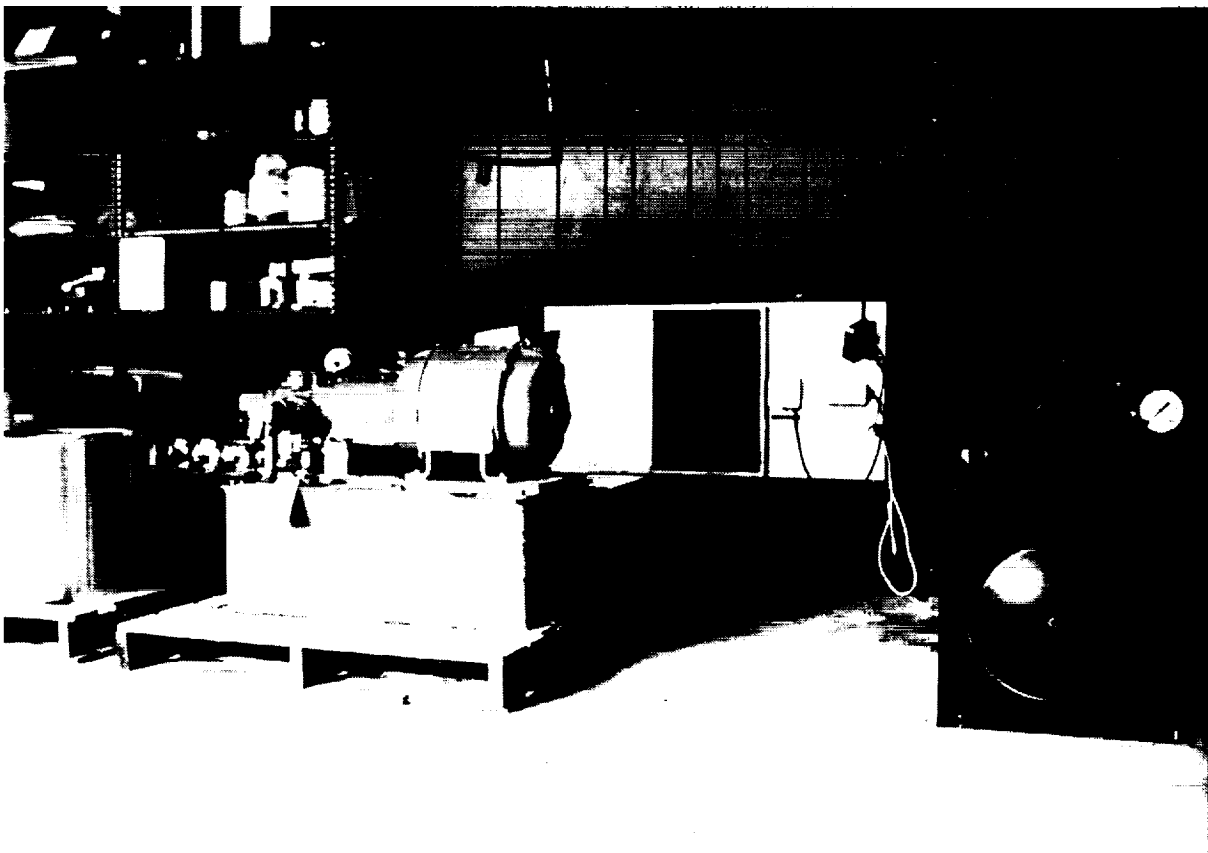


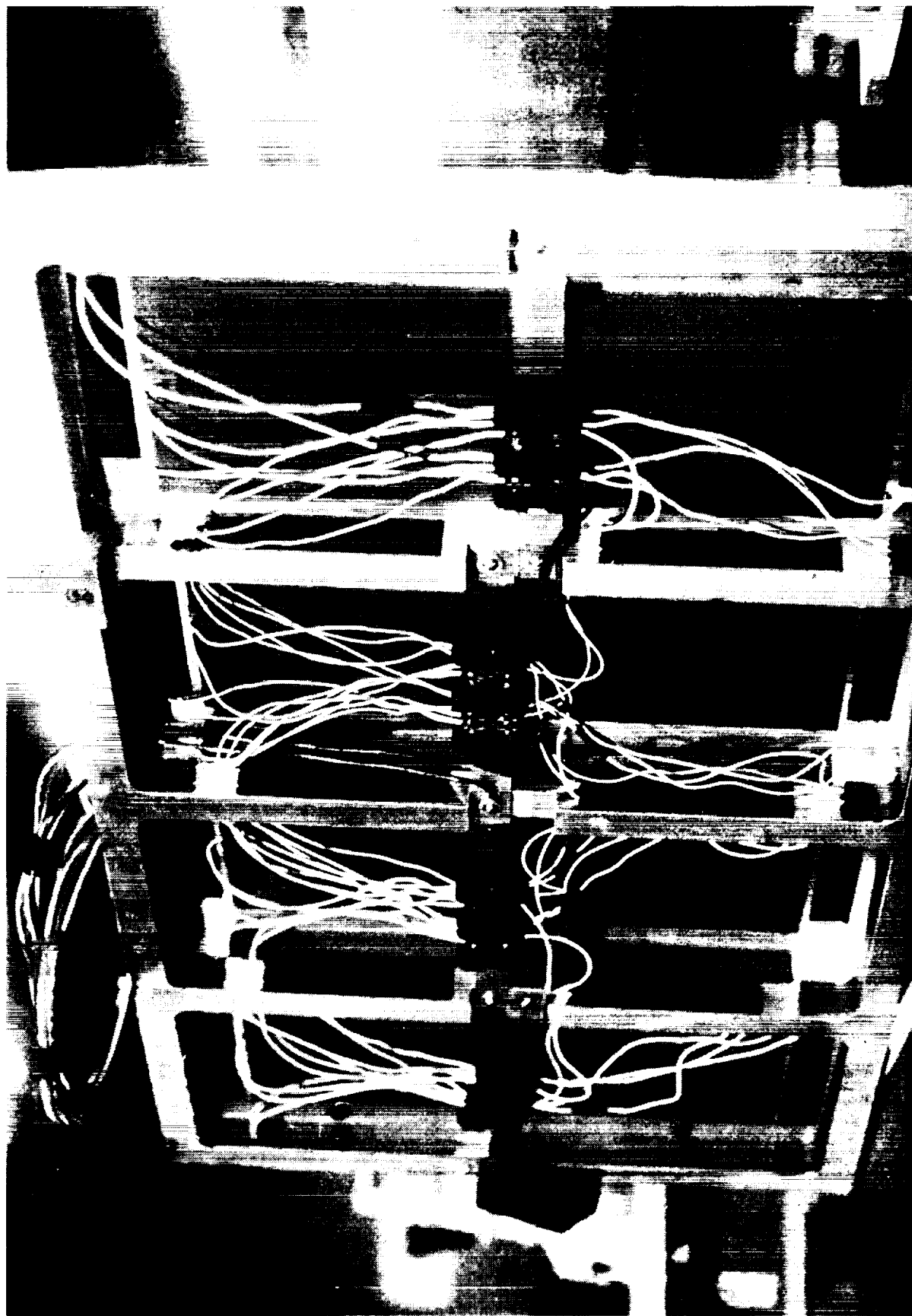
Figure 49

Panel Fabrication Area



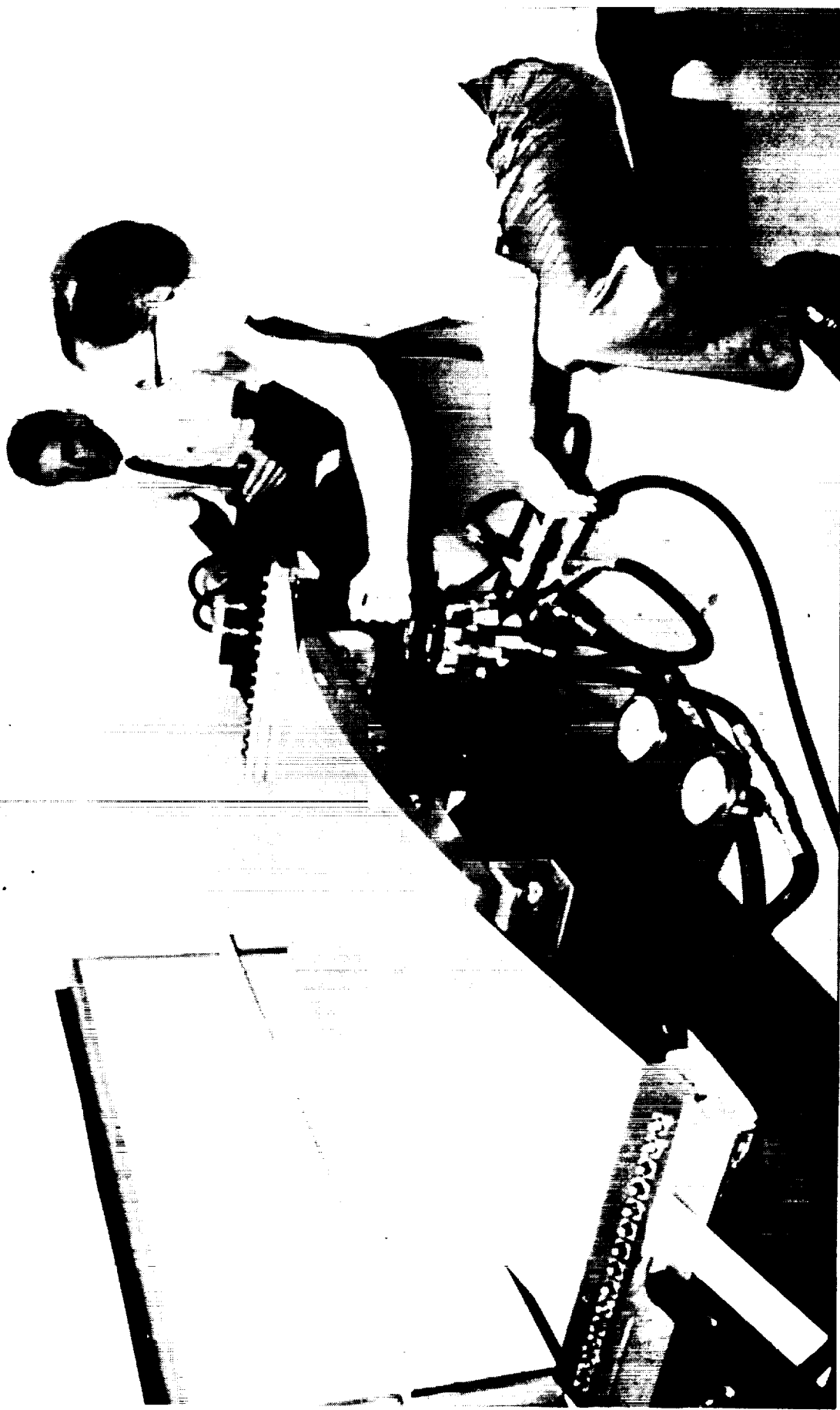
*Stretch Forming Tool*

*Figure 51*

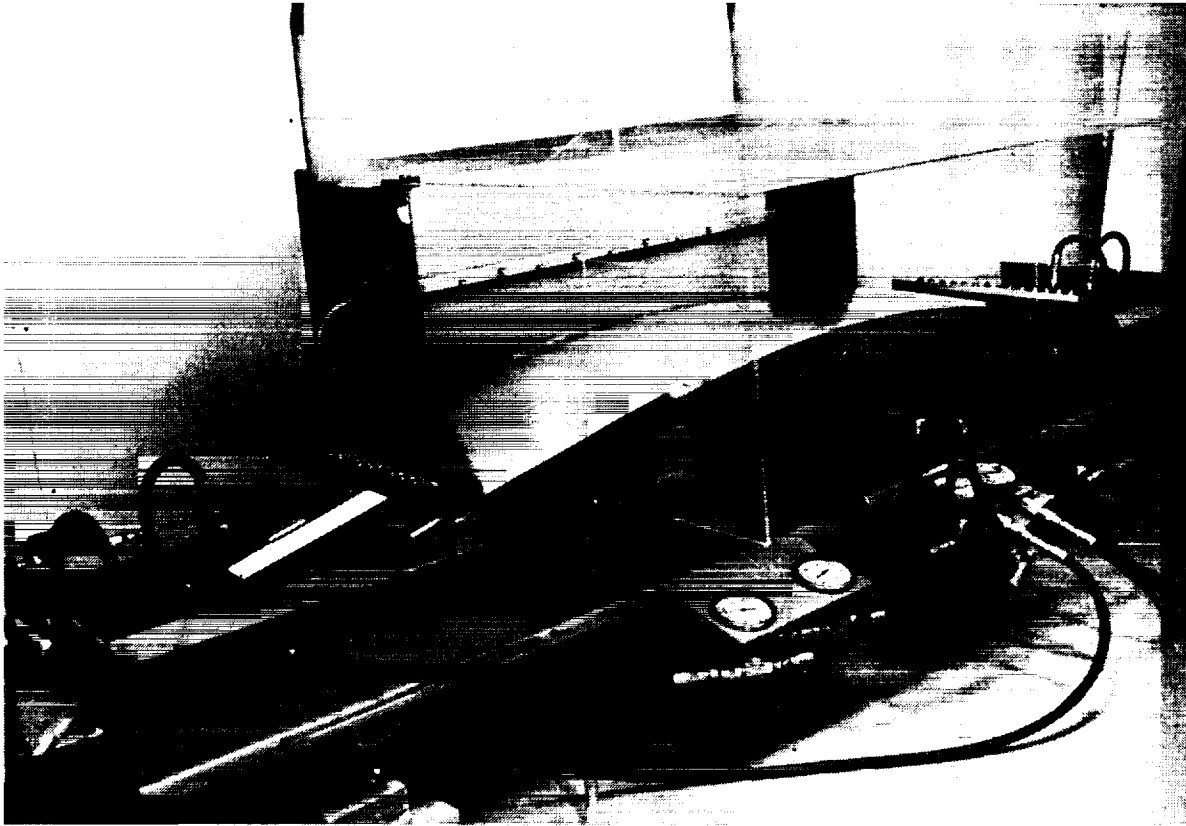


*Heaters on Underside of Tool*

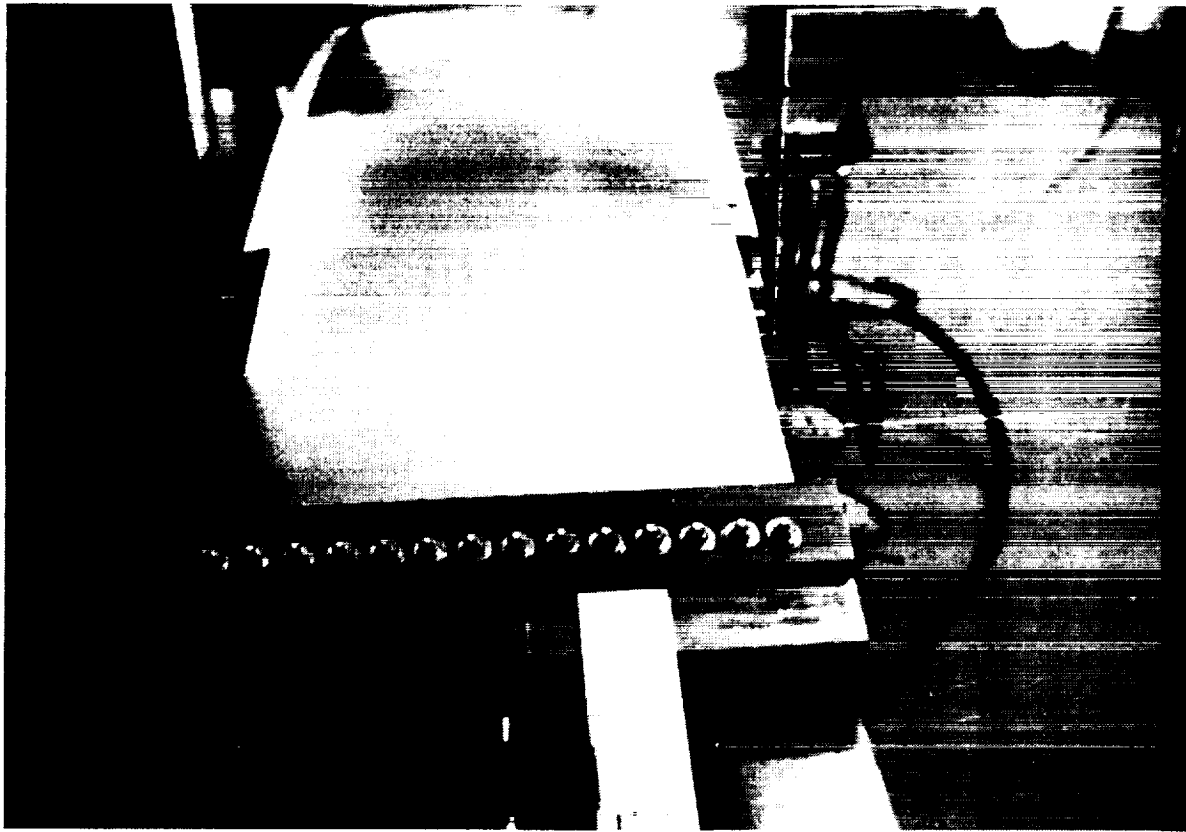
*Figure 52*



*Stretch Former without Shroud in Place*



Stretch Former with Shroud in Place **Figure 54**



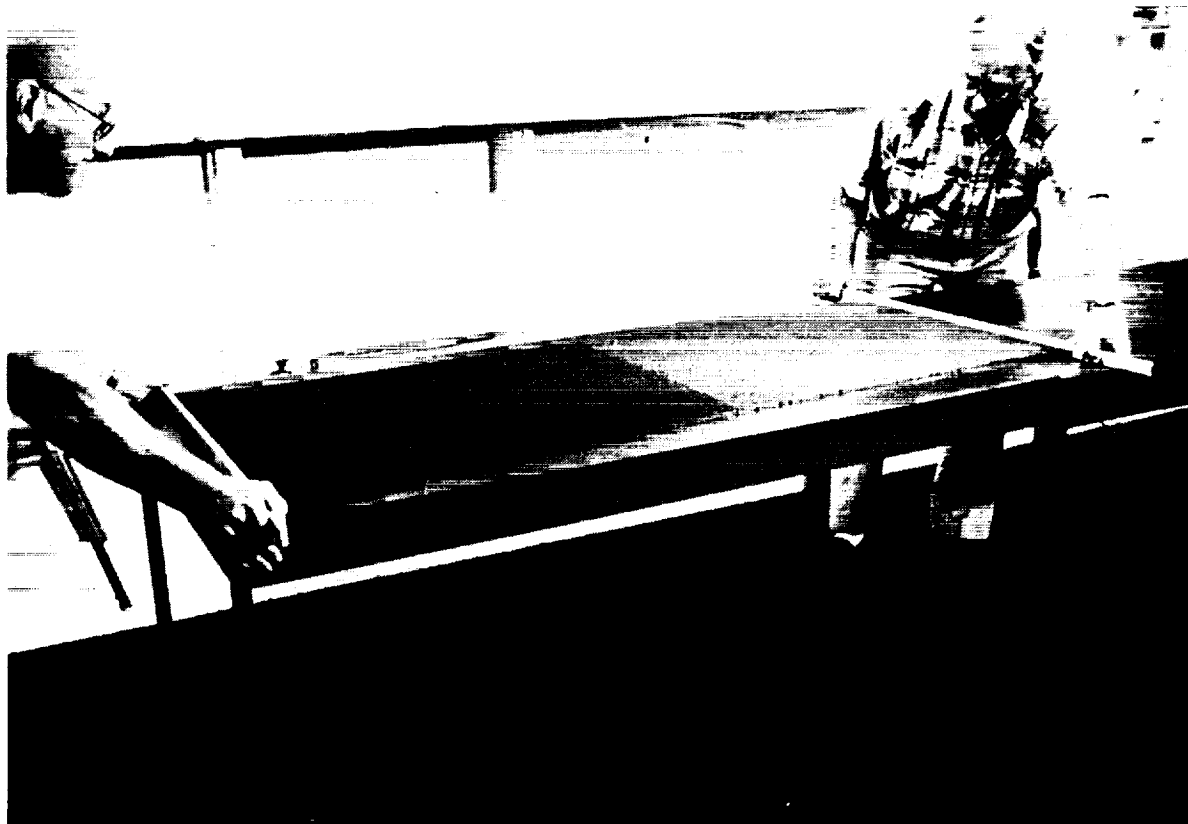
Stretch Former Viewed from  
Stretch Jaw **Figure 55**





HOBE Expansion

Figure 56



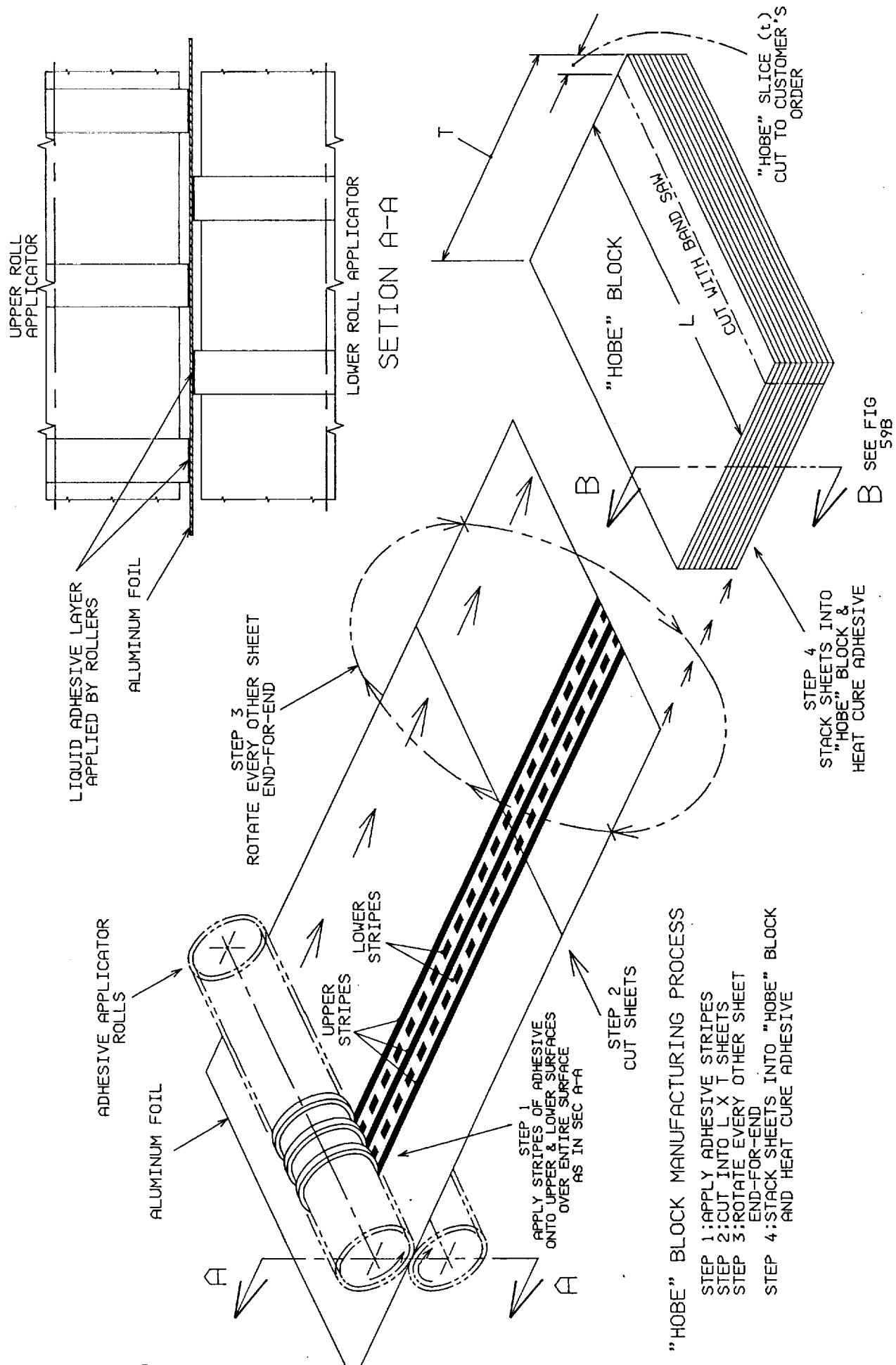
*HOBE Expansion*

*Figure 57*



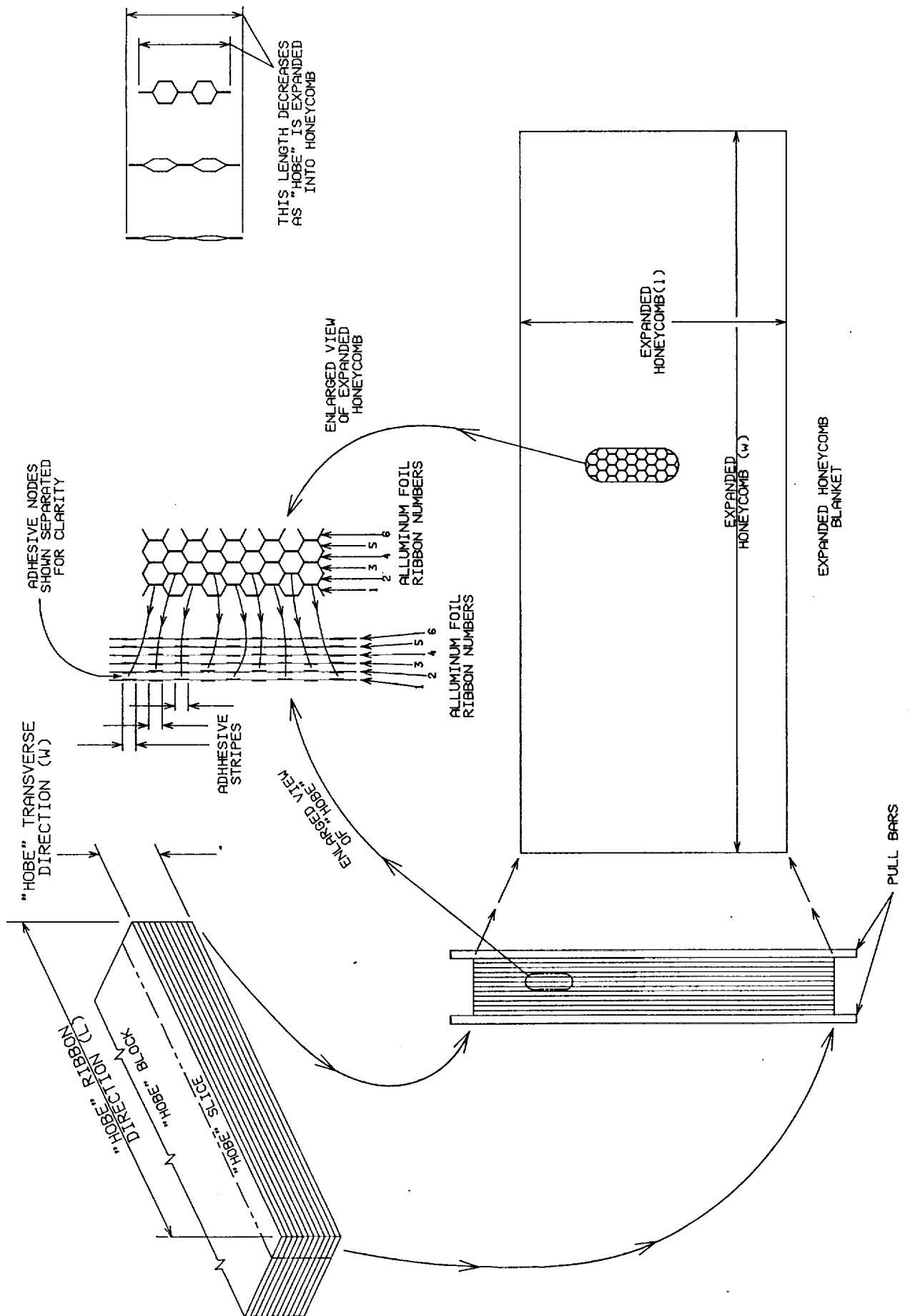
*HOBE Expansion*

*Figure 58*



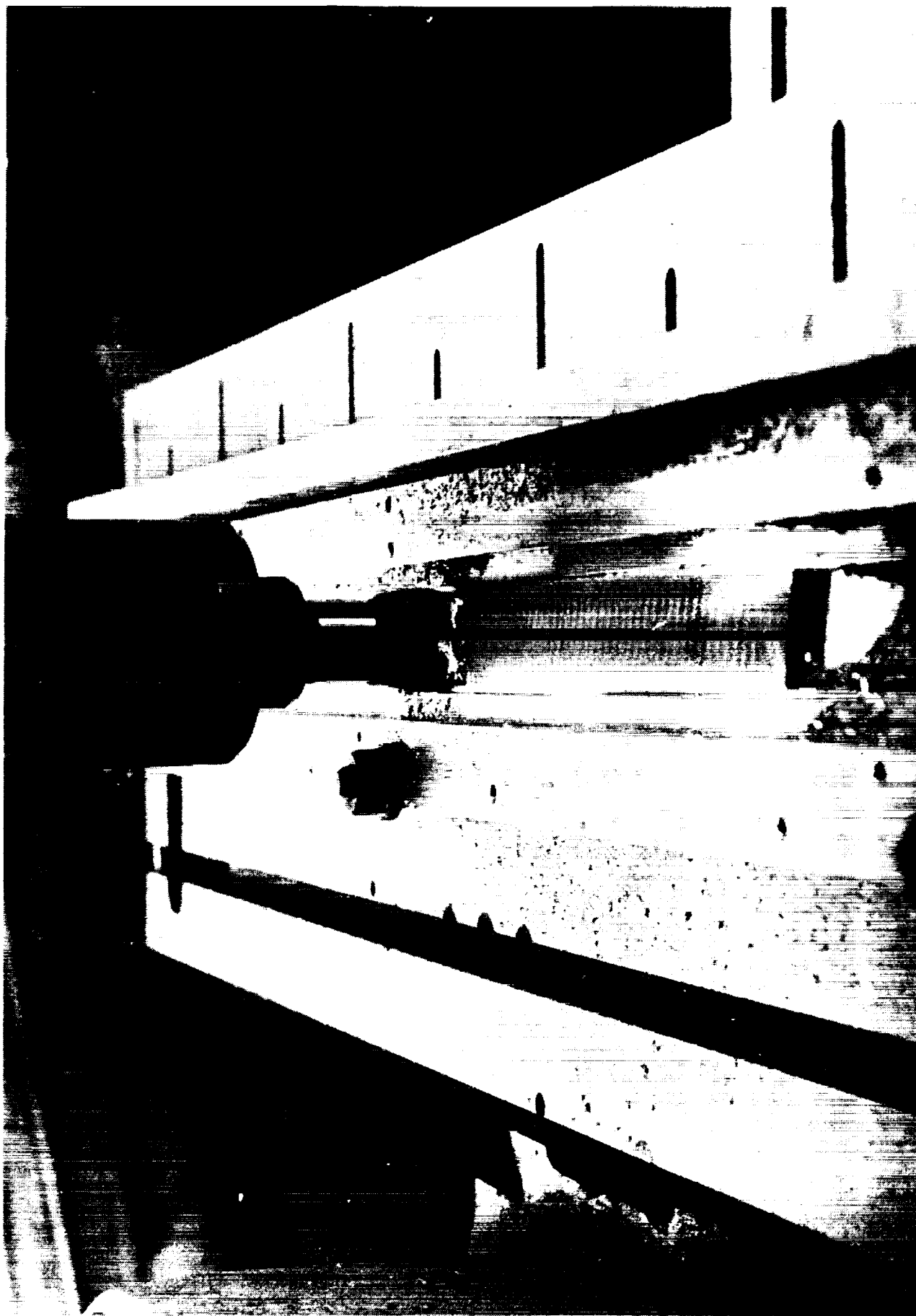
"HOBE" MANUFACTURING PROCESS

FIGURE 59A



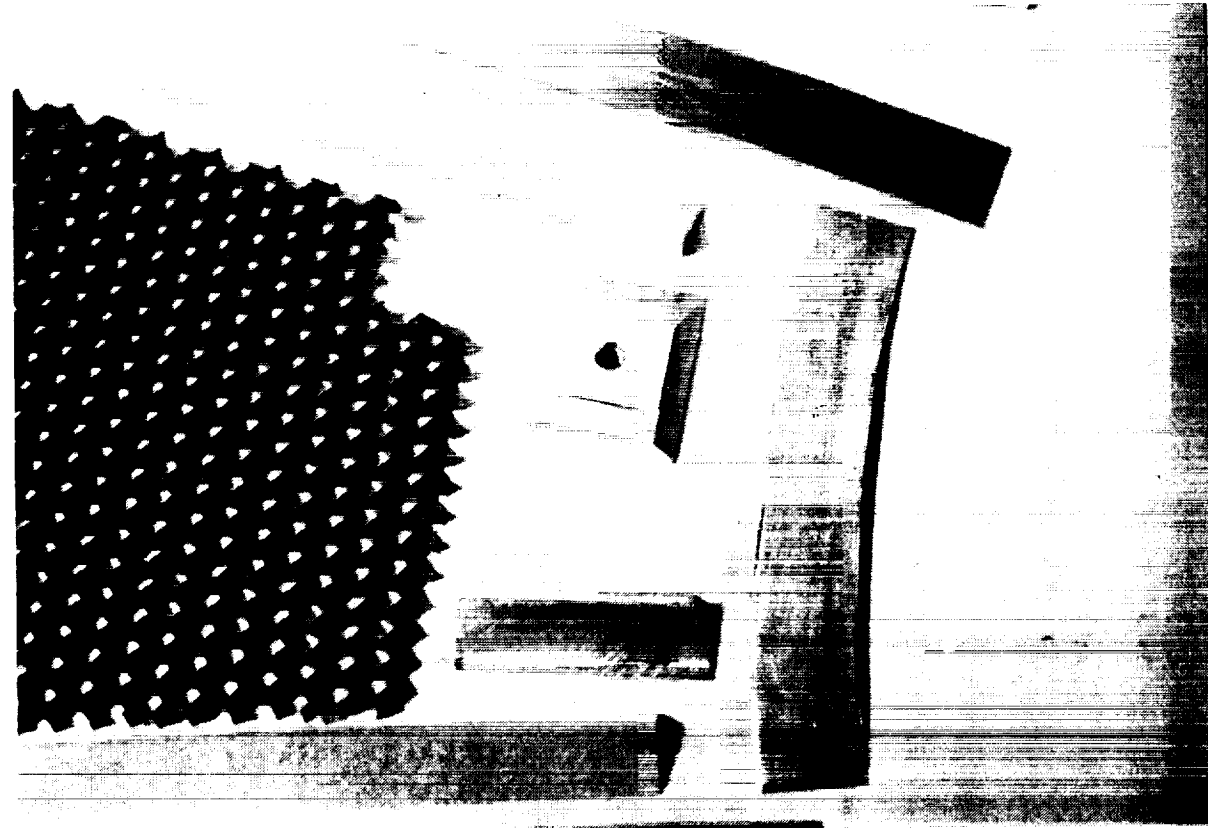
"HOBE" MANUFACTURING PROCESS

FIGURE 59B



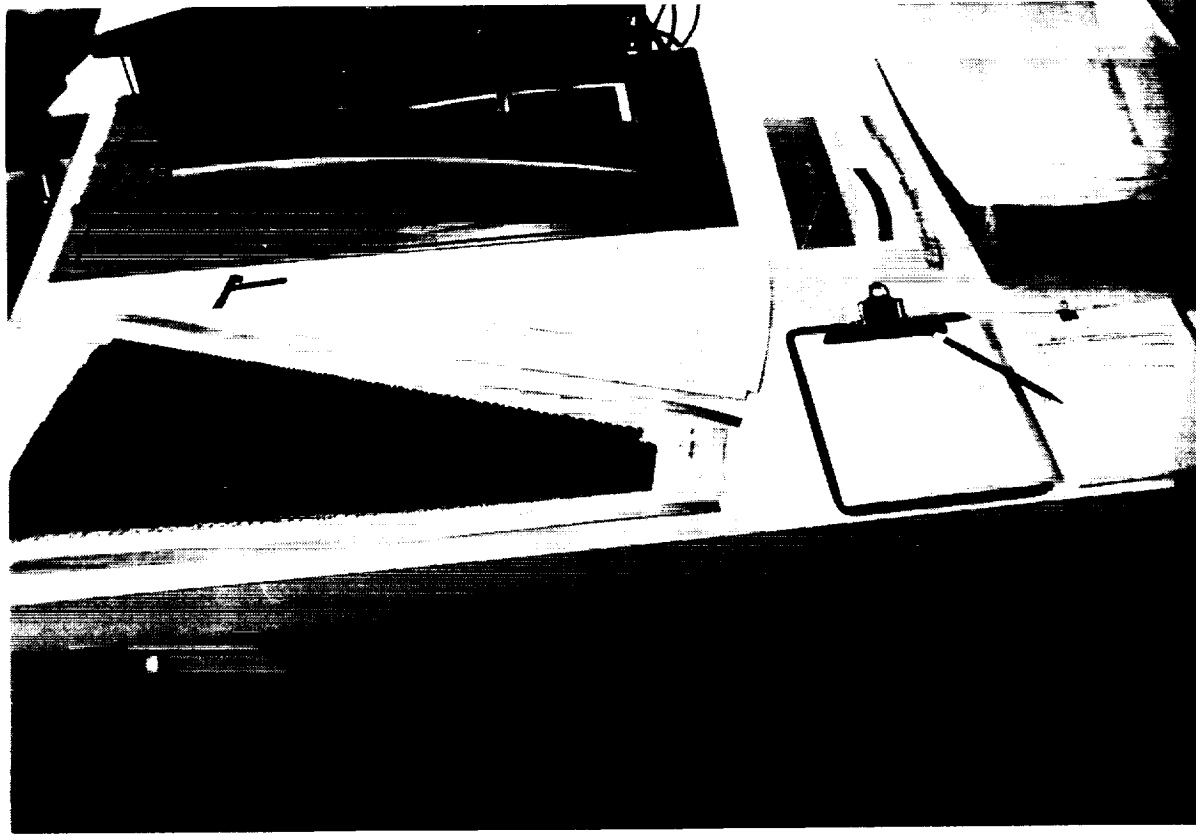
*Flycutting HOBE in Milling Machine*

*Figure 60*



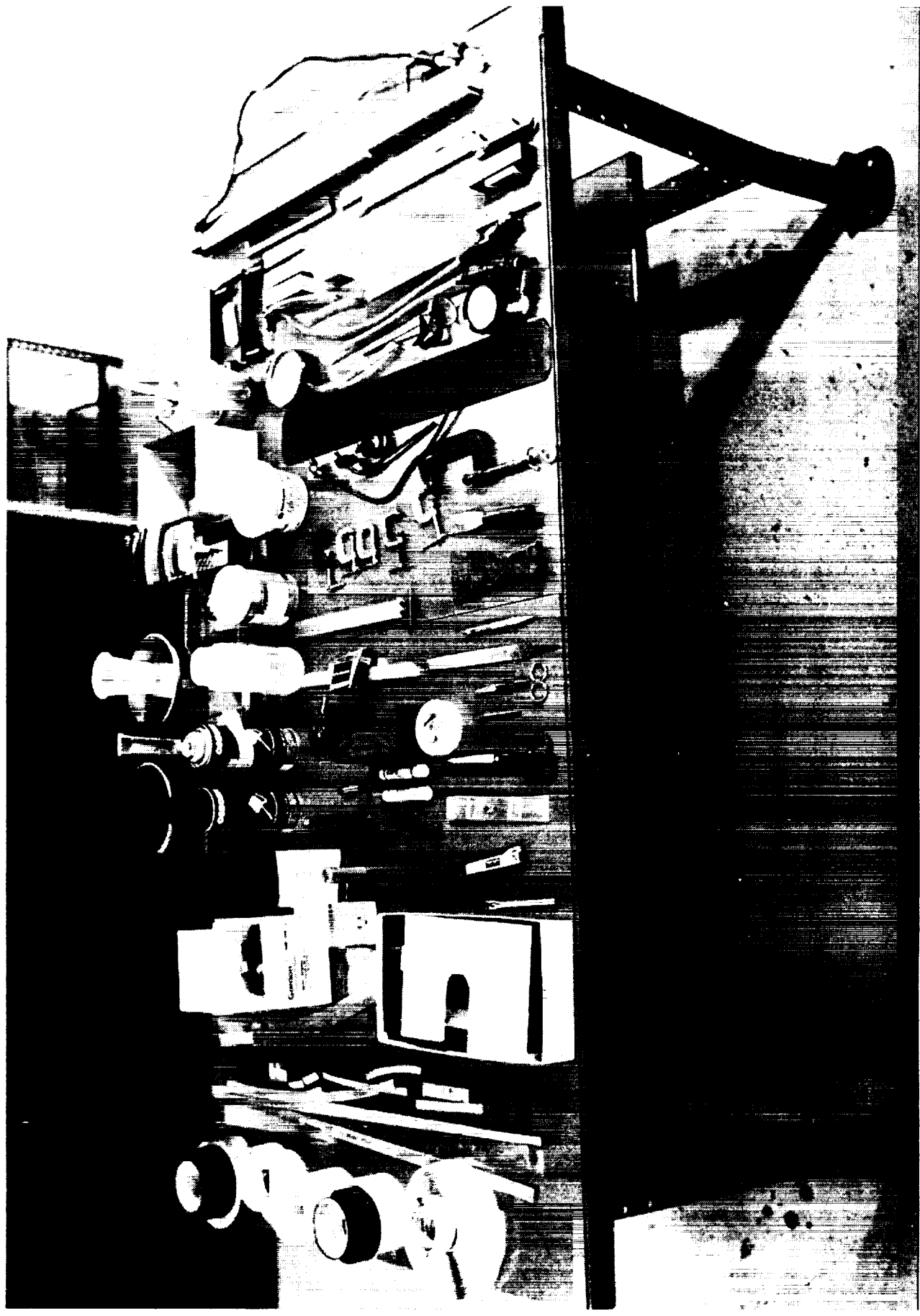
Panel Components, Close-up

Figure 61



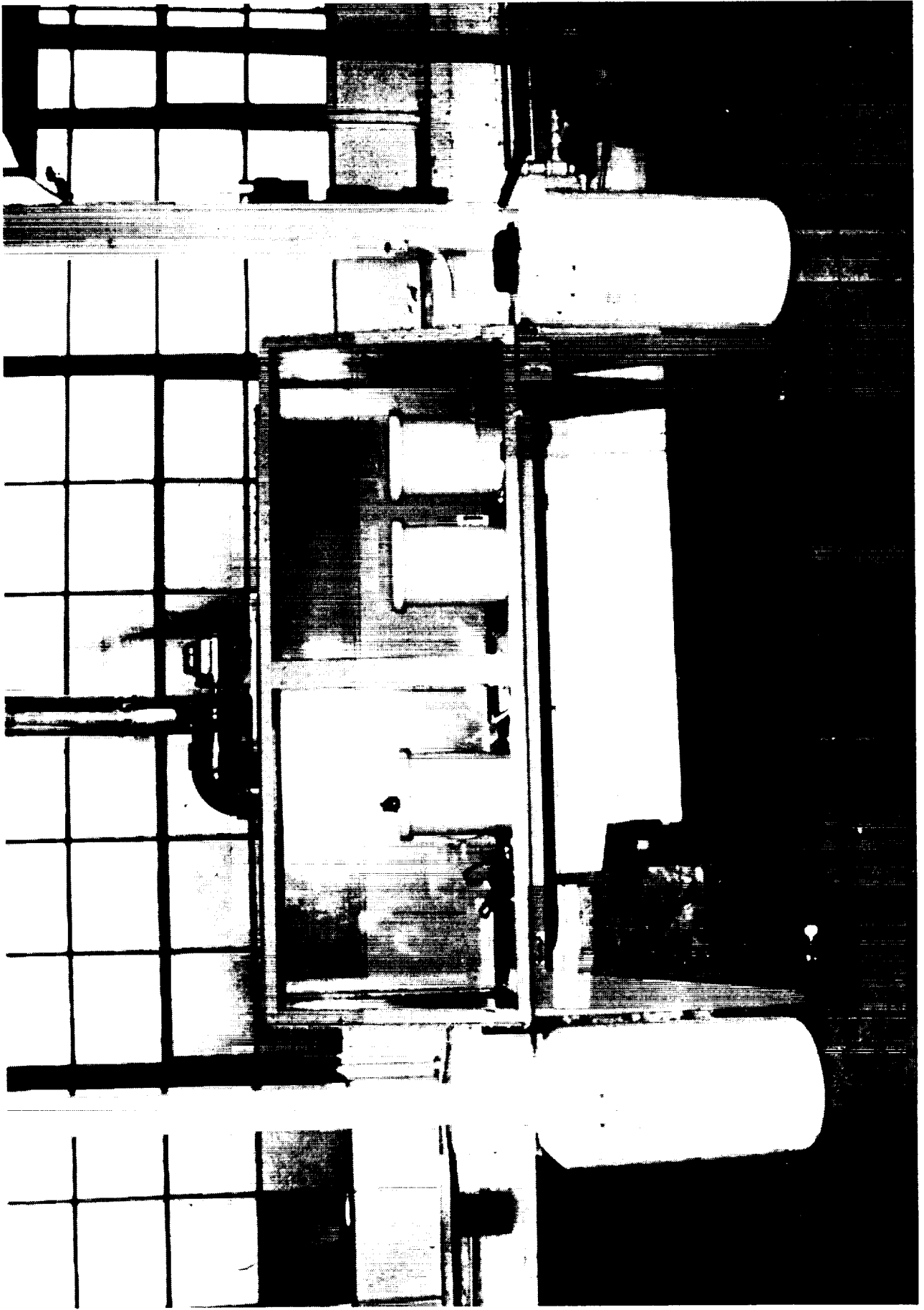
Panel Components, Templates  
& Fixtures

Figure 62



Process Equipment, Tools, and Aids

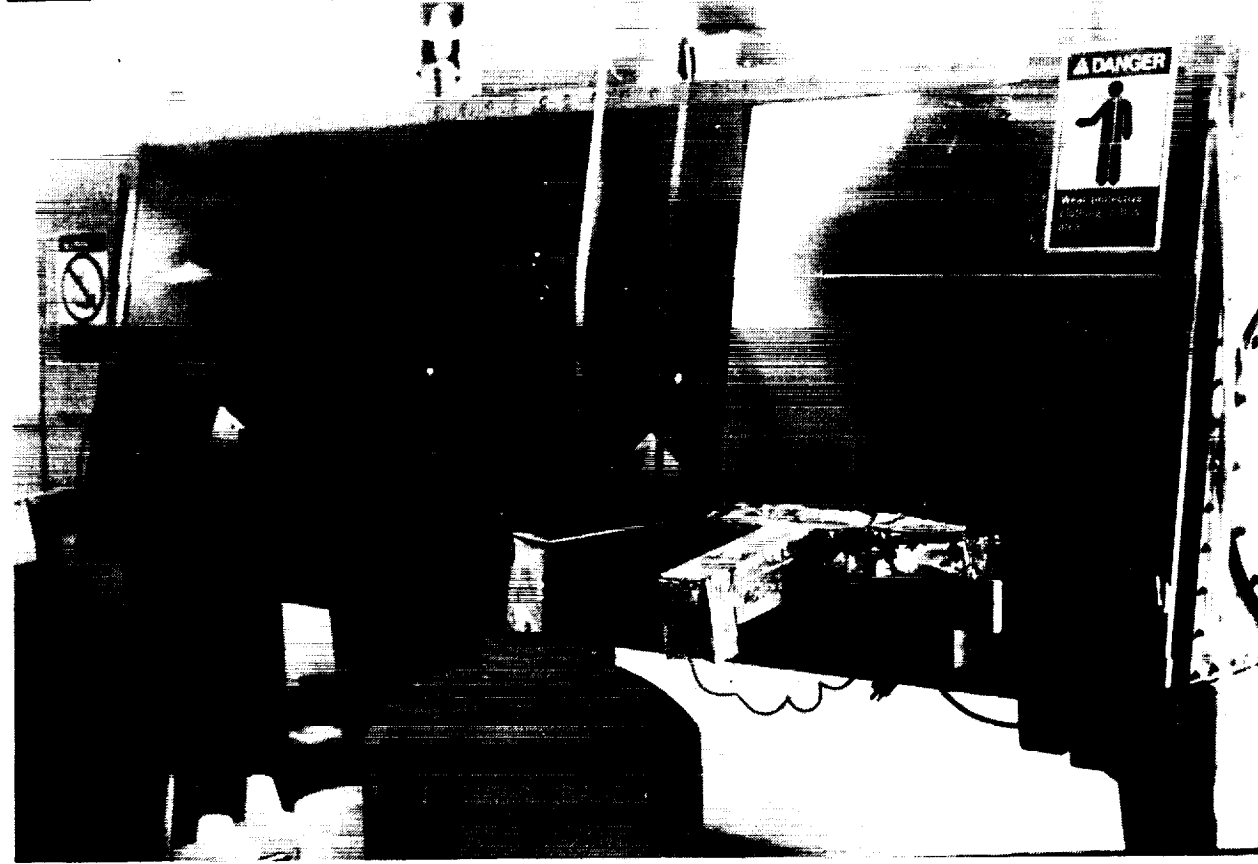
Figure 63



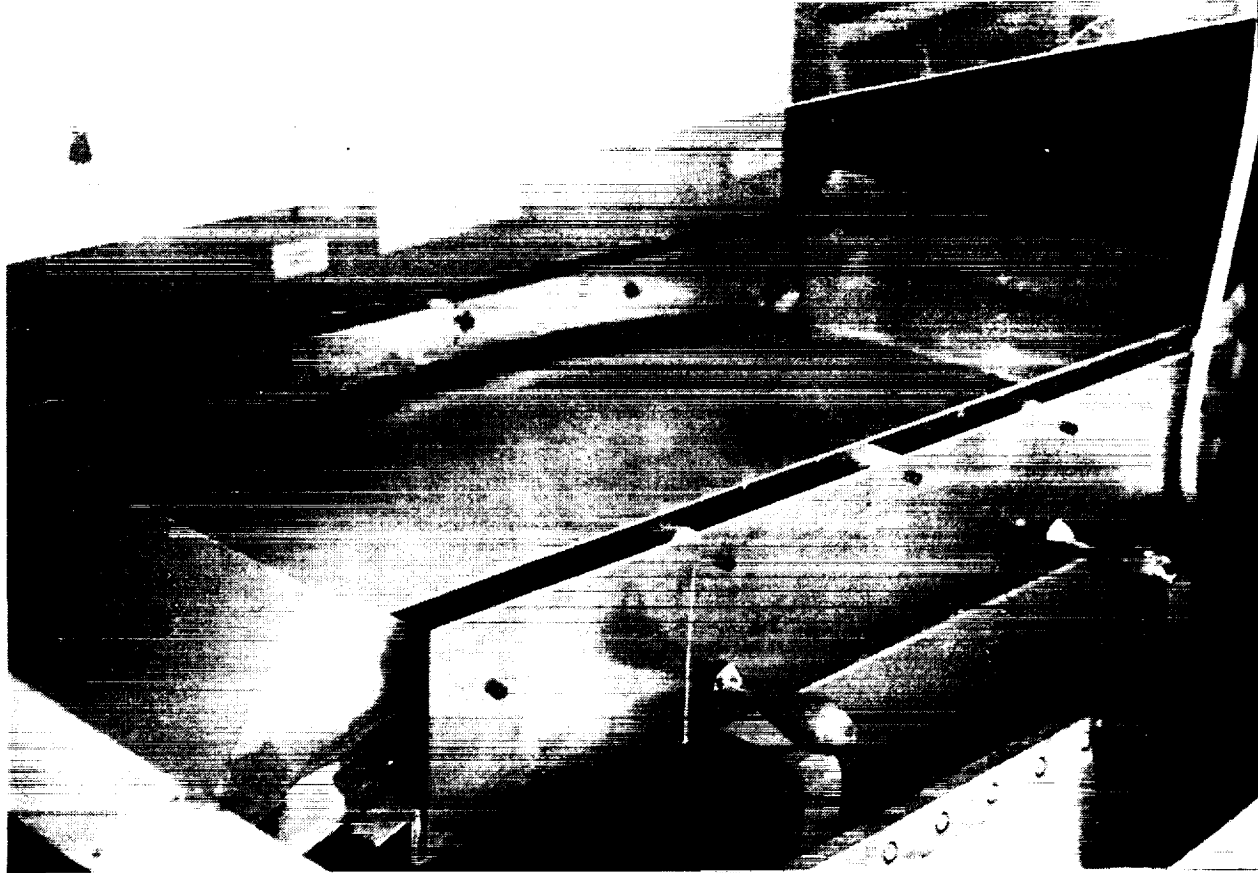
*Figure 64*

*Vented Hood & Chemical Dump Tanks*





Cleanup & Etch Drain Method **Figure 65**

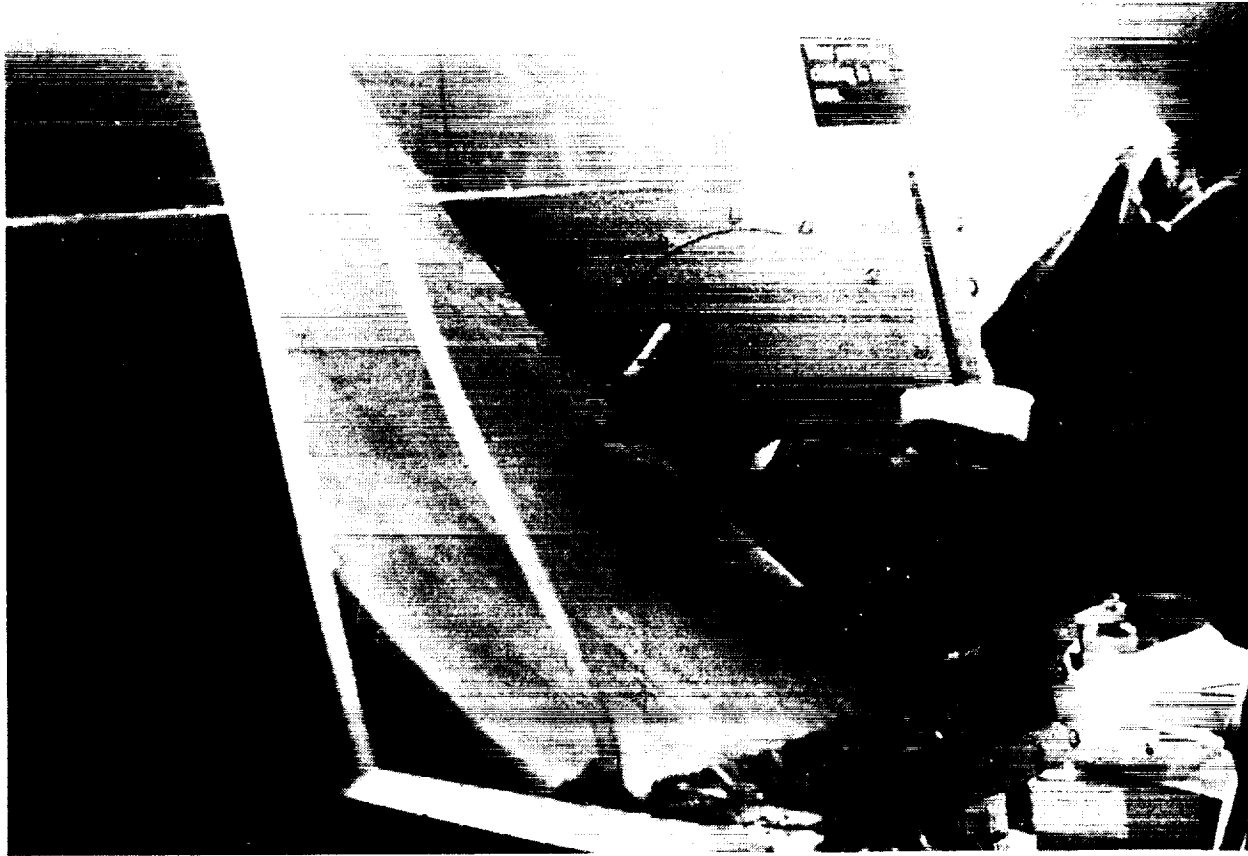


Clean & Etch of Front Face

**Figure 66**

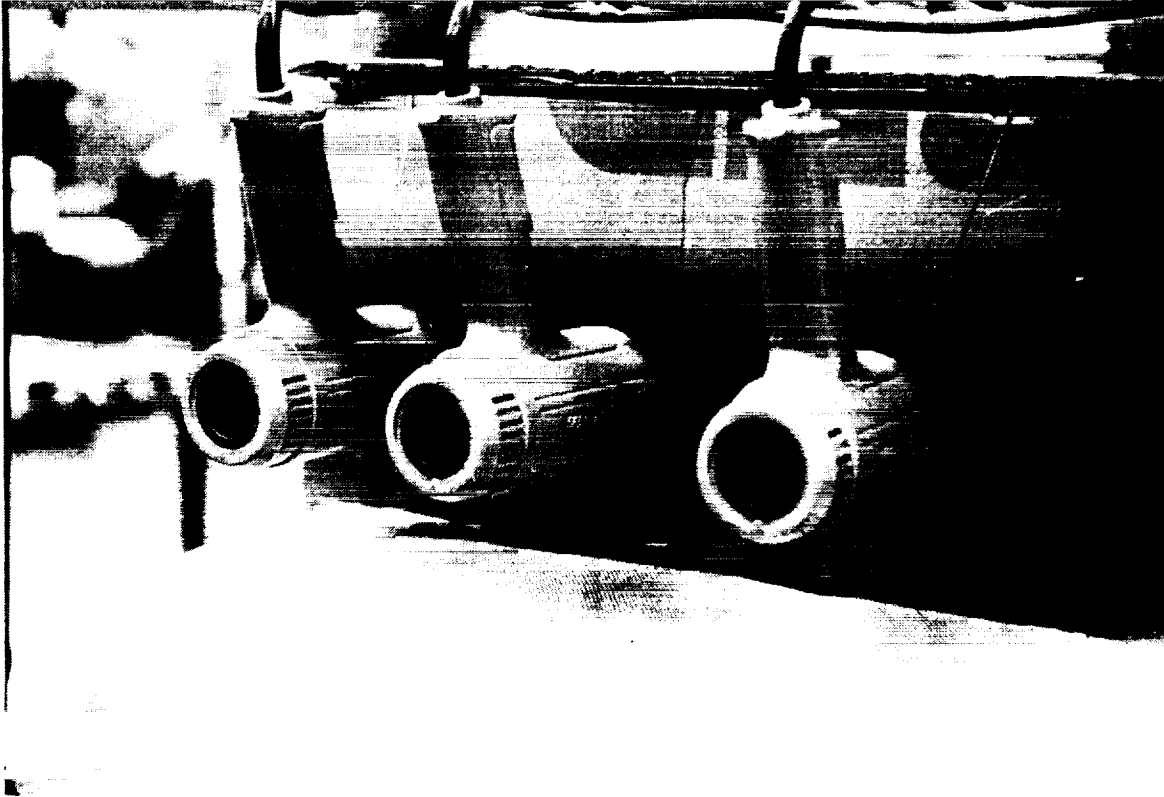


Clean & Etch of Back Face *Figure 67*



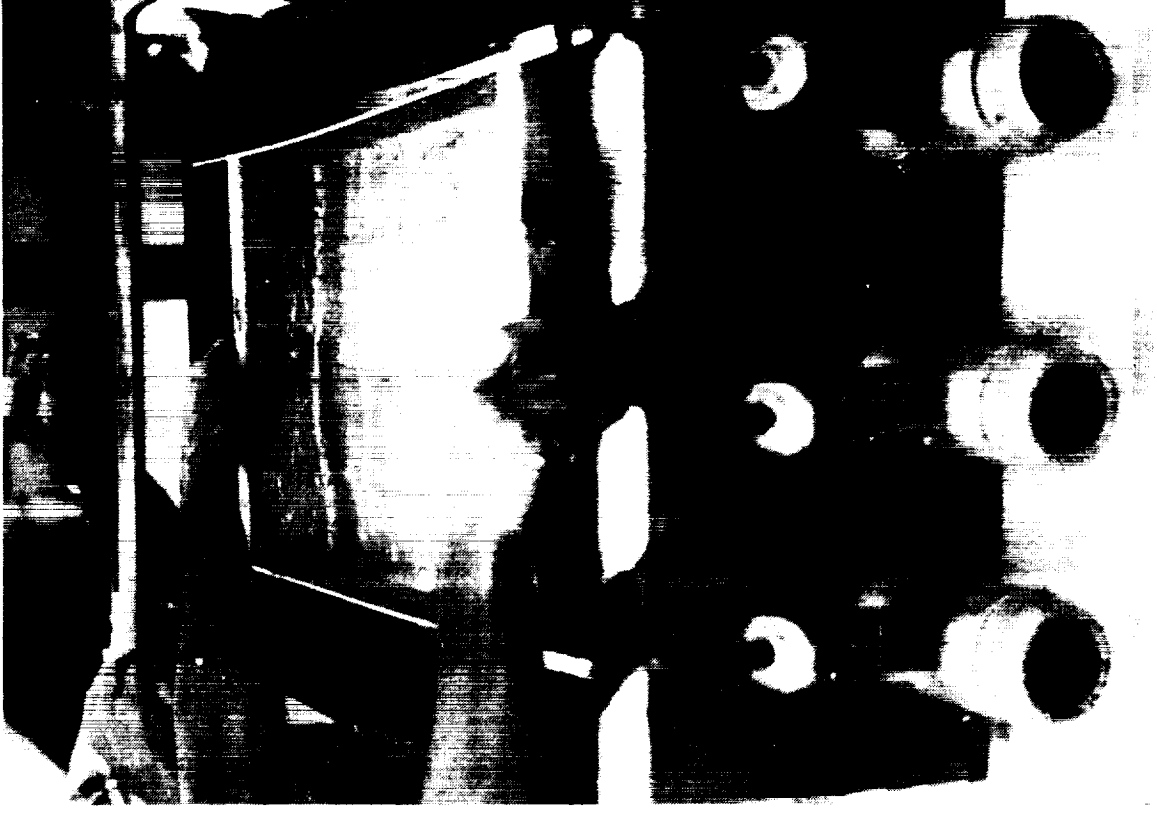
Clean & Etch of Back Face

*Figure 68*



*Hot Air Drying of Cleaned Faces*

*Figure 69*



*Hot Air Drying of Cleaned Faces Figure 70*



*Figure 71*

*Tool In Place for Lay-up Process*



*Placement of Edge Stiffener Pieces*

*Figure 72*



*Figure 73*

*Placement of Foam Edges & Dummy Corners*



*Figure 74*

*Taping Edges in Place*

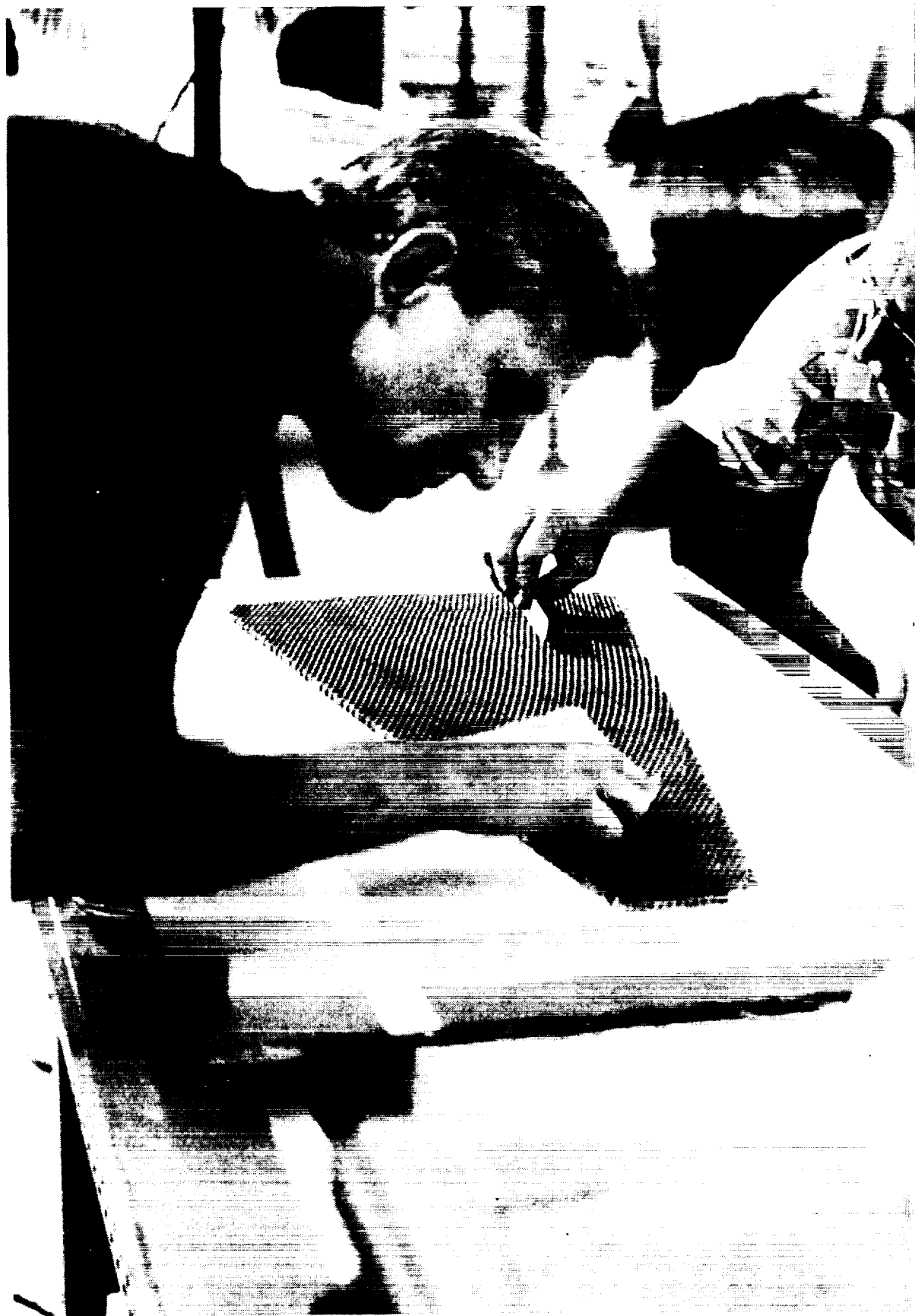
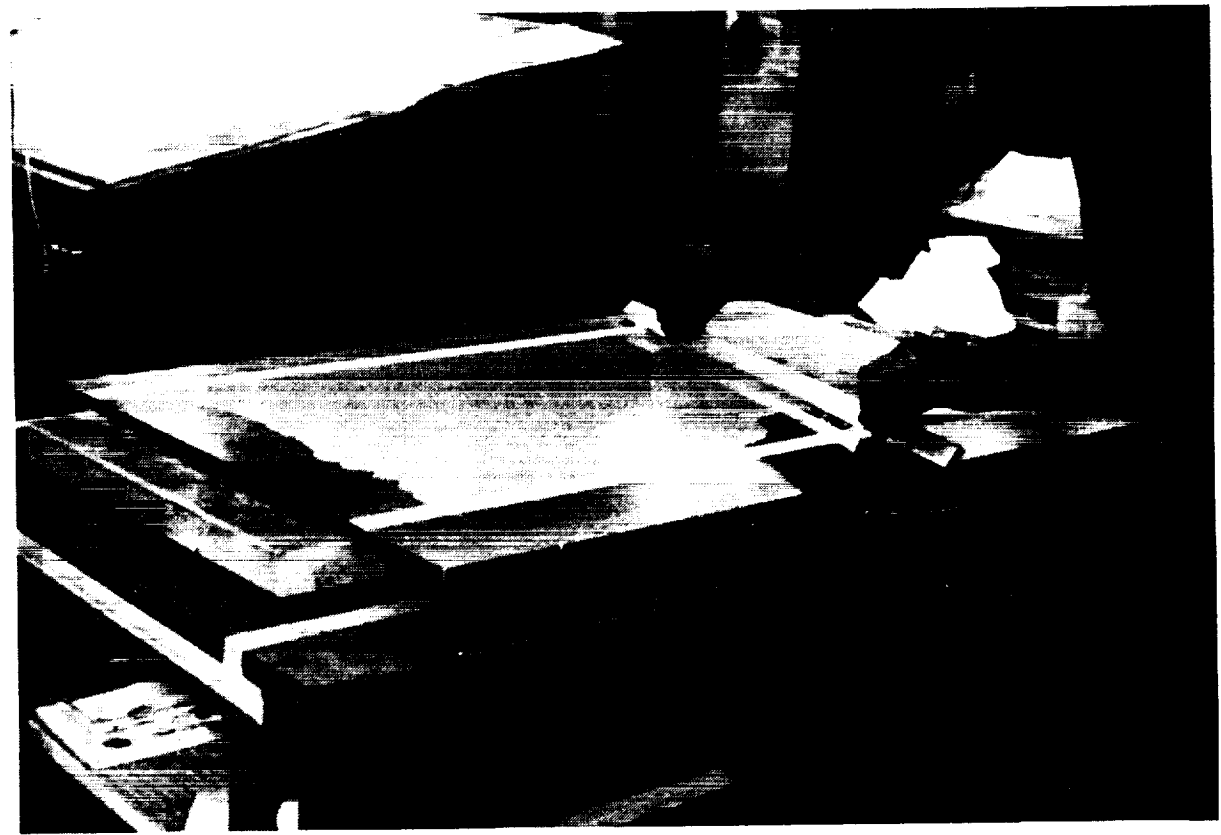


*Figure 75*

*Dipping Honeycomb Core into Adhesive*





*Screeding Adhesive Layer onto Dip Plate **Figure 76***

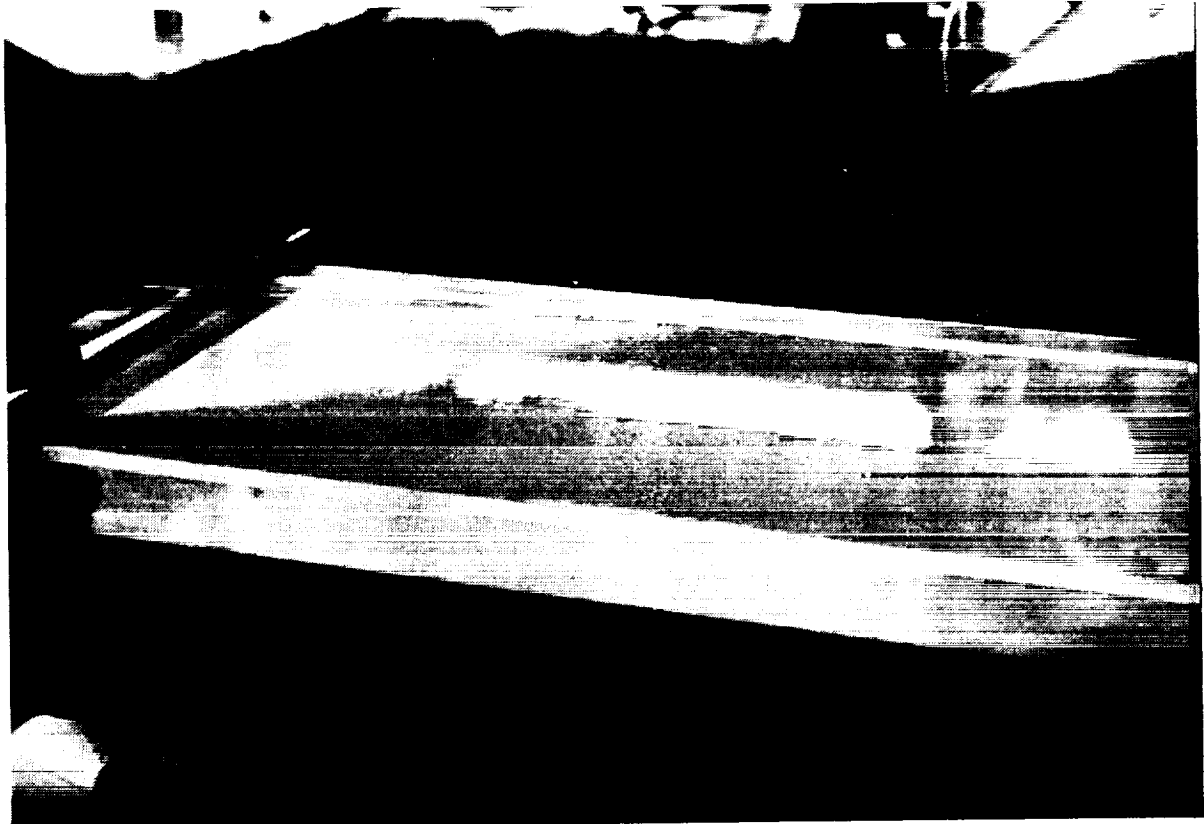


***Figure 77***



Figure 78

Placement of Honeycomb Core



HONEYCOMB IN PLACE

FIGURE 79



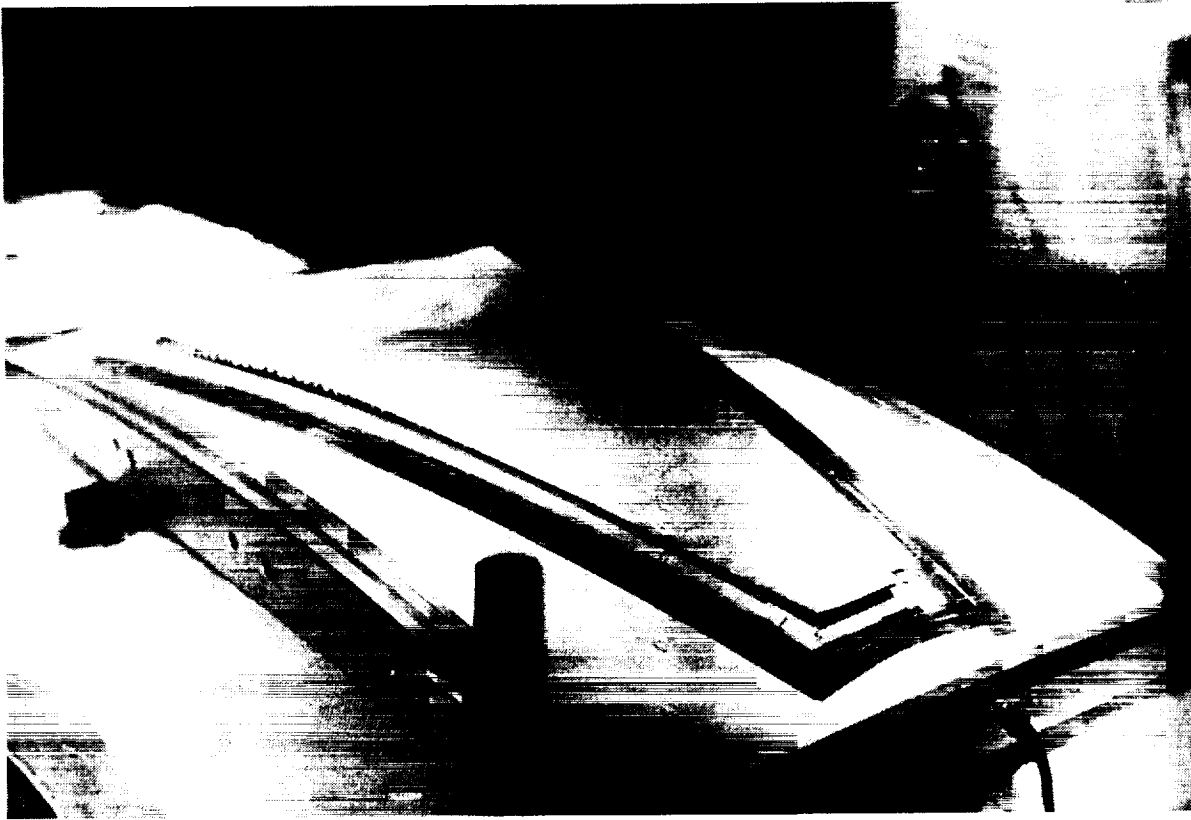
*Figure 80*

*Trimming Back Face with Template*



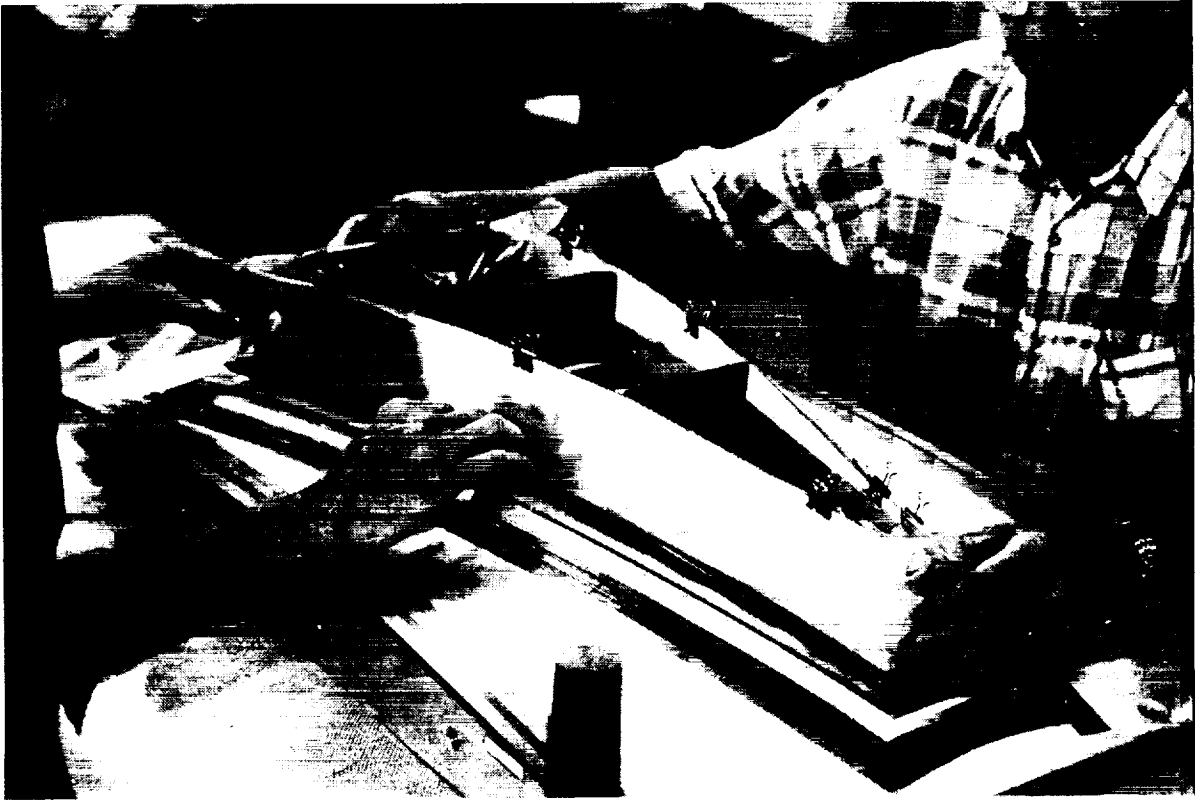
*Placement of Back Face*

*Figure 81*



*Back Face in Place*

*Figure 82*



Placement of Vacuum Bag

Figure 83

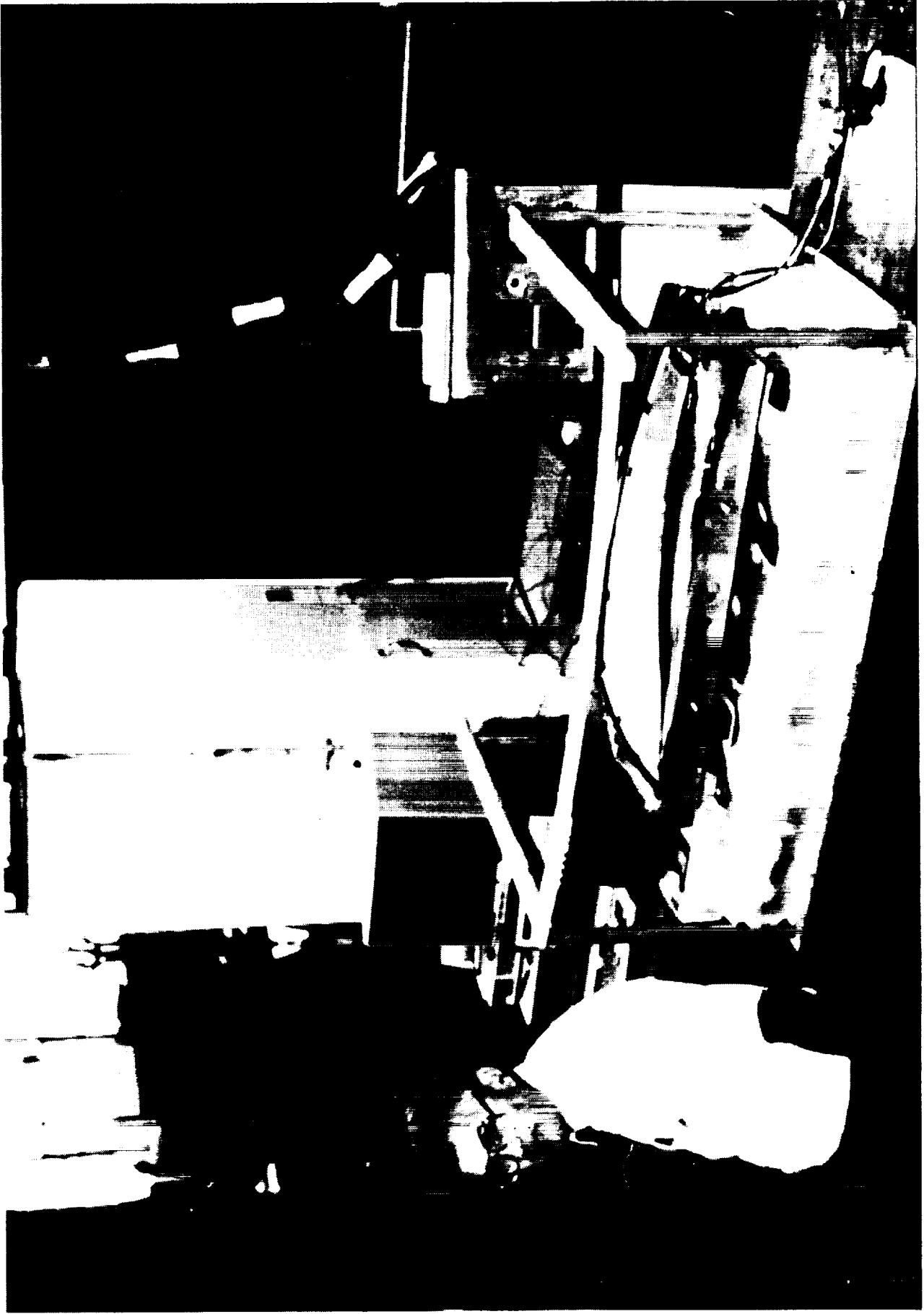


Placement of Vacuum Bag  
Sealing Tape

Figure 84



*Stretching Vacuum Bag over Sealing Tape*



*Panel Under Vacuum Bag before Cure*

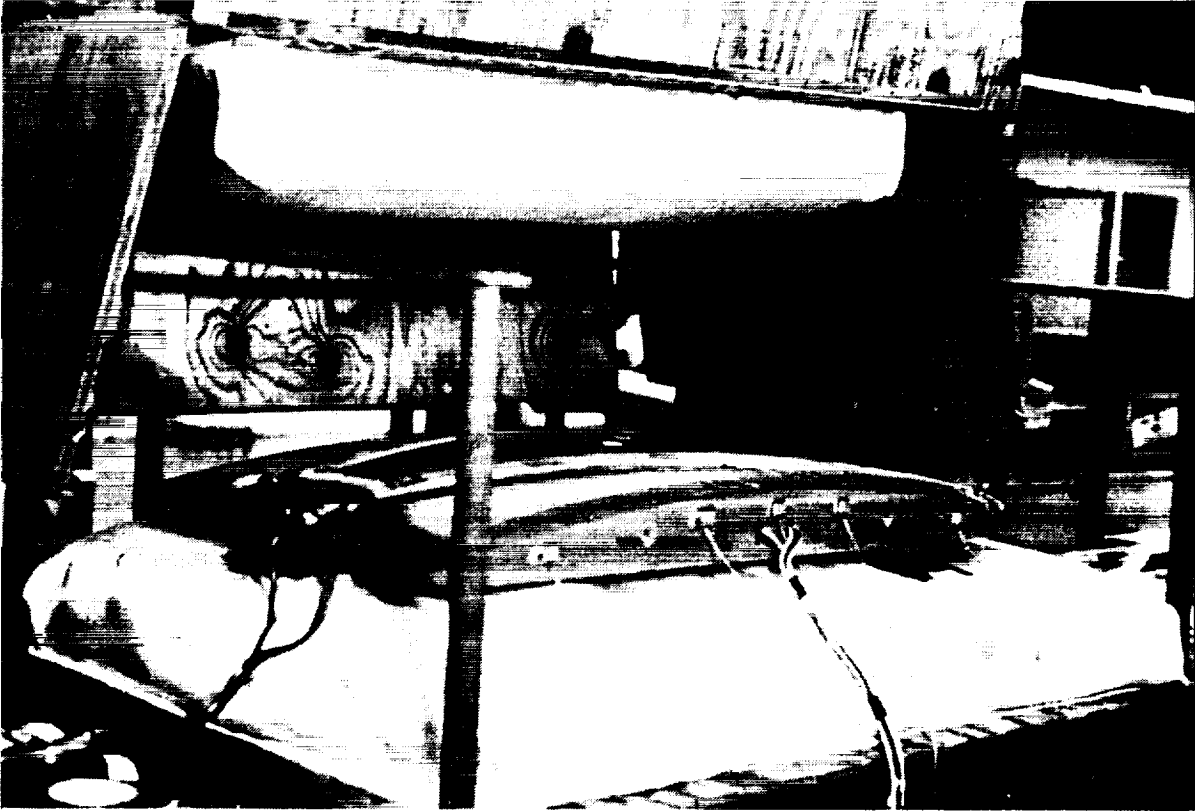
*Figure 86*





Panel Under Vacuum Bag before Cure

Figure 87



Placement of Oven Enclosure over  
Bagged Panel **Figure 88**



Placement of Insulation Pillows  
around Bagged Panel **Figure 89**



*Programming Four Zone Temperature Figure 90.*  
*Controllers*



*Panel Enclosed and Under Cure Figure 91*  
*Heat-up*



REMOVAL OF VACUUM BAG

FIGURE 92



*Removal of Tapes after Panel Cure*

*Figure 93*



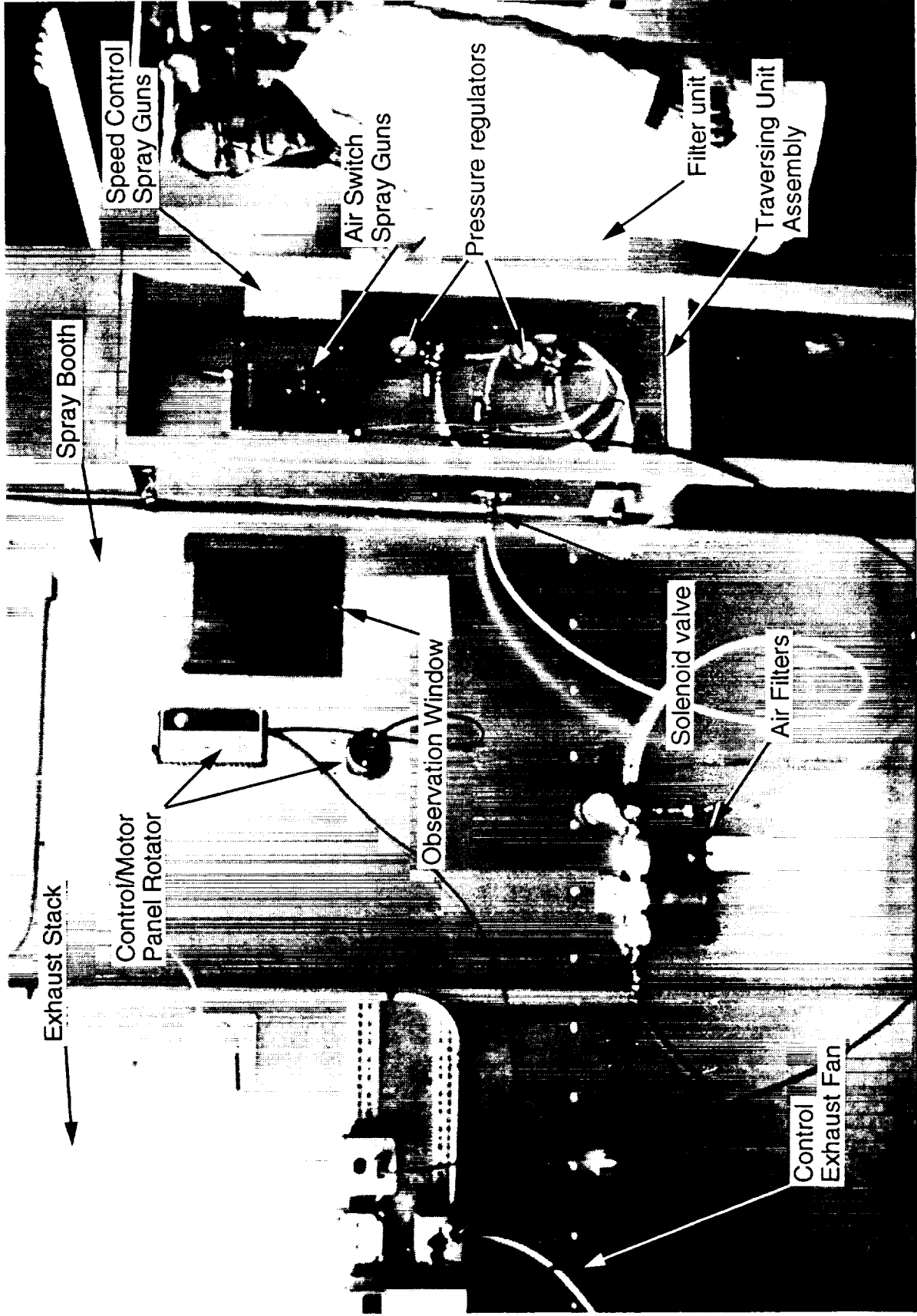
Figure 94

Removal of Cured Panel



*Figure 95*

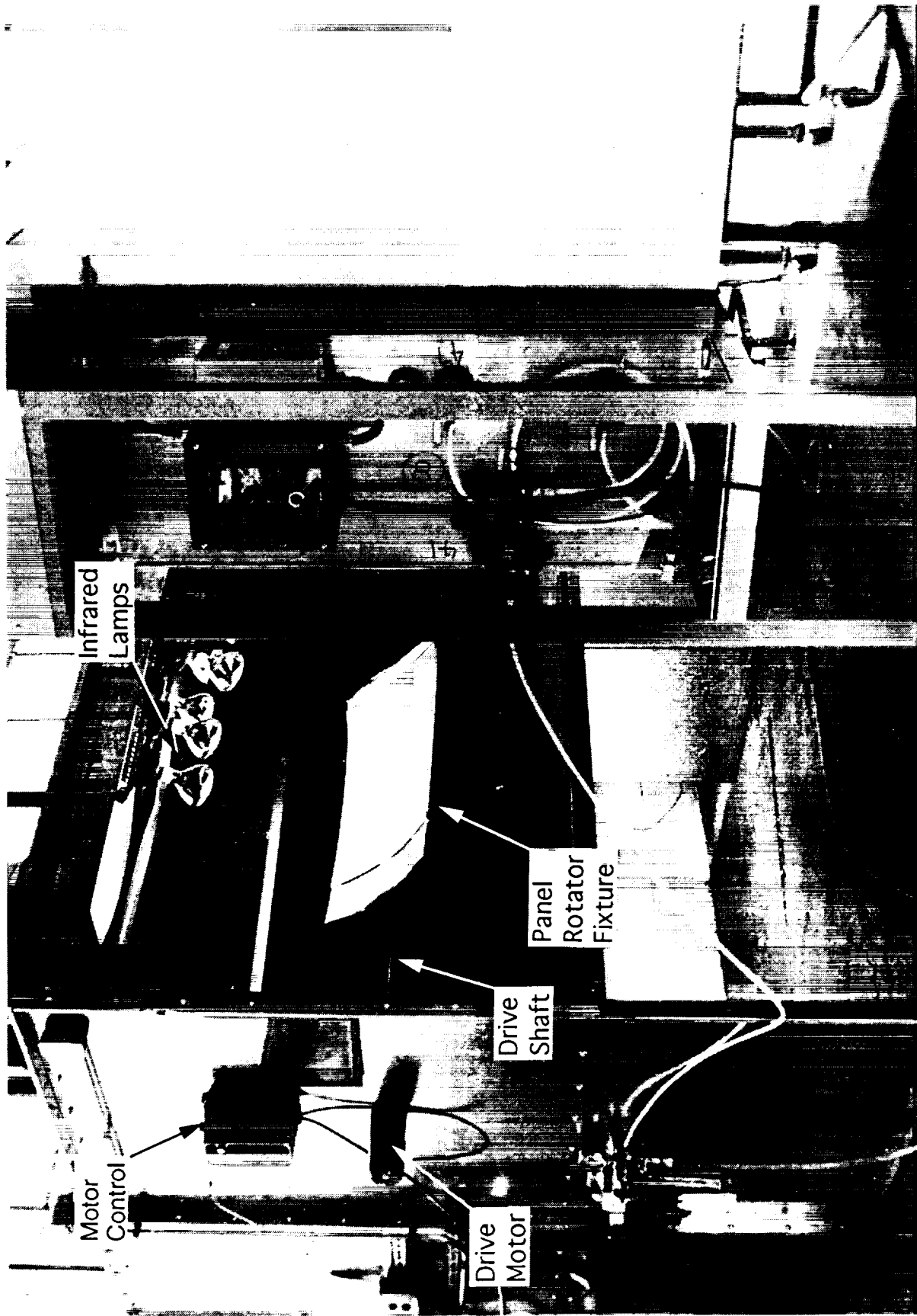
*Panel after Rough Trim*



Leveling Layer Spray Equipment

Figure 96





Heating Lamps & Panel Rotator

Figure 97

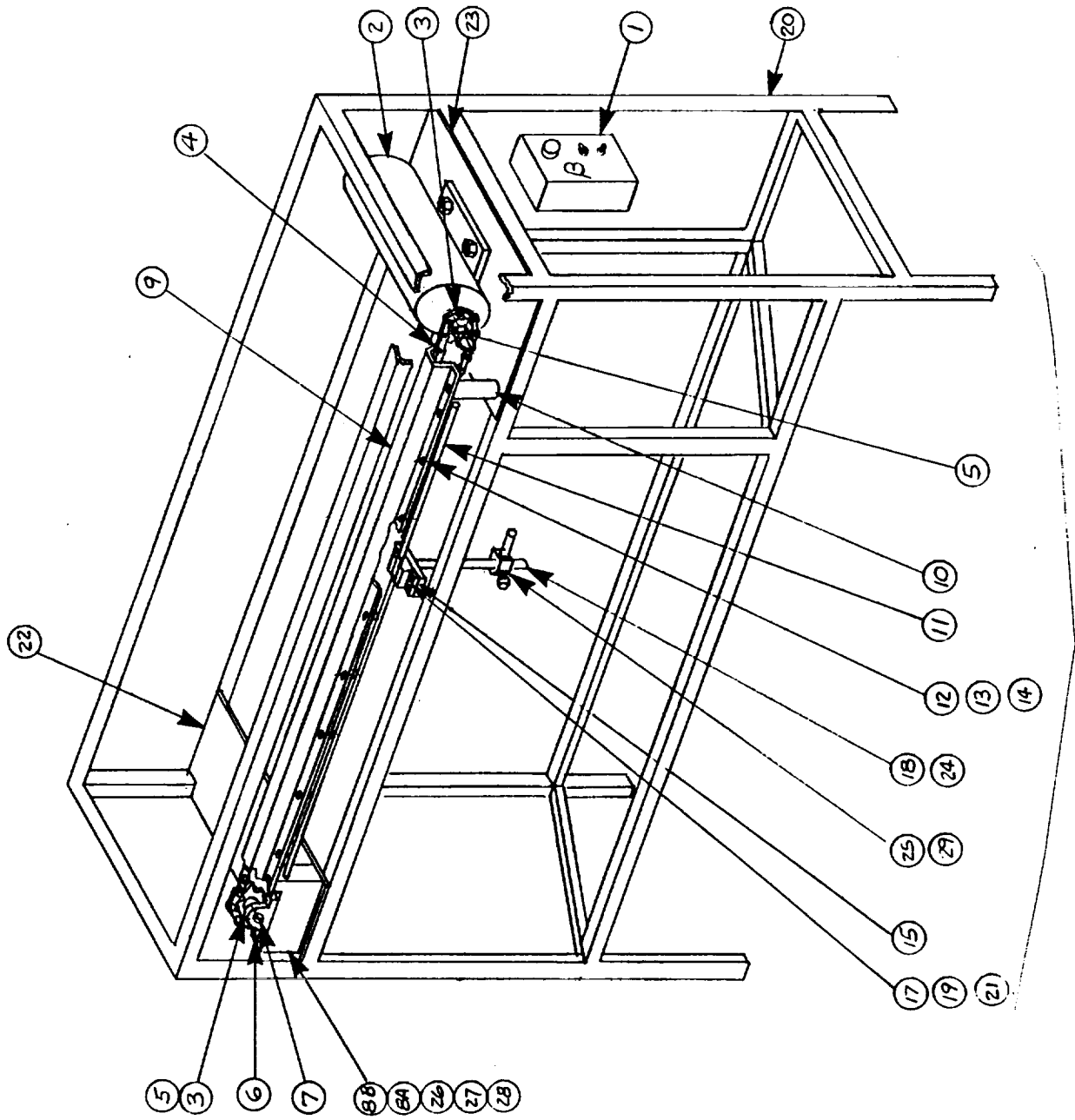


Figure 98

Traversing Mechanism Assembly

ITEM NO.	NO. REQ'D	DWG NO.	DESCRIPTION
29	2	-	HEX HD MACH SCREW 5/16-18UNC, 5/8 IN LG
28	10	-	HELICAL SPRING LOCK WASHER 3/8 LIGHT
27	6	-	HEX HD MACH. SCREW 3/8-16 UNC, .75 IN LG
26	4	-	HEX HD MACH. SCREW 3/8-16 UNC, 1.0 IN LG
25	2	1076	MOUNTING CLAMP - SPRAY GUN
24	1	1075	MOUNTING ROD - SPRAY GUN
23	1	1066	MOUNTING PLATE - MOTOR
22	1	1065	MOUNTING PLATE - SUPPORT BLOCK
21	10	-	HEX HD MACH SCREW #6-32, 1/2 IN LG
20	1	1087	EQUIPMENT CART
19	2	-	THOMPSON OPEN PILLOW BLOCK BUSHG. *SPB-8-OPN
18	1	-	HEX HD NUT 3/4 - 10 UNC STD.
17	10	-	HELICAL SPRING LOCK WASHER NO. 6 MEDIUM
16	44	-	BEARING PLATFORM
15	-	1064	HEX HD. NUT #6-32 STD.
14	44	-	SPACER - BEARING SHAFT
13	44	-	SHAFT - BEARING
12	44	1063	SUPPORT - CHAIN COVER
11	2	1084	CHAIN COVER
10	2	1061	SUPPORT BLOCK - IDLER SPROCKET
9	1	1083	SUPPORT BLOCK - IDLER SPROCKET
8B	1	1059	SHAFT - IDLER SPROCKET
8A	1	1059	BOSTON GEAR PILLW BLOCK #SL-5/8, CODE 64682
7	1	1058	STEEL KEY 3/16 SQ, 1 1/2 LG.
6	2	-	BOSTON GEAR ROLLER CHAIN 1 1/2 P, * 40
5	2	-	BOSTON GEAR SPROCKET 1/2" PITCH * 40B10-9/8, CODE 14986
4	1	-	BOSTON GEAR SPROCKET 1/2" PITCH * 40B10-9/8, CODE 14986
3	2	-	BOSTON GEAR MOTOR 1/2 HP, CAT # PM9507F-G, CODE 63226
2	1	-	BOSTON GEAR RADIOTROL CAT. # RB3R CODE 60253
1	1	-	

DESIGN CONTRACTOR  
CLEVELAND STATE UNIVERSITY  
ADVANCED MANUFACTURING CENTER

GRANT NO. 7-25-86  
TASK ORDER 2  
DR. BY ALBERT  
CHK'D BY  
DATE 7-25-86

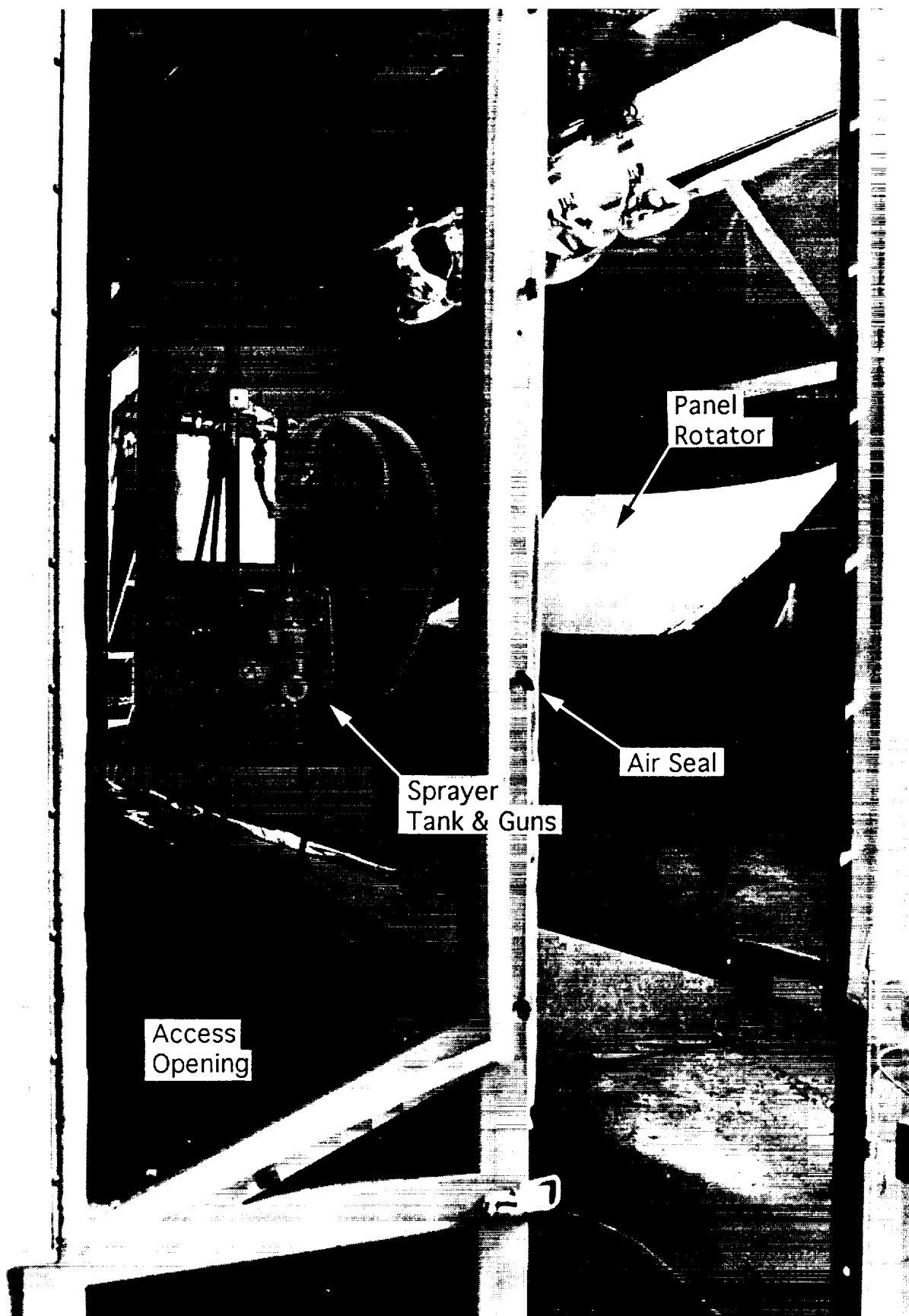
UNLESS OTHERWISE SPECIFIED  
DIM MAY VARY  
DIM MAY VARY  
ANGULAR DIM MAY VARY  
.....DIM MAY VARY  
BREAK SHARP EDGES

DR. DES. CK. D.SUP.  
D.S.HD. D.ENG. D.P.ENG.  
R.ENG. D.B.CH. D.DIV.  
R.S.HD. R.DIV.

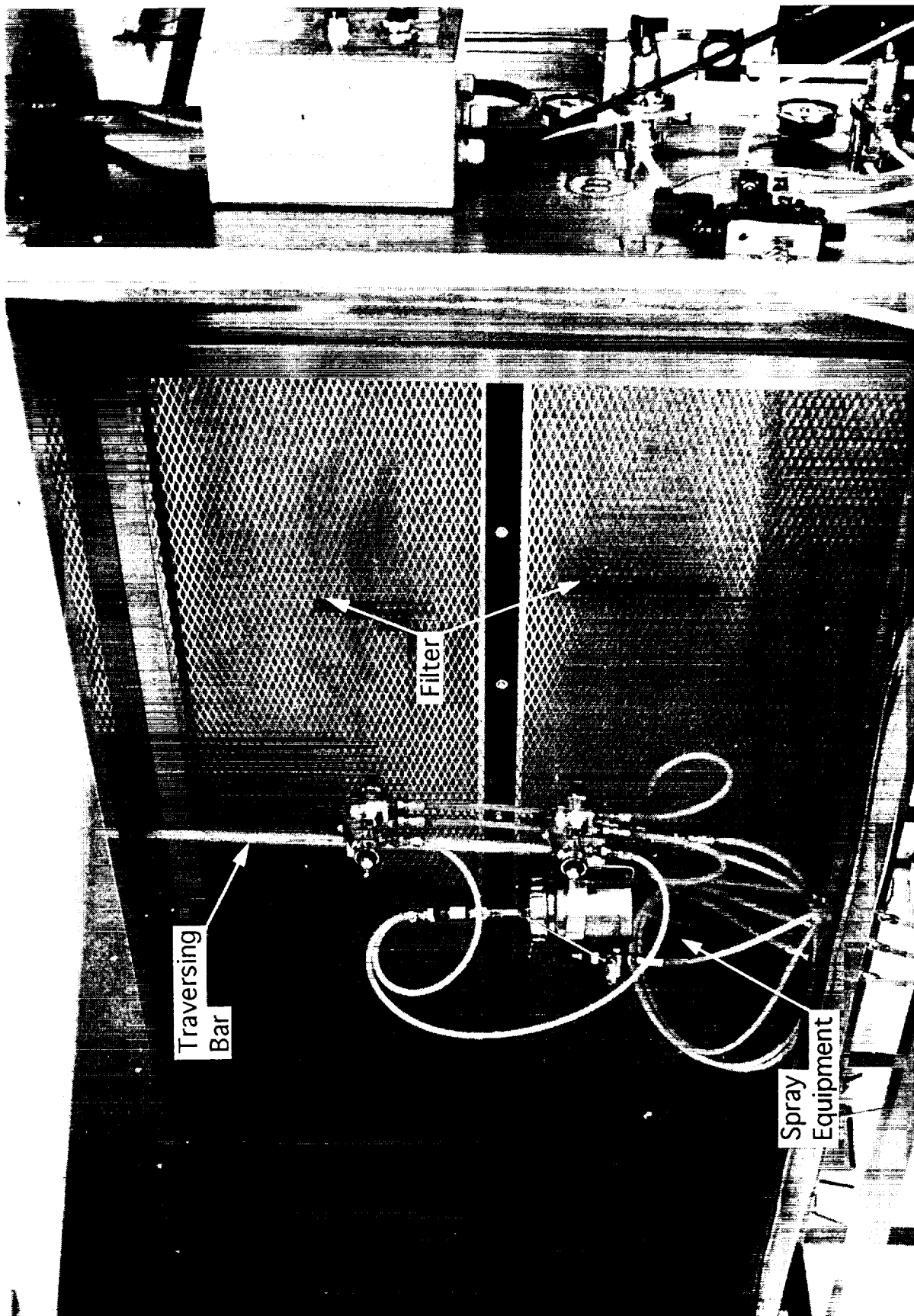
NASA NATIONAL AERONAUTICS AND SPACE ADMINISTRATION  
LEWIS RESEARCH CENTER  
CLEVELAND, OHIO

TRAVERSING UNIT  
SPRAY EQUIPMENT

SIZE -  
DRAWING NUMBER QUATIC 1085  
SCALE: 1/10115  
REV STAT BLOC NO



*View of Spray Equipment through Access Door*



View of Traversing Unit & Filter

Figure 101



*Figure 102*

*Leveling Layer Defects*



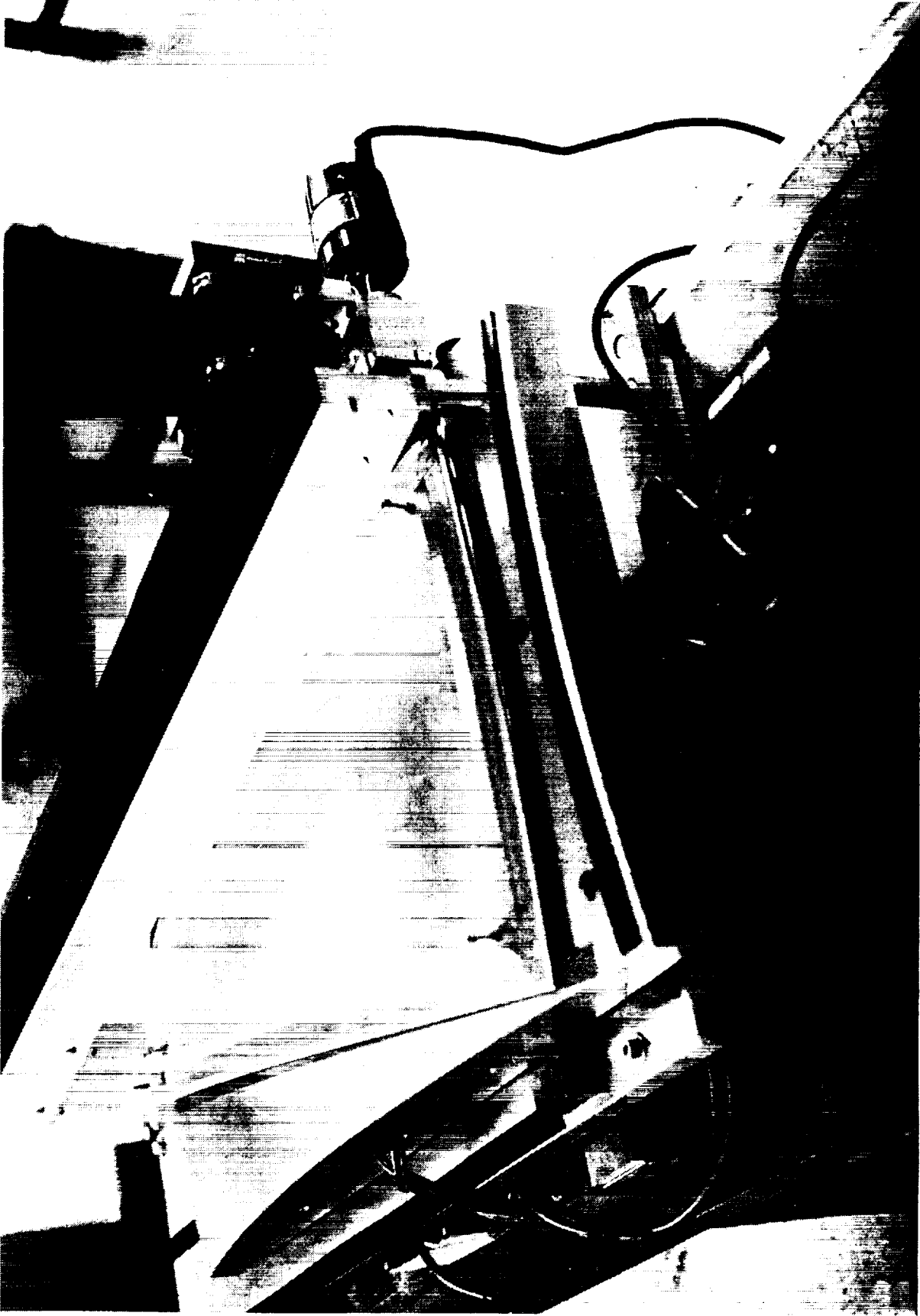
*Leveling Layer Defects*

*Figure 103*



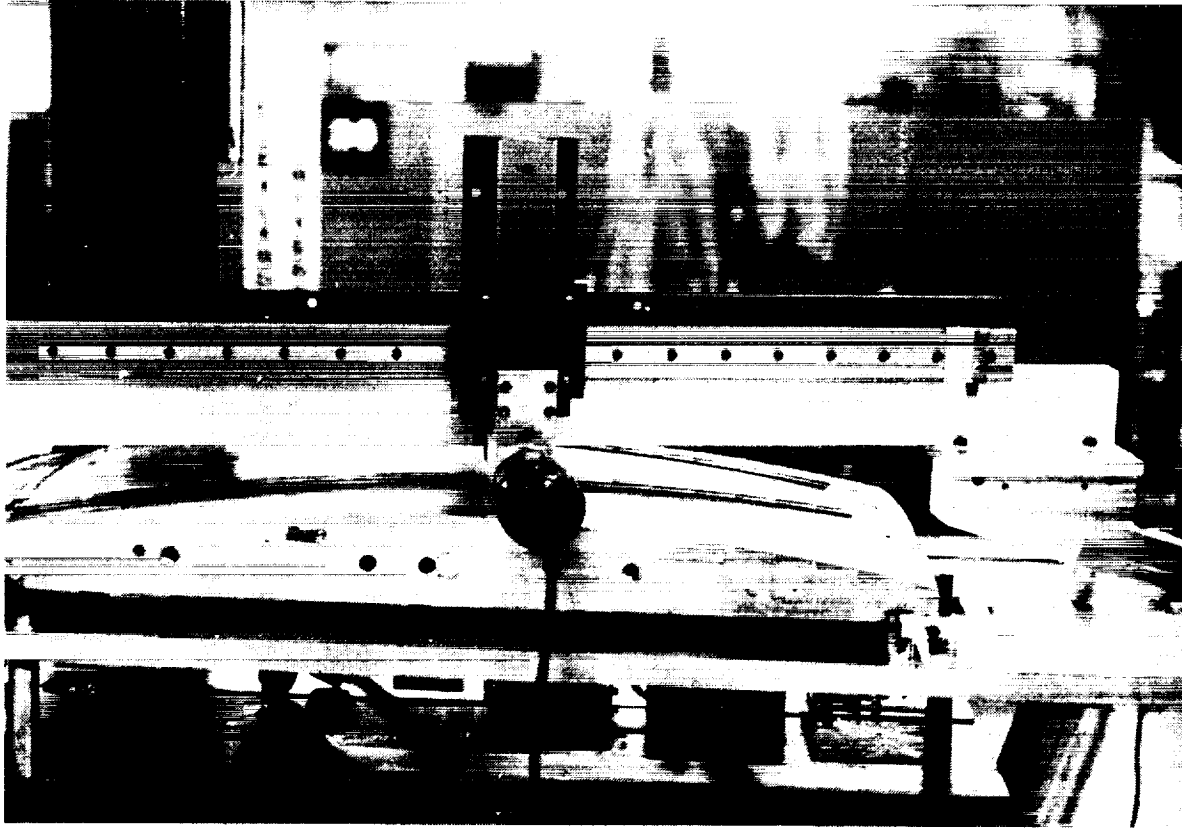
*Vacuum Evaporation Specimens*





*Panel in Trimming Fixture*

*Figure 105*



Trimming Radial Edge



Close up of Radial Edge Trimming Figure 107

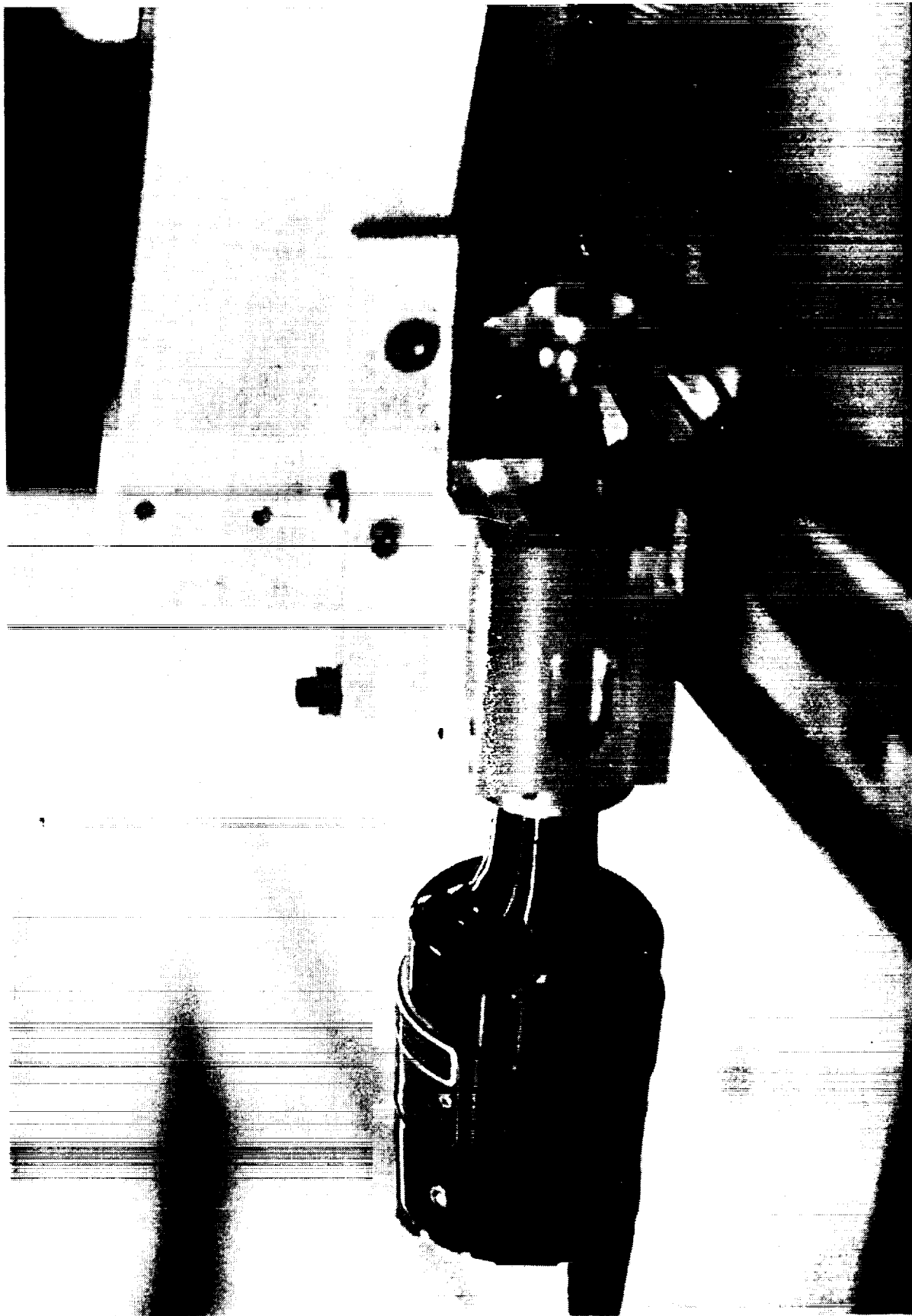
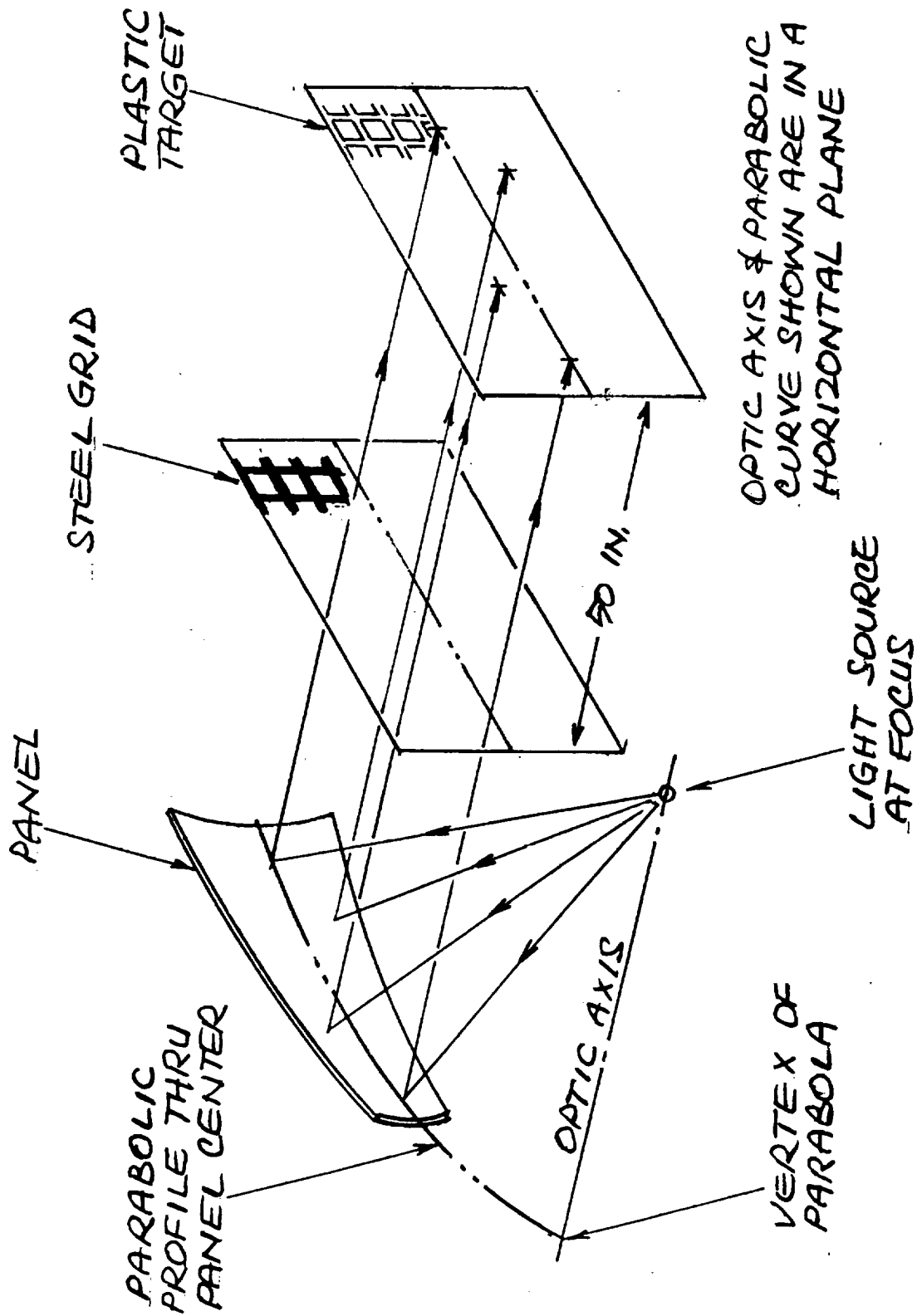


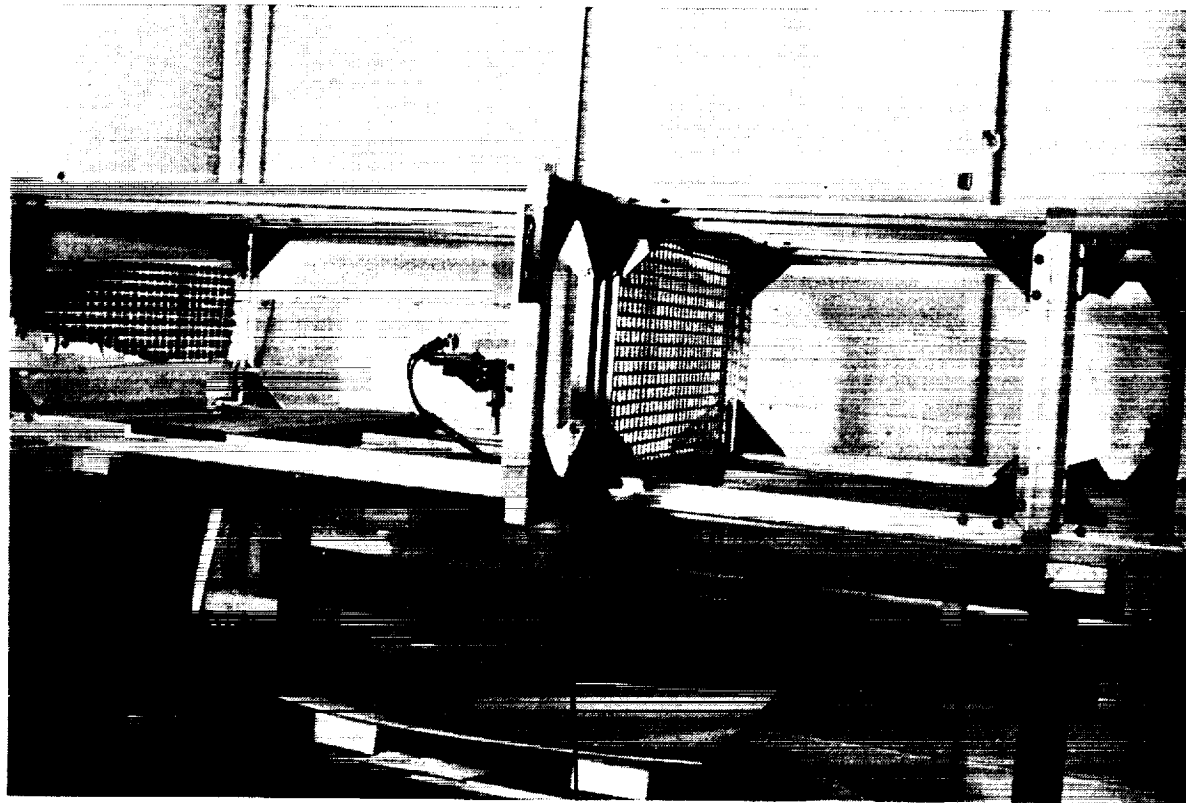
*Figure 108*

*Close-up of OD Edge Trimming*

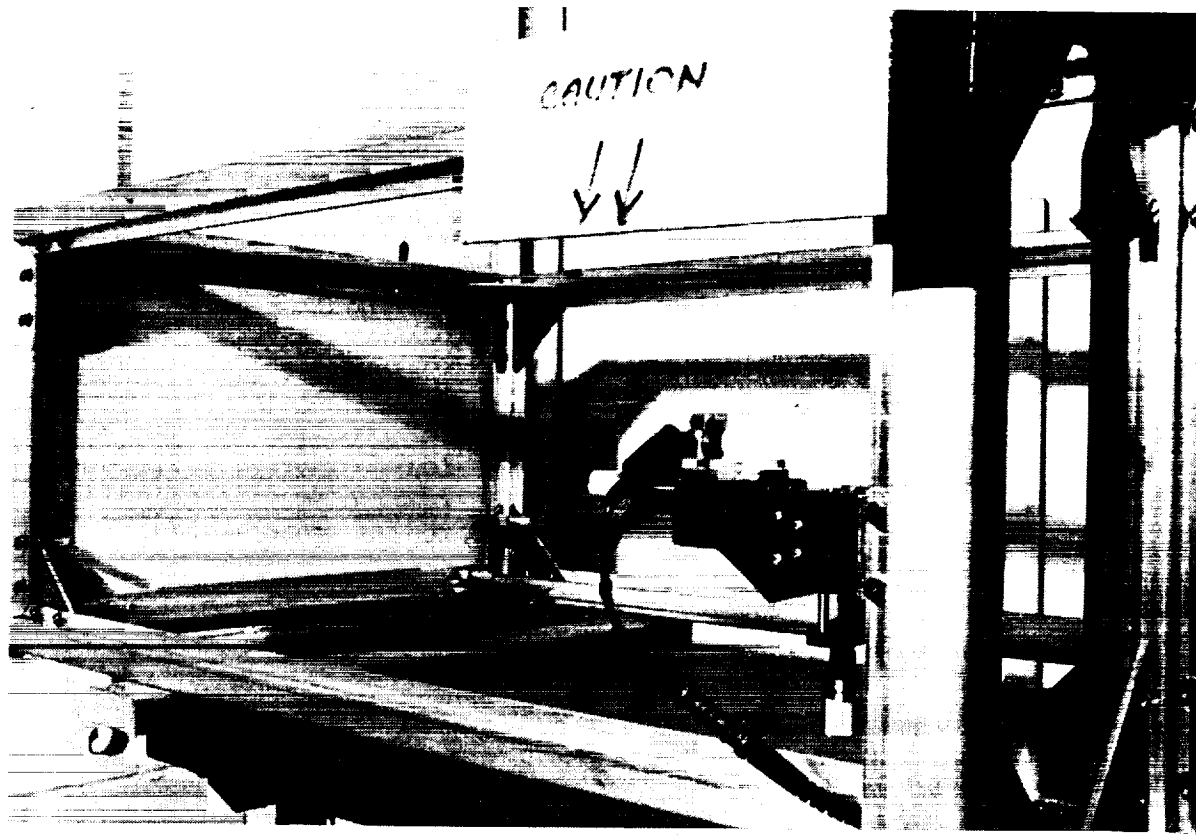
# OPTICAL INSPECTION RIG SCHEMATIC



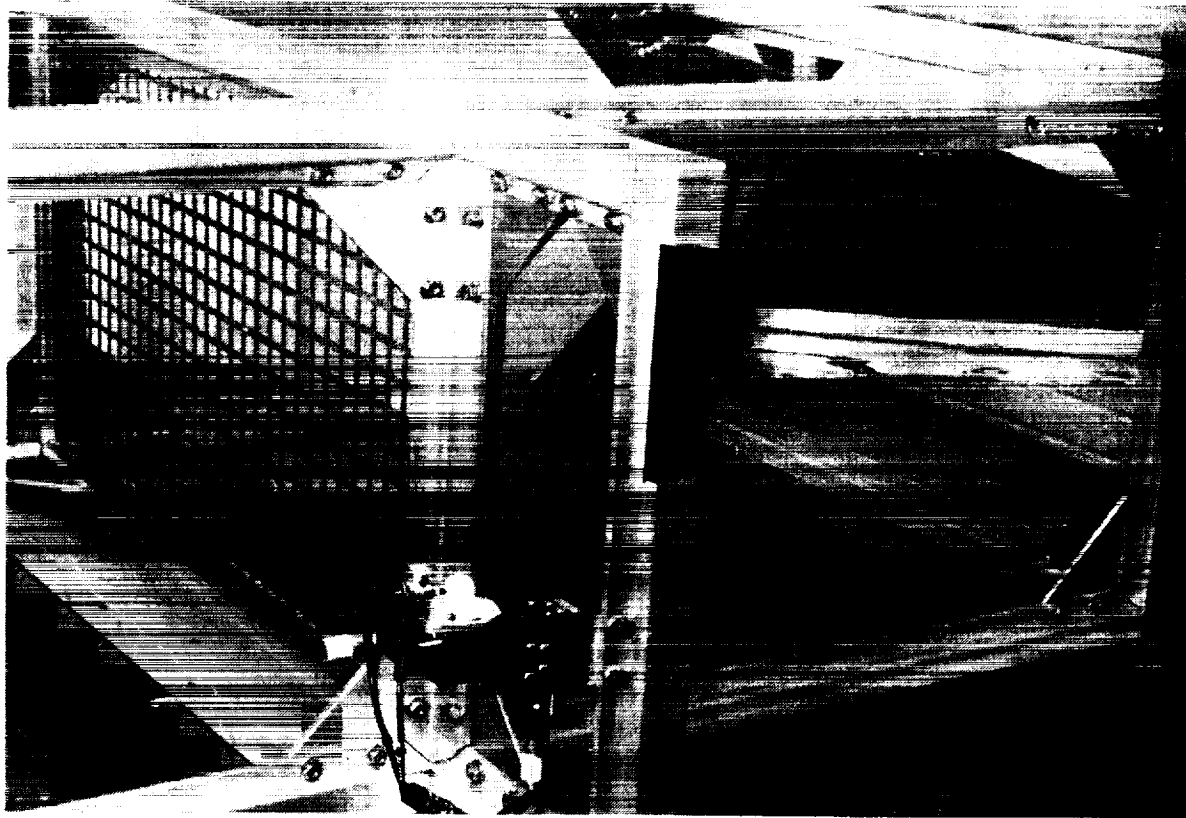
Optical Inspection Rig Schematic



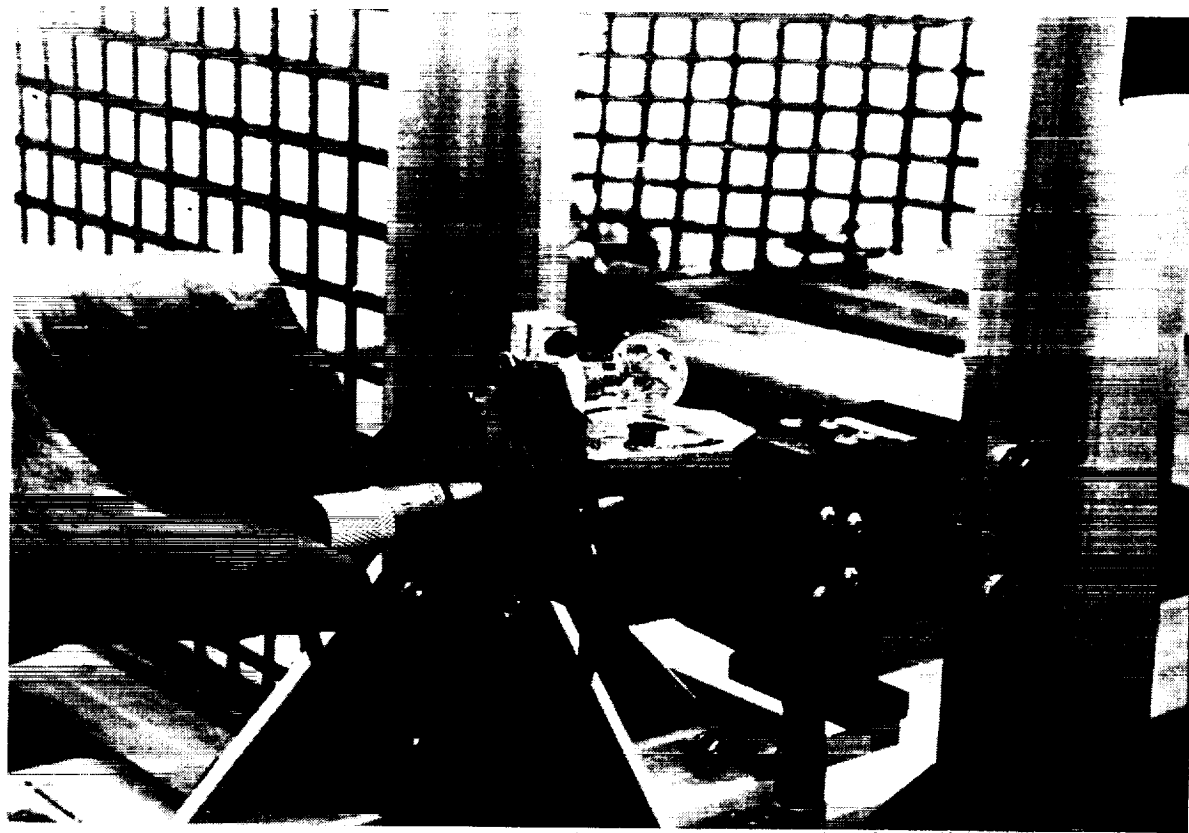
Optical Inspection Rig, Overall View **Figure 110**



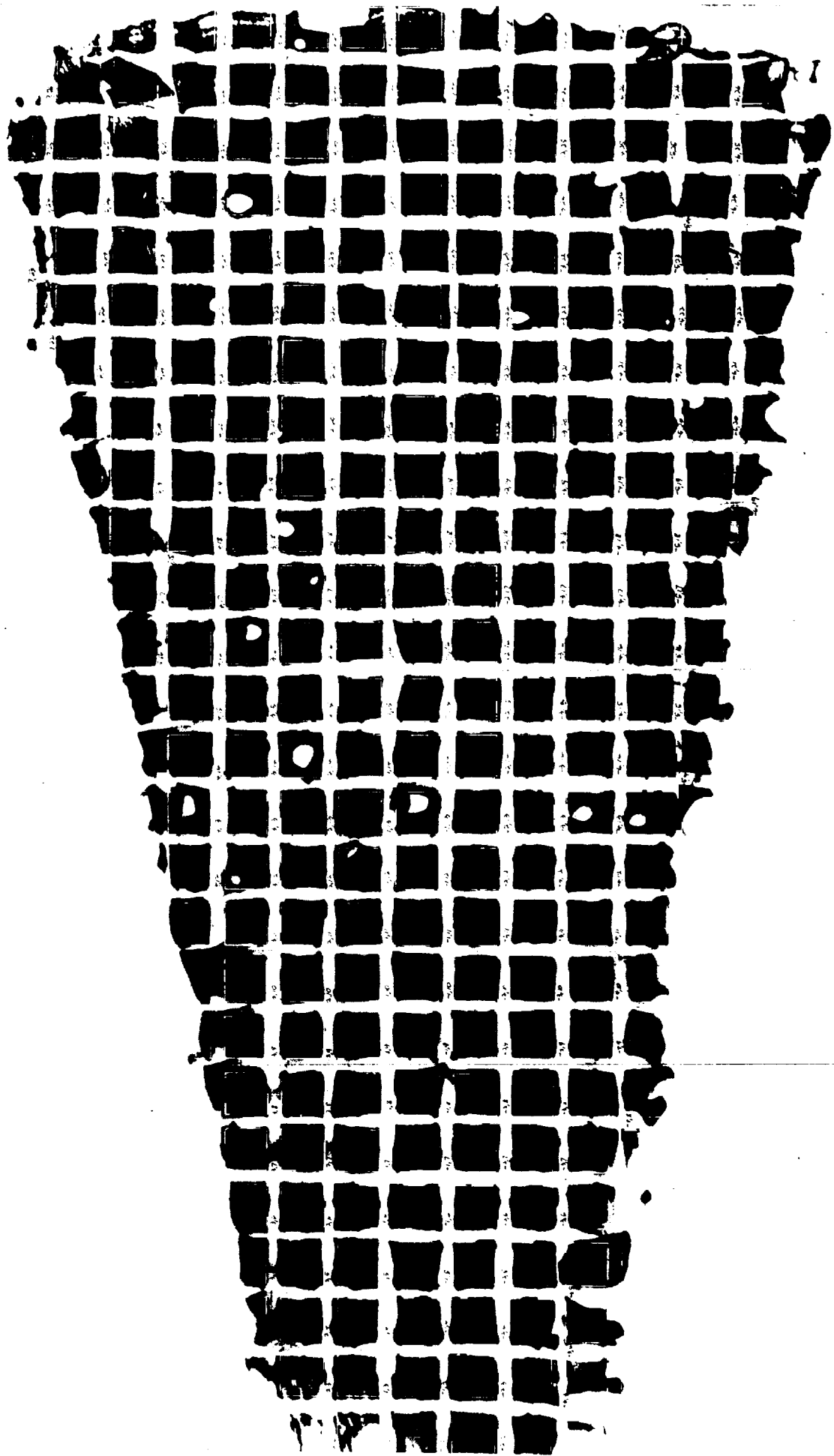
Optical Inspection Rig, Plastic Target **Figure 111**



*Optical Inspection Rig, Light Source  
& Panel*

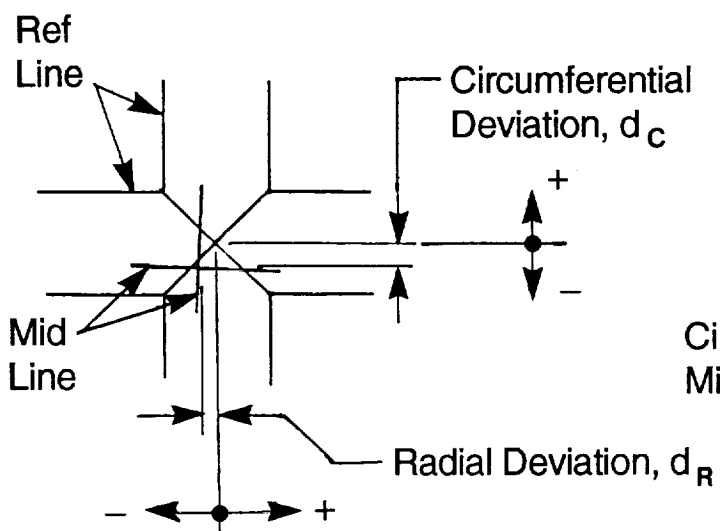


*Optical Inspection Rig, Light Source  
Adjustment*



PANEL NO. 6 INSPECTION

FIGURE 114

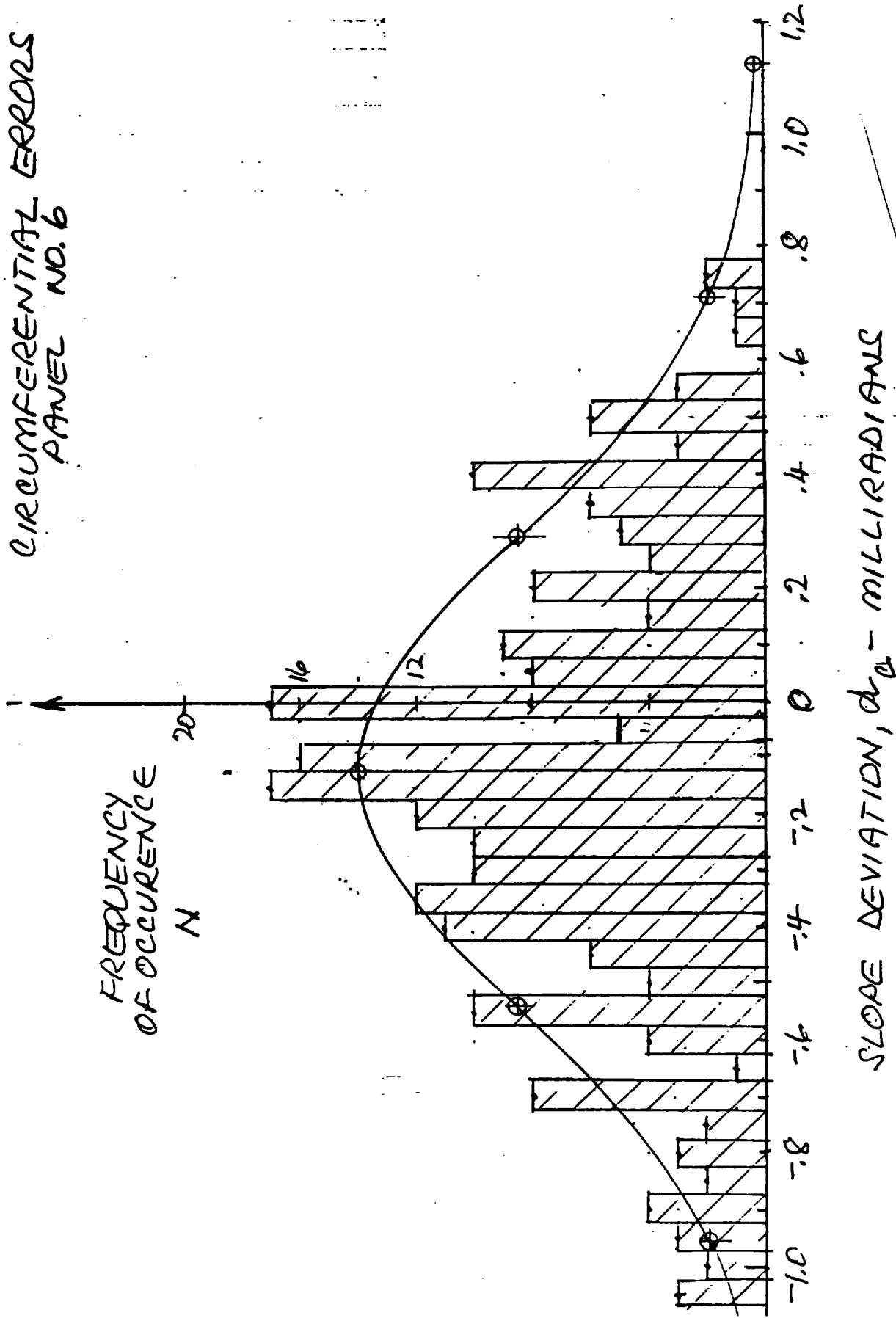


Circumferential  
Midpoints

Radial  
Midpoints

Figure 115



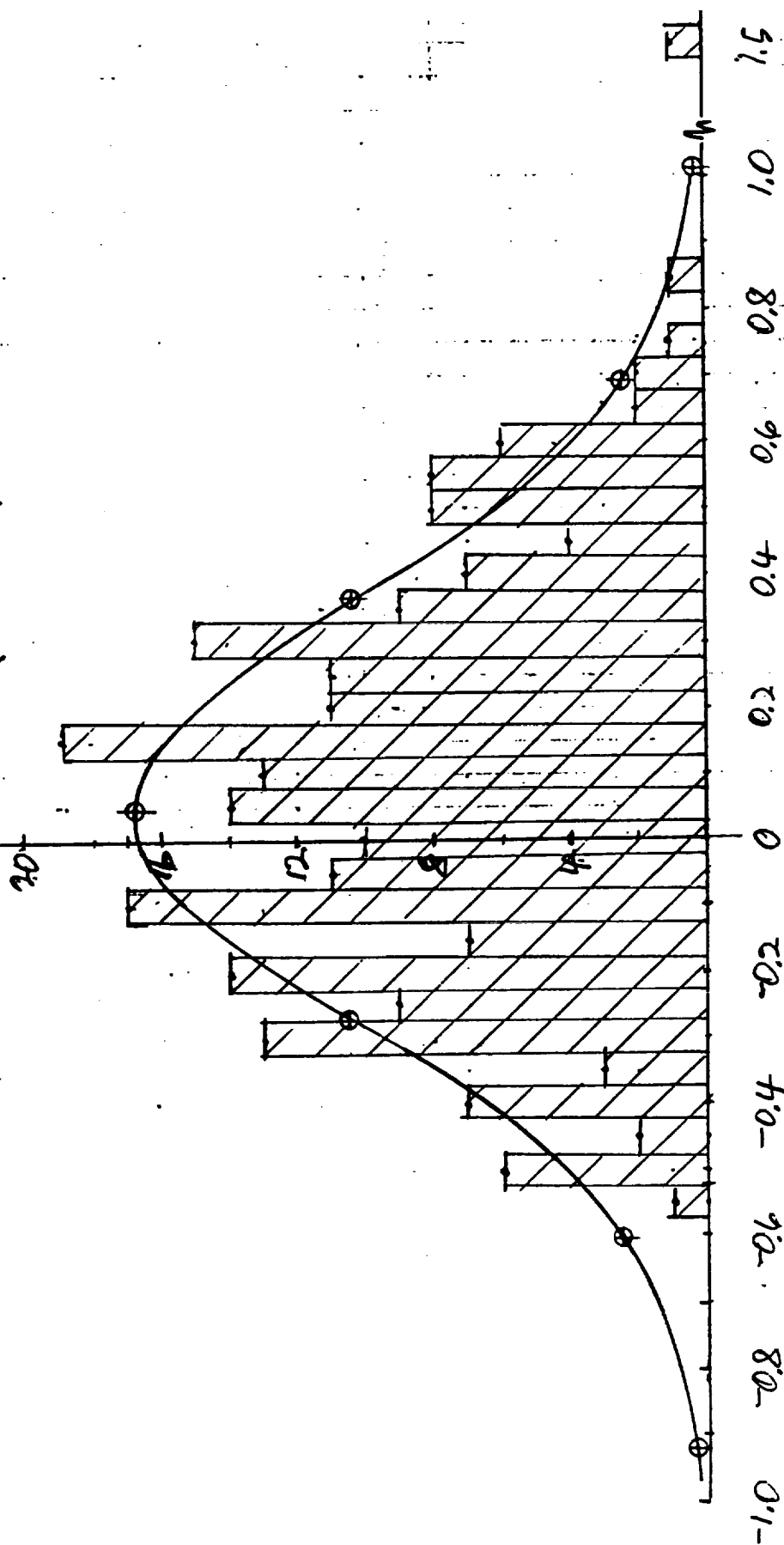


Circumferential Errors Panel No. 6

Figure 116

RADIAL ERRORS  
PANEL NO. 6

FREQUENCY OF  
OCCURRENCE, N



SLOPE ERROR,  $\alpha$  (MILLIRADIANS)

ORIGINAL PAGE IS  
OF POOR QUALITY

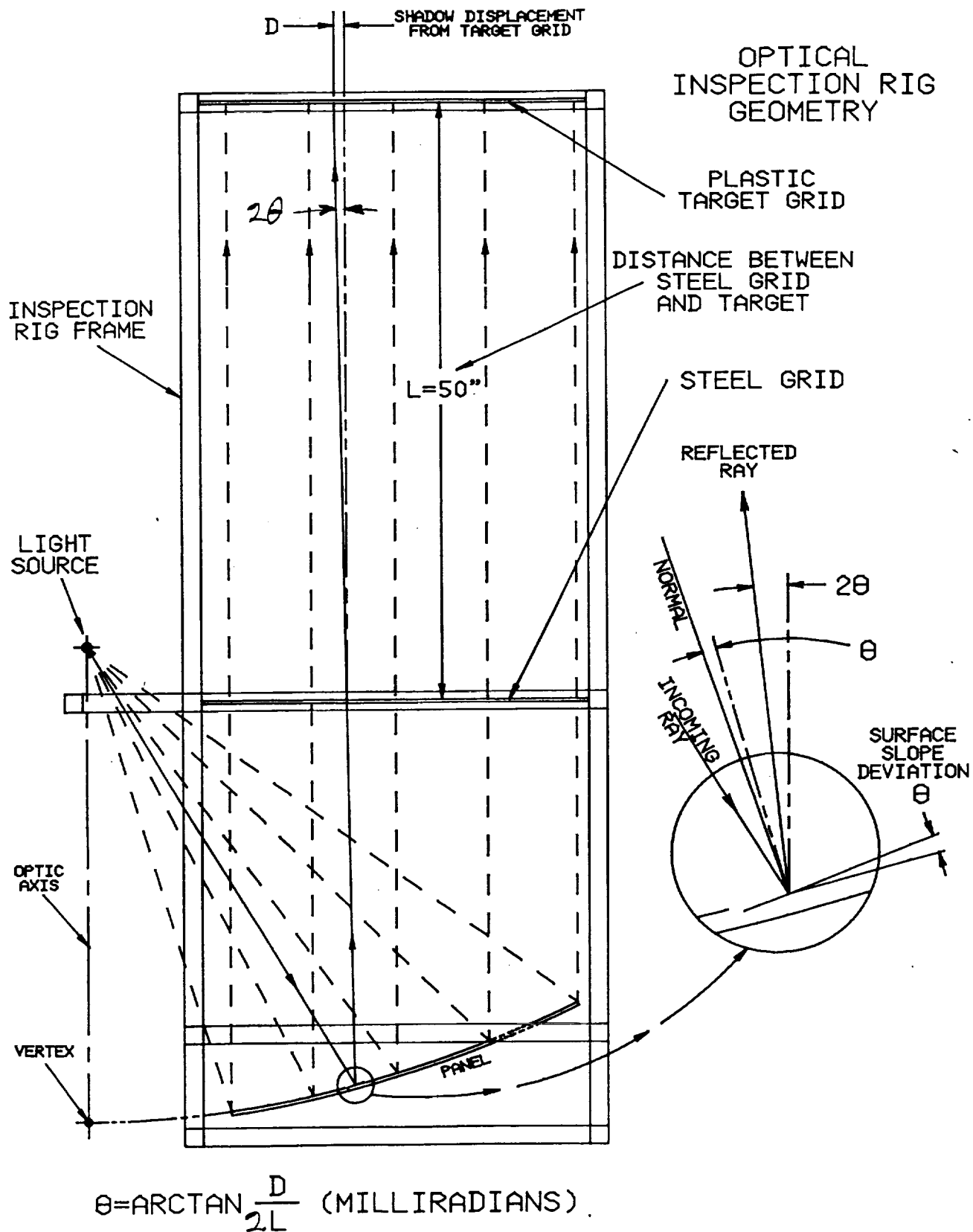


Figure 118

Optical Inspection Rig Geometry